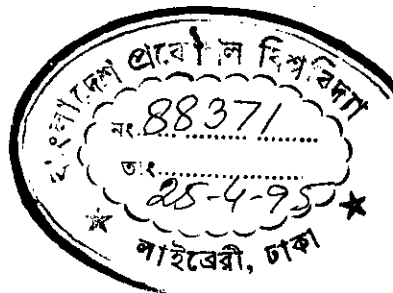# AN EXPERIMENTAL INVESTIGATION OF NATURAL CONVECTION FROM HOT SQUARE CORRUGATED PLATES TO A COLD FLAT PLATE

By

**Khan Md. Saiful Islam**

A Thesis
Submitted to the Department of Mechanical Engineering in partial fulfilment of
the requirements for the degree
of
MASTER OF SCIENCE IN MECHANICAL ENGINEERING

#88371#

BANGLADESH UNIVERSITY OF ENGINEERING AND TECHNOLOGY, DHAKA.
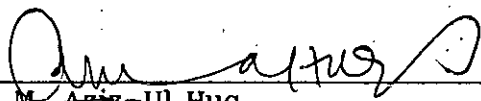FEBRUARY 1995

# CERTIFICATE OF APPROVAL

The thesis titled "An Experimental Investigation of Natural Convection From Hot Square Corrugated Plates to a Cold Flat Plate" submitted by Khan Md. Saiful Islam, Roll No. 911440P, Registration No. 85395 of M.Sc. Engineering (Mechanical) has been accepted as satisfactory in partial fulfilment of the degree of Master of Science in Engineering (Mechanical) on the 19th February 1995.


Dr. Md. Abdur Razzaq Akhanda (Supervisor)          Chairman
Professor & Head                                   Member (Ex-officio)
Mec
hanical Engineering Department
BUET, Dhaka.


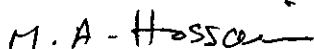Dr. A. M. Aziz-Ul Huq                              Member
Professor
Mechanical Engineering Department
BUET, Dhaka.


Dr. Md. Imtiaz Hossain                             Member
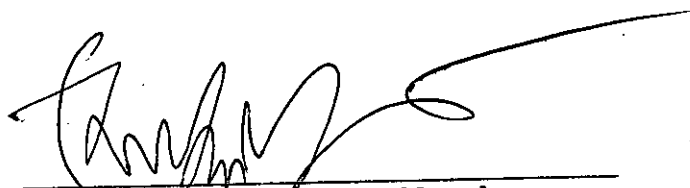Professor
Mechanical Engineering Department
BUET, Dhaka.


Professor Dr. M. Anwar Hossain                     Member
Department of Mechanical and Chemical Engg.        ( External )
Islamic Institute of Technology
Dhaka.

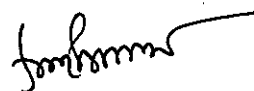# CERTIFICATE OF RESEARCH

This is to certify that the work presented in this thesis is an outcome of the investigation carried out by the author under the supervision of Dr. Md. Abdur Razzaq Akhanda, Professor & Head, Department of Mechanical Engineering, Bangladesh University of Engineering & Technology, Dhaka.

Dr. Md. Abdur Razzaq Akhanda
Supervisor

Khan Md. Saiful Islam
Author

iii

# ACKNOWLEDGEMENT

# ABSTRACT

This experimental investigation deals with the steady state natural convection heat transfer through air at atmospheric pressure from hot square corrugated plates to a cold flat plate placed above and parallel to it, where the surroundings were maintained at constant temperature. Different amplitudes of corrugation i.e., H = 10mm, 15mm and 25mm were used. The effects of angle of inclination, aspect ratio, temperature difference and Rayleigh number on average convective heat transfer co-efficients were studied which covers the ranges of:

$$0° \leq \Theta \leq 75°, \quad 1.4 \leq A \leq 9.5, \quad 10°C < \Delta T \leq 35°C, \quad 3.294 \times 10^4 \leq Ra_L \leq 1.881 \times 10^6$$

From these sets of corrugation it is investigated that for the same Rayleigh number an increase in amplitude of corrugation increases the convective heat transfer coefficient and the values are

$Nu_L$ for H = 25mm > $Nu_L$ for H = 10mm by 13%

$Nu_L$ for H = 25mm > $Nu_L$ for H = 15mm by 6%

The results are compared with those available in literature and it is investigated that for lower Rayleigh number i.e., $Ra_L$ = 0.4 $\times$ $10^6$ the Nusselt number is maximum for vee-corrugation and minimum for square corrugation, and the values are,

$Nu_L$ for Vee corrugation > $Nu_L$ for square corrugation of H = 25mm by 41%

$Nu_L$ for Sinusoidal corrugation > $Nu_L$ for square corrugation of H = 25mm by 26%

$Nu_L$ for Trapezoidal corrugation > $Nu_L$ for square corrugation of H = 25mm by 16%

$Nu_L$ for Rectangular corrugation > $Nu_L$ for square corrugation of H = 25mm by 10%

These differences are also lower for higher Rayleigh numbers i.e., 1.0 $\times$ $10^6$.

Again the following correlation for square corrugation was developed which correlates almost all the data within ± 20%

$$Nu_L = 0.295 \, [Ra_L \cos\Theta]^{0.265} \, [A]^{-0.442} \qquad \text{[a]}$$

# CONTENTS

# NOMENCLATURE

| SYMBOL | MEANING | UNITS |
|--------|---------|-------|
| A | Aspect ratio, L/H [Mean plate spacing/amplitude of currugation] | dimensionless |
| $A_{COR}$ | Projected area of the test section | $m^2$ |
| $A_{COLD}$ | Area of the cold plate | $m^2$ |
| $A_p$ | Area of any plane rectangular surface | $m^2$ |
| $A_i$ | Area of surface i | $m^2$ |
| $A_j$ | Area of surface j | $m^2$ |
| $A_s$ | Area of the wooden surface | $m^2$ |
| C | Constant | dimensionless |
| $C_p$ | Specific heat of air at constant pressure | KJ/Kg K |
| $E_b$ | Emissive power for a black surface, $\sigma T^4$ | Watt/$m^2$ |
| F | Shape factor | |
| Gr | Grashof number, $g.\beta.\Delta T d^3/v^2$ | dimensionless |
| g | Acceleration dued to gravity | m/sec$^2$ |
| h | Average natural convective heat transfer coefficient | Watt/$m^2$ K |
| H | Amplitude of the corrugation | mm |
| $I_{safe}$ | Safe current capacity of the heater coil | ampere |
| J | Radiosity [Emissive power for a black surface, $E_b$] | Watt/$m^2$ |
| K | Thermal conductivity of air | Watt/m K |
| $L_c$ | Characteristic length $(=\sqrt{A_p})$ | m |
| L | Mean plate spacing | mm |

| | | |
|---|---|---|
| m | Exponent | dimensionless |
| n | Exponent | dimensionless |
| $Nu_L$ | Average Nusselt number, $hL/k$ | dimensionless |
| Pr | Prandtl number, $\mu.C_p/k$ | dimensionless |
| q | Heat transfer rate | Watt/m$^2$ |
| q" | Heat flux rate into the test hot plate | watt/m$^2$ |
| r | Unit electrical resistance | ohms/m |
| R | Electrical resistance | ohms |
| $Ra_L$ | Rayleigh number based on mean plate spacings (L), $g.\beta.\Delta T.L^3/\nu\alpha$ | dimensionless |
| s | Maximum width of corrugation | mm |
| t | Time | Sec |
| T | Temperature | K |
| $T_a, T_\infty$ | Ambient air temperature | K |
| $T_f$ | Fluid film temperature, $[T_{COR} + T_{COLD}]/2$ | K |
| $T_{COR}$ | Temperature of the hot corrugated plate | K |
| $T_{COLD}$ | Temperature of the cold flat plate | K |
| $\Delta T$ | Temperature difference between the hot corrugated plate and flat cold plate | K |
| $\Delta T_c$ | Conduction correction | K |
| $T_s$ | Temperature of the wooden surfaces | K |
| u,v,w | Velocity components in the direction of x,y,z respectively | m/sec |
| $V_{safe}$ | Safe voltage across the heater coil | volts |
| W | Width of the enclosure | m |
| x,y,z | Spatial coordinates | |
| $X_{COR}$ | Longitudinal side of the test section of the corrugated plate | mm |

| $X_{COLD}$ | Longitudinal side of the cold flat plate | mm |
| $\Delta X$ | Thickness along x direction | in |
| $Y_{COR}$ | Lateral side of the test section of the corrugated plate | mm |
| $Y_{COLD}$ | Lateral side of the cold flat plate | mm |

**GREEK ALPHABET:**

| $\alpha$ | Thermal diffusivity. $k/\rho C_p$ | $m^2/sec$ |
| $\beta$ | Volumetric thermal expansion coefficient. $1/T_f$. | 1/K |
| $\Delta$ | Difference | |
| $\varepsilon$ | Long wave emmissivities | dimensionless |
| $\varepsilon_H$ | Hemispherical emittance | dimensionless |
| $\varepsilon_s$ | Long wave emmissivities of the wooden surfaces | dimensionless |
| $\Theta$ | Tilt angle of inclination of the enclosed air layers with the horizontal | degrees |
| $\nu$ | Kinematic viscosity of the convecting fluid (air) | $m^2/sec$ |
| $\rho$ | Density | $kg/m^3$ |
| $\sigma$ | Stefan Boltzman's constant $[=5.67 \times 10^{-8}]$ | Watt/$m^2$ $K^4$ |
| $\phi$ | Phase angle of the current | degree |

# CHAPTER 1

# INTRODUCTION

## 1.1    General

Natural convection is the result of the motion of the fluid due to density changes arising from a heating process. The movement of fluid in natural convection results from the buoyancy forces imposed on the fluid when its density in the proximity of the heat transfer surface is decreased as a result of a heating process. Buoyancy is due to the combined presence of a fluid density gradient and a body force. The body force is usually gravitational, although gravity is not the only type of force field which can produce the natural-convection currents; a fluid enclosed in a rotating machine is acted upon by a centrifugal force field, and thus could experience natural-convection currents if one or more surfaces in contact with the fluid were heated. There are several ways in which a mass density gradient may arise in a fluid but in the most common situation it is due to the presence of a temperature gradient. The density of gases and liquids depends on temperature, generally decreasing due to fluid expansion with increasing temperature.

Natural convection currents transfer internal energy stored in fluid elements in the same manner as forced convection currents. However the intensity of mixing is generally less in natural convection and consequently the heat transfer co-efficients in natural convection are lower than those in forced convection. The analysis of heat transfer by convection is complicated by the fact that the motion of the fluid plays an important role in heat transfer. The temperature distribution in natural convection depends on the intensity of the fluid currents which is really depended on the temperature potential itself. So the qualitative and quantitative analysis of natural convection heat transfer are quite difficult. For this reason the theoretical analysis of natural convection heat transfer for most of the practical situations is absent in the literature. So, at this present stage the necessity of the experimental investigation is seriously felt.

1

## 1.2    Natural Convection in an Enclosure

A large number of engineering applications frequently involve heat transfer between surfaces that are at different temperatures and are separated by an enclosed fluid. These applications span such diverse fields as solar energy collections, nuclear reactor operation and safety, the energy efficient design of buildings, rooms and machinery, waste disposal and fire prevention and safety, also cooling of microelectric components. The surfaces may be plane horizontal or vertical or inclined.

Recently the heat transfer characteristics for non-plane [Vee, sinusoidal rectangular & trapezoidal corrugated] horizontal as well as inclined fluid layers have been reported. The main feature of these types of natural convection heat transfer problems is that the boundary layer thickness, if there be any, is comparable with the dimensions of the enclosed fluid layers.

### 1.2.a    Horizontal Fluid Layers

In fluids whose density decreases with the increasing of temperature, no natural convection currents occur in such a fluid which is enclosed between two parallel horizontal plates as long as the temperature of the upper plate is higher than the temperature of the lower one. In that case heat will be transferred only by conduction. The situation is different when a fluid is enclosed between two horizontal surfaces of which the upper surface is at lower temperature than the lower one. For fluids whose density decreases with increasing temperature leads to an unstable situation. Benard [1900] mentioned this instability as a "top heavy" situation. In that case fluid is completely stationary and heat is transferred across the layer by the conduction mechanism only. Rayleigh [1916] recognized that this unstable situation must break down at a certain value of Rayleigh number above which a convective motion must be generated. Jeffreys [1928] and Low [1929] calculated this limiting value of $Ra_L$ to be 1708, when the air layer is bounded on both sides by solid walls. With the optical investigation in a trough filled with water carried out by Schmidt and Saunders [1938] this limiting value [$Ra_L = 1708$] also has been confirmed. Above this critical value of $Ra_L$ a peculiar natural convection flow pattern arises. The flow field becomes a celluler structure with more or less regular hexagonal cells. In the interior of

2

these cells the flow moves in an upward direction and along the rim of the cells it returns down. According to Ostrach [1957] when the top and the bottom surfaces are rigid, the turbulence first appears at $Ra_l = 4380$ and the flow becomes fully turbulent at $Ra_l = 4500$ for plane horizontal air layers but at lower values of $Ra_l$ for water with same boundaries.

## 1.2.b        Inclined Fluid Layers:

The convective motion of an inclined fluid layer heated from below is more or less similar to horizontal fluid layer. Purely convective motion is gained after decaying of two distinct flow regimes – conductive regime and postconductive regime. At very small Rayleigh number the motion is relatively simple. It consists of one large cell which fills the whole slot, the fluid rising from the hot wall, falling down the cold wall and turning at the opposite ends of the slot. This flow pattern is known as base flow according to Ayyaswamy [1973]. The heat transfer in this flow regime is purely conductive [i.e., Nu = 1] except at the extreme ends where there is some convective heat transfer associated with the fluid turning. For air this conductive regime exists if the Rayleigh number is less than a critical value $Ra_c$. This limit has been defined by Buchberg et al. [1976] as follows:

$$Nu = 1 \quad \text{for } Ra_l < 1708/Cos\Theta$$
$$\text{i.e., } Ra_c = 1708/Cos\Theta$$

At $Ra_c$, the base flow becomes marginally unstable and the resulting flow begins to take the form of steady longitudinal rolls i.e., rolls with their axis along the upslope.

At $Ra_l \gg Ra_c$, the flow becomes convective. The resulting flow begins to take the boundary layer structure with the resistance to heat transfer lying exclusively in two boundary layers, one on each of the boundary surfaces.

## 1.3    Motivation Behind the Selection of the Problem:

Most works have addressed natural convection in rectangular geometries in horizontal or vertically imposed heat flux of temperature difference. Little work has been carried out in which the conditions are neither horizontal nor vertical.

Natural convective heat transfer across inclined fluid (air) layer heated from below is of importance in many engineering applications. It is of particular importance in flat-plate collectors where it can constitute the main mode of heat loss. Solar engineers are concerned about natural convection heat loss from the absorber plate of the flat plate solar collector to the adjacent flat glass covers. The efficiency of the collector among other things increases with the decreasing of heat loss through the cover plates. Generally the absorber plate is made flat. Several studies have proved the advantageous effect of vee corrugated absorber plate. Investigation carried out by Arnold et al. [1978], Buchberg et al. [1976], Graff et al. [1953], Difederico et al. [1966], Dropkin et al. [1966, 1965, 1959], Hart et al. [1971], Hollands et al. [1976, 1975, 1973, 1965], Koschmieder et al. [1974], O'Toole et al. [1961] and Schluter et al. [1965] have already discussed the natural convection heat transfer across air layer bounded by two parallel flat plates at different angles of inclination, including $\Theta = 0^0$, Elsherbiny et al. [1977] the natural convection heat transfer from a hot vee corrugated plate to a cold flat plate.

Kabir [1988] reported results on natural convection heat transfer from a hot sinusoidal corrugated plate to a cold flat plate for different aspect ratios and different angles of inclination including horizontal.

Feroz [1992] reported results on natural convection from hot trapezoidal and rectangular corrugated plates to a flat plate for different aspect ratios and different angles of inclination.

Works were reported on natural convection heat transfer across air layer in an enclosure bounded by two flat plates, from a hot vee corrugated plate to a cold flat plate, from a hot sinusoidal plate to a cold flat plate, also from hot trapezoidal and rectangular corrugated plates to a cold flat plate. But no work is reported on natural convection heat transfer from hot square corrugated plates to a cold flat plate. In previous works no report has focused attention on the variation of natural convection with the variation of amplitude of corrugation. Hence through the present investigation an effort has been made to fill up the existing gap in the information on natural convection heat transfer.

4

## 1.4   The Present Study:

Previously no work has reported the variation of natural convection with the variation of amplitude of corrugation. So, the present study is an experimental investigation on the natural convection heat transfer rate from hot square corrugated plates to a cold plate with air as the working fluid. The geometry and dimensions of the corrugated plates tested are reported in figure 3.1 from the sketch of the inclined air layer bounded by square corrugated plate and flat plate.

**Main objectives of the present work were:**

a.   To determine the average natural convective heat transfer co-efficients [h].

b.   To determine the dependence of average heat transfer co-efficient on aspect ratio [A].

c.   To study the variation of average heat transfer co-efficient with the angle of inclination [Θ] of the corrugated plate with the horizontal.

d.   To observe the variation of average heat transfer co-efficient with different thermal potential [ΔT].

e.   To observe the variation of natural convection with the variation of amplitude H of corrugation.

f.   To compare the results of this study with earlier relevant investigations.

g.   To develop possible correlations which will correlate all the experimental data within reasonable limit.

Here to meet the above objectives, experimental set-up of Kabir [1988] was redesigned and modified for the present investigation. Supply of power to the experimental rig by electric heater was varied by using a Variac with the variation of aspect ratio to keep a particular constant thermal potential [ΔT]. The cold flat plate was cooled by continuous water circulation. In the fabrication of hot plate assembly, square corrugated plates of different depths (amplitudes) were fabricated from G.I. Sheets.

The aspect ratio was varied between 1.40 and 9.5 by changing the mean plate spacing [L]. The angle of inclination covered was between $0^0$ and $75^0$ and the range of temperature difference in the experiment was in between $10^0$C and $35^0$C.

5

The Rayleigh number covered in this study was:

$$3.294 \times 10^4 \leq Ra_L \leq 1.881 \times 10^6$$

Correlation in the form of $Nu_L = C [Ra_L Cos\Theta]^D [A]^E$ was developed. The results obtained in the present study are compared with other studies related to the problem under investigation, in the form of plots and percentage variation.

# CHAPTER 2

# LITERATURE REVIEW

## 2.1 General:

Natural convection heat transfer through a layer of air bounded by two parallel plates heated from below is important in numerous engineering problems. Specially the natural convection heat loss across an inclined air layer is of interest to the designers of solar collectors, because any reduction of heat loss from the absorber plate through the cover plates improves the efficiency of the collector. A large number of engineering applications frequently involve heat transfer between surfaces that are at different temperatures and are separated by an enclosed fluid. These applications span such diverse fields as solar energy collections, nuclear reactor operation and safety, the energy efficient design of buildings, rooms and machinery, waste disposal and fire prevention and safety, also on cooling of microelectric components. The surfaces may be plane horizontal or vertical or inclined.

Natural convection currents occur in a fluid enclosed between two parallel horizontal plates if the temperature of the lower plate is higher than that of the upper one. For fluids whose density decrease with the increasing temperature, an unstable state, named as 'top heavy', is observed at a very small Rayleigh number. In this state, the fluid is completely stationary and heat is transferred across the fluid layer by a conduction mechanism. This unstable state breaks down at a certain critical value of Rayleigh number [which depends on the boundary conditions].

At $Ra_c$, the unstable state becomes marginally unstable as any disturbance in the fluid will result in fluid motion with no dampening. This flow state is known as postconductive state. It is laminar and has nearly a hexagonal cell structure. The flow moves upward in the interior of these cells and returns downward along its rim.

At $Ra_t$ >> $Ra_c$, the flow becomes convective with the breaking down of laminar flow into turbulent flow. The resulting flow begins to take the boundary layer structure in which the resistance to heat transfer lie exclusively in two boundary layers on the two boundary surfaces.

## 2.2    Natural Convection Heat Transfer In Plane Horizontal Fluid Layers:

In most researches heat transfer in confined spaces have been carried out with the parallel plates in a horizontal position. A considerable number of experiments have been conducted on air, on water and on oil and the results have been reported by investigators.

An experimental investigation performed by Thomson [1882] on natural convection heat transfer through a layer of soapy water between horizontal plates heated from below. He noted the presence of cellular patterns in soapy water whose mean temperature was greater than the ambient. Benard [1900] also performed similar experimental investigation but his working fluid was paraffin oil and published photographs taken with a beam of parallel light which had passed through the layer of this paraffin oil. Those photographs clearly indicated the presence of a hexagonal cellular convection patterns. Sterling and Scriven [1964] concluded that the cellular convection patterns observed by Thomson and Benard were caused by surface tension rather than by thermal gradient.

8

Most elaborated experiment performed by Mull and Reiher [1930] on free convection heat transfer in horizontal air layer, who presented their experimental results by plotting $K_e/K_c$ versus $Gr_L$ and obtained a smooth curve in the range of $2.1 \times 10^3 < Gr_L < 8.89 \times 10^6$. They assumed $K_e$ as an equivalent thermal conductivity considering the effect of conduction, convection and radiation i.e., $K_e = K_c + K_r$, where $K_c$ is an equivalent thermal conductivity taking into effects both conduction and convection, and Kr an equivalent thermal conductivity for radiation. Jakob [1946] plotted the data of Mull and Reiher in log-log coordinates and showed that there is at least one point of inflection in the curve and finally developed the following correlations:

$$Nu = 0.195 [Gr_L]^{1/4}; \qquad \text{for } 10^4 < Gr_L < 4 \times 10^5$$
$$= 0.068 [Gr_L]^{1/3}; \qquad \text{for } Gr_L > 4 \times 10^5$$

Hollands, et. al. [1974] carried out an experimental investigation on natural convection through an air-layer between two parallel copper plates, heated from below. They performed their experiment by varying pressure from 10 Pa to 700 KPa by inserting the plates in a pressure vessel. Actually the variation in $R_a$ over a wide range without altering the plate spacing or the temperature difference between the plates was attained through the variation of pressure. Tests were carried out at mean plate spacings of 10mm, 25mm and 35mm covering the range of Ra from subcritical to $4 \times 10^6$. They reported that when their data along with the data of Chu and Goldstein [1969] for air were analysed, the value of the index for Ra were the same as one-third [1/3] while Chu and Goldstein for their data found that:

$$Nu \propto [Ra_L]^{0.294} \qquad \text{[air]}$$
$$Nu \propto [Ra_L]^{0.278} \qquad \text{[water]}$$

Rossby [1969] also reported different power law for different Prandtl number fluids as follows:

Nu   $\alpha$   $[Ra_L]^{0.281}$;   for silicon oil [Pr = 11600]

Nu   $\alpha$   $[Ra_L]^{0.257}$;   for mercury [Pr = 0.025]

O' Toole and Silveston [1961] developed the correlation equations for natural convection heat transfer across horizontal fluid layers by taking all the data available in the literature at that time. On the basis of $Ra_L$ they differentiated the flow into the following three regions:

Initial region       :    $1700 < Ra_L < 3500$

Laminar region       :    $3500 < Ra_L < 10^5$

Turbulent region     :    $10^5 < Ra_L < 10^9$

They also developed the following correlations:-

Nu = 0.229 $[Ra_L cos\Theta]^{0.22}$;     $5900 < Ra_L cos\Theta < 10^5$

Nu $\alpha$ $[Ra_L]^{0.305}$;              for turbulent region

A number of investigators have also reported the 1/3 power law of dependency of Nusselt number on Raleigh number. Mulkus [1963] and Globe et. al [1959] also found the asymptotic behaviour of Nusselt number and obtained Nu $\alpha$ $[Ra_L]^{1/3}$. Through numerical solution of the governing differential equations Herring [1965, 1964] also predicted Nu $\alpha$ $[Ra_L]^{1/3}$ by neglecting the non-linear interaction terms.

## 2.3 Natural Convection Heat Transfer In Plane Inclined Fluid Layer:

Natural convection in inclined layers of fluid heated from below and cooled from above has received extensive attention owing to its importance in engineering applications, including solar heating, nuclear reactor operation and safety, energy efficient design of buildings, machinery and cooling of microelectronic components.

Investigation was carried out by Graaf et. al. [1953]. They performed measurements on heat transfer rate for the angles of inclination ranging from $0^0$ to $90^0$ in $10^0$ steps and covered the range, $10^3 < Ra_L \cos\Theta < 10^5$.

Dropkin et. al. [1965] performed an experimental investigation of natural convection heat transfer in liquids [water, silicon oils and mercury] confined in two parallel plates, inclined at various angles with respect to the horizontal. They carried out their experiments in rectangular and circular containers having copper plates and insulated walls and covered the range, $5 \times 10^4 < Ra_L < 7.17 \times 10^8$ and $0.02 < Pr < 11560$. They got the following correlations:

$$Nu = C \, [Ra_L]^{1/3} \quad [Pr]^{\,0.074}$$

where the constant C is a function of the angle of inclination. It varies from C = 0.069 for the horizontal plates to C = 0.049 for vertical plates.

Ayyaswamy et. al. [1974] carried out a theoretical investigation on natural convection heat transfer in an inclined rectangular region and their results were limited to $0^0 < \Theta < 120^0$, $0.2 < A < 20$ and Ra up to $10^6$. But Ayyaswamy et. al.

[1973] investigated the boundary layer domain and observed that:

$$Nu_{(\theta)} = Nu_{(\theta=90^0)} \; [\sin\Theta]^{1/4}; \; 0^0 < \Theta < 110^0$$

Hollands et. al. [1975] performed an experimental investigation on free convection heat transfer rates through inclined air layers of high aspect ratio (AR), heated from below. The covered range of Rayleigh number was from subcritical to $10^5$ and angle of inclination was $0^0 \leq \Theta < 70^0$. They gave the following correlation:

$$Nu = 1 + 1.44 \; [1-1708/Ra_L \; \cos\Theta]^*$$
$$[1 - (\sin 1.8\Theta)^{1.6} \times 1708/Ra_L \; \cos\Theta] +$$
$$[(Ra_L \; \cos\Theta)^{1/3}/(5830^{1/3}) - 1]^*$$

$[^*$ denotes that when the arguments inside the bracketed terms become negative, the value of bracketed terms must be taken as zero].

Computation of natural convection heat transfer characteristics of flat plate enclosures, using interferometric techniques, was carried out by Randall et. al. [1977]. The effects of Grashof number, tilt angle and aspect ratio on both the local and average heat transfer co-efficient were determined. The Grashof number range tested was $4 \times 10^3$ to $3.1 \times 10^5$ and the aspect ratio, defined as the ratio of enclosure length to plate spacing, varied between 9 and 36. The angles of inclination of the enclosure were $45^0$, $60^0$, $75^0$ and $90^0$. They reported that the average heat transfer rate at an angle of inclination of $90^0$ decreased by 18% from that at $45^0$ and developed the following correlation:

$$Nu_L = 0.118 \; [Gr_L \; Pr \; \cos^2 (\Theta-45)]^{.29}$$

## 2.4 Natural Convection Heat Transfer In Vee Corrugated Enclosure:

Experimental investigations on natural convection heat transfer from a horizontal lower vee corrugated plate to an upper cold flat plate for Rayleigh number from $7 \times 10^3$ to $7 \times 10^5$ were first carried out by Chinnappa [1970]. The vee angle was $60^0$ and aspect ratios were 0.64, 0.931, 0.968, 1.1875 and 1.218. Experimental fluid was air in all the test runs. The following correlations were obtained:

$Nu_L = 0.54 [Gr_L]^{0.36};$ $\qquad 7 \times 10^3 < Ra_L < 5.6 \times 10^4$

$Nu_L = 0.139 [Gr_L]^{0.278};$ $\qquad 5.6 \times 10^4 < Ra_L < 7 \times 10^5$

Elsherbiny et. al. [1977] investigated free convection heat transfer in air layers bounded by lower hot V-corrugated plate and upper cold flat plate for Rayleigh number $10^4 < Ra_L < 4 \times 10^6$ and angle of inclination 0, 30, 45 and 60 degrees. The V-angle was 60 degree and aspect ratios were 1.0, 2.5 and 4.0. Experimental fluid was air in all test runs. He found that the convective heat transfer across air layers bounded by V-corrugated and flat plates was greater than those for two flat parallel plates upto a maximum of 50%.

The correlation given by them was as follows:

$Nu = Nu_c + K [1 - Ra_c/Racos\Theta]^* [Ra_c (sin 1.8\Theta)^{1.6}/Ra cos\Theta$

$\qquad + B [(Ra cos\Theta)^{1/3}/(3377)^{1/3}) - F]^*$

where,

| | | |
|---|---|---|
| $Ra_c$ | $=$ | $1708 + 945/(A-0.5)^{0.923}$ |
| $K$ | $=$ | $1.44 [ 1-1.15/A + 6.74/A^2 - 5.28/A^3]$ |
| $B$ | $=$ | $1.33/cos (\Theta-23.5)$ |
| $F$ | $=$ | $1.515-3.417 \times 10^{-2}\Theta + 1.289 \times 10^{-3}\Theta^2 - 1.158$ |
| | | $\times 10^{-5} \Theta^3$ |

$\Theta$ is in degrees and the asterisk brackets go to zero when the arguments inside them are negative.

Randall [1977] studied the average heat transfer co-efficients for natural convection between a V-corrugated plate and a parallel flat plate. He used interferometric techniques to find out the temperature distribution in the enclosed air space. From this temperature distribution he found the wall temperature gradient and hence estimated the local heat transfer co-efficient. The measurements were carried out for $10^3 < \text{Gr} < 3 \times 10^5$. The vee angle was $60^0$ and aspect ratios were 0.75, 1 and 2, angle of inclination were $0^0$, $45^0$ and $60^0$. Finally the following correlation was obtained:

$$\text{Nu} = C \ \text{Gr}_L^n.$$

where,

| 0 | A | C | n |
|---|---|---|---|
| $0^0$ | 0.75 | 0.060 | 0.41 |
| | 1.0 | 0.060 | 0.41 |
| | 2.0 | 0.043 | 0.41 |
| $45^0$ | 0.75 | 0.75 | 0.36 |
| | 1.0 | 0.082 | 0.36 |
| | 2.0 | 0.037 | 0.41 |
| $60^0$ | 0.75 | 0.162 | 0.30 |
| | 1.0 | 0.141 | 0.30 |
| | 2.0 | 0.027 | 0.42 |

## 2.5 Natural Convection Heat Transfer In Sinusoidal Corrugated Enclosures:

The experimental investigation on the natural convection heat transfer from a lower horizontal sinusoidal corrugated plate to an upper cold flat plate for a range of Rayleigh number $5.50 \times 10^3$ to $2.34 \times 10^6$ and angle of inclination [$\Theta$],

from $0^0$ to $75^0$ was carried out by Kabir [1988]. The sinusoidal leading angle was $72^0$ and aspect ratios covered were 2.0 to 5.75. Experimental fluid was air in all the test runs. Finally the following correlation was obtained.

$$Nu_L = 0.0132 \, [Ra_L \, cos\Theta]^{0.51} \, [A]^{-0.35}$$

The above equation correlates all the experimental data within ± 10% and is valid for $5.56 \times 10^3 \leq Ra_L \leq 2.3 \times 10^6$, $2.0 \leq A \leq 5.75$ and $0^0 \leq \Theta \leq 75^0$.

## 2.6    Natural Convection Heat Transfer In Rectangular and Trapezoidal Corrugated Enclosures:

The experimental investigation on the natural convection heat transfer from a lower horizontal Rectangular and Trapezoidal corrugated plates to an upper cold flat plate for a range of Rayleigh number $9.84 \times 10^4 \leq Ra_L \leq 2.29 \times 10^6$ and angle of inclination [$\Theta$] from $0^0$ to $75^0$ was carried out by Feroz [1992]. The aspect ratios covered were $2.6 \leq A \leq 5.22$. Experimental fluid was air in all test runs. Finally the following correlations were developed.

$$Nu_L = 0.0112 \, [Ra_L Cos\Theta]^{0.521} \, [A]^{-0.4546} . [\text{Trapezoidal corrugation}] \quad Nu_L = 0.0102 \, [Ra_L Cos\Theta]^{0.530} \, [A]^{-0.4923} . [\text{Rectangular corrugation}]$$

Both of these correlations correlate data to ± 15%.

# CHAPTER 3

# THEORY

## 3.1 Description of the Problem:

Natural convection heat transfer in an inclined rectangular enclosure is a function of temperature difference between the hot and cold plates, boundary conditions, angle of inclination of the enclosure with the horizontal and the properties of confined convective fluid. Also the natural convection heat transfer is a function of geometry of the hot plate, which is the basis for sketching the present problem of variation of natural convection from hot square corrugated plate to a cold flat plate.

The present investigation in rectangular region was carried out with three sets of bottom hot square corrugated plates having amplitude of 10mm, 15mm and 25mm. In all cases the upper cold plate was flat. The convective fluid was air. The side walls of the enclosure were made adiabatic and flat.

In the present experimental setup the spacing between the hot and cold plate was varied to get different aspect ratio `A' defined as the ratio of mean plate spacing to amplitude of corrugation. The vertical side walls of the enclosure and the bottom hot corrugated plates were maintained at the same temperature. Also the upper wall of the lower guard heater assembly was maintained at the temperature same as that of lower hot corrugated plate. At steady state the heat flux [q"] to the cold flat plate was by conduction, convection and radiation. But

for Rayleigh numbers well above the critical value, conduction heat transfer was considered insignificant. So total heat flux, q" had two components. Convection heat flux, $q_{conv}$" and radiation heat flux qr". In case of a fixed temperature potential ($\Delta$T) the radiative heat flux becomes constant and the convective heat transfer varies on aspect ratio 'A' and angle of inclination of the enclosure. The radiative heat-flux, $q_r$" was calculated by using the formula drived in Appendix-A by considering hot corrugated plate and cold flat plate behaved as black bodies. The convective heat flux $q_{conv}$" was calculated by substructing the value of $q_r$" from the total heat flux, q". Heat flux from the hot corrugated plate was calculated by measuring the current and the voltage supply of the main heater. In this chapter article 3.2 describes the mathematical equations required for calculating $q_r$", $q_{conv}$" and natural convective heat transfer co-efficient [h].

## 3.2 Mathematical Equations:

The mathematical equations that were used to calculate h, $Nu_L$ and $Ra_L$ are given below:

$$q_r" = \sigma.\varepsilon_{COR}. [(T_{COR})^4 - (T_{COLD})^4] \qquad [3.1]$$

$$q" = VIcos\phi/A_{COR} \qquad [3.2]$$

$$h = [q" - q_r"]/[T_{COR} - T_{COLD}] \qquad [3.3]$$

$$Nu_L = h.L/K \qquad [3.4]$$

$$Ra_L = g.\beta [T_{COR} - T_{COLD}] . L^3/\nu.\alpha \qquad [3.5]$$

All properties of air were evaluated at film temperature, $T_f$ where,

$$T_f = [T_{COR} + T_{COLD}]/2$$

17

# CHAPTER 4

# EXPERIMENTAL SET-UP

**4.1    General Description of the Set-up:**

The experimental set-up made up by Kabir (1988) was redesigned to meet the requirements of the present experiment. The details of the experimental set up and test section is shown in figures 4.1 and 4.2. There is a provision for the experimental set up to incline by an alignment plate in the range, $0^0$ to $90^0$ at a step of $15^0$. The air gap depth was varied by changing the position of the cold plate in relation to the hot plate from 35mm to 95mm. Experimental hot plate assembly was heated by the main electric heater sandwiched in between the hot corrugated plates by supplying a constant voltage from the voltage stabilizer. The guard heater assemblies were also heated by electric heaters sandwiched in between the inner and the outer wooden strips. The cold flat plate was placed above the hot corrugated assembly by four vertical clamps, fixed on the upper guard heater. This cold plate assembly was cooled by passing a steady flow of cooling water from the overhead tank, where the head of overhead tank was kept constant. A digital milli-voltmeter was used to measure the temperature of the test section of the hot plate and cold plate through thermocouples no. 1 to 9 and 37 to 41 respectively. It was also used to monitor the surface temperatures of the guard heater assemblies through 27 Chromel-Alumel thermocouples. To obtain the total heat input to the experimental test section of the hot plate, the input current to the corresponding heater [main heater] was measured by a digital ammeter and the voltage across the main heater was measured by a precision digital voltmeter.

## 4.2    The Test Section

The test section consisted of

a.     The hot plate assembly

b.     The outer guard heater assembly

c.     The cold plate assembly

d.     The alignment plate and supporting  frame.

### 4.2.1        The Hot Plate Assembly

The main section of the hot plate assembly is the test section. The hot plate assembly was made of G.I. sheets having three different amplitudes of square corrugation i.e. 10mm, 15mm and 25mm, with total dimension of 456mm X 534mm. An asbestos cloth of 12mm thick was placed on the upper side of the lower corrugated plate to insulate it electrically from the electrical heaters placed on this asbestos cloth ( Fig. 4.3 ). Another asbestos cloth was placed over the heaters to make the upper corrugated plates of the assembly well insulated from the sandwiched electrical heaters. There were three heaters on the hot plate assembly. One was used to heat the experimental test section and the other two heaters were used as end and side guard around the test section. These guard heaters were provided to reduce the end conduction losses from the experimental hot plate to a minimum level. For this purpose these guard heater sections were separated from the experimental hot plate section by cutting the top corrugated plate into five pieces forming separate guard heater sections and the central experimental test section. The test section was 152mm X 230mm; 152mm across the corrugation and 230mm along the corrugation.

19

The end and side guard heater sections were 152mm wide on all the sides of the experimental hot plate section. Thus the over all dimensions of the hot plate assembly was 456mm X 534mm. This hot plate assembly was placed inside a rectangular ring of 483mm X 560mm. The rectangular ring was made of 76mm wide and 19.05mm thick wooden strip. Details of the hot plate assembly have been shown in figure 4.3 and details of design and fabrication process of the heaters are given in the Appendix-A.

The outer surfaces of both the test section, end and side guard heater section were painted black with dull black plastic paint. The test section was separated from both the end and side guard sections by asbestos powder to reduce conduction loss.

## 4.2.2      The Outer Guard Heater Assembly:

The main feature of the outer guard heater assembly is to isolate the test hot plate section thermally from the surrounding surfaces except from the top. This assembly mainly consisted of upper guard heater ring and lower guard heater box. The heat input was varied by using variacs – 4, 5 and 6 to maintain the temperature difference between the test hot plate and its surrounding surfaces zero. Under this condition all the heat input to the experimental hot plate section would be transferred by conduction, convection and radiation only to the cold flat plate which was placed above the hot plate.

### 4.2.2a    The Upper Outer Guard Heater Ring:

The upper outer guard heater ring was a rectangular shaped structure which consisted of the following sections:

a.    Inner wooden rectangular ring

b.    Inner asbestos rectangular ring

c.    Outer asbestos rectangular ring

d.    Outer wooden rectangular ring

The inner wooden rectangular ring in which the test section was placed having a dimension of 483mm x 564mm. The inner and outer wooden rings were held together with a 579mm X 660mm outside dimension, 12mm thick and 48mm wide wooden annular ring at the top of the upper guard heater assembly. The height of the upper guard heater assembly was 139mm. The inner and outer asbestos rectangular rings were fitted inside the annular space between the outer and inner rectangular wooden rings. The outer asbestos ring 127mm wide was fitted inside the outer wooden ring and the inner asbestos ring of the same width was fitted outside the inner wooden ring. The heater was made by wrapping 29 SWG Nichrome wire on the mica sheet sandwiched in between the inner and the outer asbestos ring. The capacity of the heater was 105 Watt. A cross section of the upper outer guard heater assembly is shown in figure 4.4. Both the outside and inside surfaces of the upper guard heater ring was painted with dull black plastic paint.

21

### 4.2.2b    The Lower Outer Guard Heater Box:

The lower outer guard heater box was rectangular in shape and consisted of the following sections:

a.    Inner wooden rectangular box

b.    Inner asbestos rectangular box

c.    Outer asbestos rectangular box

d.    Outer wooden rectangular box

The inner wooden rectangular box over which the hot plate assembly was placed was of 483mm x 564mm x 16mm in inside dimension. The outer wooden box having outside dimension of 579mm X 660mm X 76mm was made of 12mm thick wooden strip. The outside dimension of the inner wooden box was 507mm X 588mm X 40mm. The outer asbestos box having dimension of 555mm X 636mm X 64mm was fitted the inner surface of the outer wooden rectangular box and the inner asbestos box having dimension of 531mm X 612mm X 52mm was fitted over the outer surface of the inner wooden box i.e. over the inner surface of the outer asbestos box. Two separate Nichrome heaters were sandwiched in between the inner and the outer asbestos rings, one was lower bottom guard heater and the other was lower side guard heater. A cross section of the lower outer guard heater assembly is shown in figure 4.5. The outer surfaces of the outer wooden rectangular box was painted black with dull black plastic paint.

### 4.3.2 The Cold Plate Assembly:

The cold plate assembly was a sealed 550mm X 470mm X 19.05mm rectangular box made of 3.175mm thick mild steel plates painted with dull black plastic paint. Provision of water circulation was made from a reserve tank through inlet and outlet connections. The outlet and inlet connections were placed on the upper surface of this box. The flat bottom surface of this assembly, facing the corrugated plate was acting as a receiver of heat that was convected and radiated from the hot corrugated plate. The whole cold plate assembly was placed above the hot corrugated plate and held by the vertical clamps, fixed on the upper outer guard heater assembly. These clamps had arrangements to change the spacing between the hot corrugated plate and the cold flat plate from 19.5mm to 109.5mm in steps of 10mm. The cold plate assembly is shown in figure 4.6.

### 4.2.4 The Alignment Plate and Supporting Frame:

The hot and the cold plate assembly along with the guard heaters were placed inside of a rectangular frame made of 38.1mm X 38.1mm X 6.35mm mild steel angle on the two side supports of this frame, each of them is attached with the plate assembly by means of two bolts. Another two bolts were fixed at the centre of the two opposite longitudinal sides of the frame and passed through the holes of the side supports so that the frame and the plate assembly with the guard heaters could swivel about a horizontal axis i.e. the lateral axis of the hot plate through these bolts. The rectangular frame is shown in figure 4.7.

Two circular disc of mild steel having diameter of 102mm and thickness of 6.35mm namely as alignment plates were connected at the centre of the two opposite lateral sides of the rectangular frame by means of two screws passed through 6.5mm diameter holes located on each disc at 40mm apart and the holes of the two 57mm X 57mm hanging side supports made of 6.35mm thick mild steel sheet that were welded with the supporting frame at its centre. These discs had also several holes of diameter 6.5mm along a circle of radius 38mm. The angle of inclination of the test section was varied by means of these holes by changing the inclination angle from $0^0$ to $90^0$ in steps of $15^0$. One of the alignment plate is shown in figure 4.8.

A supporting stand consisting of two pairs of legs 915mm apart connected by a flat mild steel bar. The height of this stand was 460mm. The rectangular frame along with the two alignment plates was connected with this stand at the top centre of its legs by means of two bolts passed through the 16mm diameter central holes of the alignment plates and the two holes located at the centre of the two lateral sides of the frame so that the frame and the plate assembly with the guard heaters could also swivel about a horizontal axis i.e. the longitudinal axis of the hot plate. The connection between the rectangular frame and the supporting stand is shown in figure 4.9.

The angle of inclination of the test section of the hot corrugated plate could set at a desired value by means of two screws passed through the corresponding peripheral holes of diameter 6.5mm of the alignment plates as mentioned above and the two holes 76mm apart located at the top of the two legs of the supporting stand. The supporting stand is shown in figure 4.10.

24

## 4.3    The Reserve Water Tank:

The reserve water tank was an overhead tank– a simple cylindrical drum made of galvanized iron sheet. The water level in the tank was kept constant during experiments by controlling the water flow using the inlet and outlet valves of this tank. The cold plate assembly was cooled by passing a steady flow of cooling water from this tank through rubber pipes of 12.5mm dia.

## 4.4    Instrumentation:

There were provisions for measuring angle of inclination, air gap between the hot and the cold plates and the temperature at different points of the experimental set–up in the present investigation. There were five variacs and one stabilizer to supply regulated voltage at different sections of the experimental set up. Each variac had graduated scale on it to measure the voltage supplied to heaters. Also the voltage supplied and current by the stabilizer to the test section was measured by a precision Normameter MP–14. Again the details of the instrumentation and measurement procedure is depicted in detail in chapter 5.

# CHAPTER 5

# EXPERIMENTAL MEASUREMENTS
# AND
# TEST PROCEDURE

## 5.1    Temperature Measurement

The accuracy of the value of natural convection was dependent on the accuracy
of the measurement of temperature and input power (voltage and current value).
For this reason, precision instruments were used. Temperature at different
sections of the experimental set-up were measured by fortyone 36 SWG Chromel-
Alumel thermocouples connected to a millivoltmeter of MP-12 having a range of −
$50^0$C to $750^0$C [for K type] to show the temperature directly through two selector
switches each having 24 points. Out of these, nine thermocouples of no. 1 to 9,
were fixed on the bottom surface of the test section of the hot corrugated plate
and five thermocouples of no. 37 to 41, were fixed on the bottom surface of the
cold plate facing the corrugated plate and the rest were fixed on the guard
heater sections. The positions of thermocouples are shown in figures 5.1 to 5.5.
These thermocouples were calibrated in between $0^0$ (melting ice temperature) and
$100^0$C (saturated steam temperature). There was a maximum variation of 0.10%
between the actual and the standard reading within the working range of the
experiment. The calibration curve for thermocouple no. 5 is shown in figure 5.6.

For greater accuracy the temperature of the exposed top surface of the
experimental hot corrugated plate $[T_{COR}]$ was determined after necessary
conduction correction. Appendix B contains the outline of the procedure for
calculating the conduction correction.

## 5.2    Heat Flux Measurement

Amount of heat supplied per unit area of the test section through heater was the heat flux. Heat flux from the hot corrugated plate was calculated by measuring the current and the voltage supply to the main heater.

A digital voltmeter of model Normameter MP-14 was employed to measure the voltage across the stabilizer which supplied the necessary heat to the test section of the hot plate assembly. The voltmeter had the range of 0-750 volts.

A digital ammeter of model Normameter MP-14 was employed to measure the current supplied to the test section of the hot plate. This ammeter had the range of 0 to 10 amps.

## 5.3    Test Procedure

Three sets of corrugation having different amplitudes (H = 10mm, 15mm, 25mm) of corrugation were used. For all sets temperature difference [$\Delta$T], angles of inclination of the air layer [$\Theta$] and the air gaps [L] were measured. The experimental fluid was air at atmospheric pressure. Experiments were carried out under steady state condition. The experiment was carried out first using corrugation having H = 10mm, then on H = 15mm and then on H = 25mm. The test was carried out according to the following procedures:

a.    Before starting the experiment the room temperature was recorded for selecting $T_{COR}$ to maintain a steady $\Delta$T [say, $\Delta T = T_{COR} - T_{COLD} = 10^0C$] since $T_{COLD} = T_{ROOM}$.

b.    The spacing between the hot corrugated plate and the cold flat plate was measured as the distance between the bottom surface of the cold plate and the mid section of the troughs and crest of the corrugated plate [Fig. 4.2]. The spacing L i.e. air gap of L = 35mm was kept by fixing the cold plate to the appropriate holes of the clamps fixed on the upper outer guard heater assembly.

c.   Then the rig was aligned to horizontal position for angle of inclination $\Theta = 0^0$.

d.   Then all the heater circuits were switched on and at the same time, the water line of the cold plate and the reserve tank were opened.

e.   To maintain the temperatures of thermocouples 1 to 36 at $T_{COR}$ the voltages of test section and guard heater sections were varied by stabilizer and variacs. The cold plate was also maintained at the room temperature by controlling the water flow through it to maintain $\Delta T$ constant during a particular test run.

f.   When steady state was reached i.e. $T_{COR} - T_{COLD} = 10^0$ readings of temperatures of thermocouples No. 1 to 9 and 37 to 41 were recorded. At the same time readings of ammeter and voltmeter connected to the test section of the hot plate was also noted, to obtain the heat input.

g.   The procedures of steps (e) and (f) were repeated for inclination angles $\Theta = 30^0$, $45^0$ and $75^0$ keeping air gap, L = 35mm constant throughout.

h.   Then by changing the air gap, [L] to the other values of 55mm, 75mm, and 95mm operations from step [c] to step [g] were repeated.

i.   Then for other values of $\Delta T$ i.e. for $26^0$C and $35^0$C all the operations described in steps [b] to [h] were repeated. Thus one full set of readings were completed.    -

For one full set of data, i.e. for H = 10mm forty eight sets of readings were recorded. Similarly for H = 15mm and 25mm the procedures (a) to (i) were repeated respectively. Thus total of 144 sets of readings were obtained. The ranges of parameters for different corrugations were as follows.

For H = 10mm

| | |
|---|---|
| Rayleigh Number, | $Ra_L = 3.299 \times 10^4$ to $1.8814 \times 10^6$ |
| Heat flux, | $q" = 57$ to $276 \ W/m^2$. |
| Temperature difference between hot plate and Cold plate, | $\Delta T = 10^0C$ to $35^0C$ |

| | |
|---|---|
| Temperature of the hot plate, | $T_{CO2} = 36^0C$ to $64^0C$ |
| Inclination angle, | $\Theta = 0^0$ to $75^0$ |
| Air gap, | $L = 35mm$ to $95mm$ |

For H = 15mm.

| | |
|---|---|
| Rayleigh Number, | $Ra_L = 3.294 \times 10^4$ to $1.8814 \times 10^6$ |
| Heat flux, | $q" = 59$ to $280 W/m^2$ |
| Temperature difference between hot plate and Cold plate, | $\Delta T = 10^0C$ to $35^0C$ |
| Temperature of the hot plate. | $T_{CO2} = 36^0C$ to $64^0C$ |
| Inclination angle, | $\Theta = 0^0$ to $75^0$ |
| Air gap, | $L = 35mm$ to $95mm$ |

For H = 25mm.

| | |
|---|---|
| Rayleigh Number, | $Ra_L = 3.294 \times 10^4$ to $1.8814 \times 10^6$ |
| Heat flux, | $q" = 60$ to $285 W/m^2$ |
| Temperature difference between hot plate and Cold plate, | $\Delta T = 10^0C$ to $35^0C$ |
| Temperature of the hot plate, | $T_{CO2} = 36^0C$ to $64^0C$ |
| Inclination angle, | $\Theta = 0^0$ to $75^0$ |
| Air gap, | $L = 35mm$ to $95mm$ |

## 5.4 Reduction of Data

Convective heat transfer co-efficient was calculated from convective heat flux. The heat flux, q" obtained from readings of voltmeter and ammeter was the combination of convective and radiative heat flux. So in calculating convective heat flux, the radiative heat flux was deducted from this measured heat flux. To find out the radiative heat Stefan-Boltzman equation for grey surface [equation 3.1] was used. The outline for obtaining the emissivity of the test section of the hot corrugated plate has been given in appendix-C, and the emissivity for the square corrugated plates having opening angle of $90^0$ has been found to be 0.95.

# CHAPTER 6

# RESULTS AND DISCUSSION

This experimental investigation deals with the steady state natural convection heat transfer from hot square corrugated plates through air to a cold flat plate placed above and parallel to the hot corrugated plate. The assembly being inclined at various angles with respect to horizontal was carried out in a finite rectangular enclosure having adiabatic surroundings. Three types of corrugation having amplitudes, H = 10mm, 15mm and 25mm were used. Experiments covered a range of Rayleigh number from $3.2940 \times 10^4$ to $1.8814 \times 10^6$ and angle of inclination from $0^0$ to $75^0$. The temperature difference ($\Delta$T) between the hot and cold plates was kept constant at $10^0$C, $26^0$C and $35^0$C.

The temperature distribution over the experimental hot corrugated plate and cold plate for different aspect ratios [A or L/H] and different inclination angles [$\Theta$] was found to be isothermal. The temperature distribution for a typical illustration for hot and cold plate is shown in figures 6.1 to 6.3 and figures 6.4 to 6.6 respectively.

The effect of aspect ratio [L/H] on heat transfer rate across rectangular regions for various angles of inclination [$\Theta$] and temperature difference ($\Delta$T) for all types of corrugation, is shown in figures 6.7 to 6.10. Each figure is drawn for a particular $\Theta$ with different values of $\Delta$T and H. From graphs 6.7 to 6.10, it is observed that for both types of corrugation "h" increases with increasing of aspect ratio for a certain $\Delta$T upto a certain limit and then decreases. But the

31

limiting value of aspect ratio upto which, "h" increases are found to be different for different $\Delta T$ and for different corrugations. It is also observed from figures 6.7 to 6.10 that for same $\Delta T$ and $\Theta$, an increase in the amplitude of corrugation the value of 'h' increases upto a certain value of aspect ratio for each type of corrugation. But after that the values of aspect ratio, 'h' decreases sharply with increasing in amplitude of corrugation and aspect ratios. The reason of such occurance is that increasing of gap between the hot corrugated plate and the cold flat plate increases the aspect ratio and permits better mixing of the fluid leading to an enhancement of heat transfer rate. But this enhancement of heat transfer rate has got a certain limit and beyond this limit heat transfer co-efficient are found to decrease with the increasing of aspect ratio. This is due to the fact that beyond these limiting values of "A" the convective currents appear to be weak to reach the cold flat plate and transfer less heat after crossing a larger distance. As aspect ratio is the ratio of mean plate spacing to the amplitude of corrugation, so for same aspect ratio an increase in amplitude of corrugation the mean plate spacing increases. So the limiting value of aspect ratio was found to be different for different types of corrugations.

Figures 6.11 to 6.19 also show the variation of 'h' with aspect ratio (A), each of which was drawn for a particular value of $\Delta T$ and H. It is observed that for each value of aspect ratio with an increase in the value of inclination angle heat transfer coefficient decreases and it is maximum at $0^0$. This is perhaps due to the fact that the Rayleigh number for breaking down of unstable situation in order to set convective motion within the fluid increases with the increasing of angle of inclination. Again the effect of fluid stagnation in the corrugation cavity at higher angle of inclination may also not be ruled out as the fluid flow direction appears to be perpendicular to the corrugation channel.

Figures 6.20 to 6.22 shows that for $0 \leq \Theta \leq 75^0$ and at constant $\Delta T$, heat transfer coefficient increases with an increase of aspect ratio `A' upto a certain value. But this limiting value of `A' was found to be different for different amplitudes of corrugations. The limiting values of `A' were—

for  H  =  10mm      A  $\approx$  4 to 7

    H  =  15mm      A  $\approx$  3.5 to 6

    H  =  25mm      A  $\approx$  2.5 to 4

To show the effect of temperature potential on heat transfer rate for various angles of inclination [$\Theta$] and aspect ratios [A] for both types of corrugation, figures 6.23 to 6.26 were plotted which presents h vs $\Delta T$ for a particular "L" with different values of $\Theta$. From these figures it is clear that average heat transfer coefficient increases more or less linearly with the increasing of temperature potential. The reason is that for higher values of $\Delta T$ heat fluxes are also higher which enhance heat transfer i.e. increase convective heat transfer coefficient for both types of corrugation.

Results are presented in terms of Nusselt number and angle of inclination for a particular value of `L' and Rayleigh numbers [$Ra_L$] in figures 6.27 to 6.30. From these figures it is clear that at a constant L and Rayleigh number, Nusselt number decreases with the increasing of angle of inclination for all types of corrugation. Nusselt number is also found to be maximum at $\Theta = 0^0$ [horizontal] for all Rayleigh numbers. This is due to the fact that as angle of inclination [$\Theta$] increases from $0^0$, the hydrodynamic instabilities begin to interfere with the motion induced by thermal instabilities. But thermal instabilities are dominant at lower angles of inclination.

Figures 6.31 to 6.38 show the relationship between the Nusselt number and $Ra_L \cos\Theta$ for different values of L and angles of inclination [$\Theta$]. From these figures it is observed that for all types of corrugation, Nusselt number increases with increasing of Rayleigh number at a particular L and angle of inclination. This is due to the fact that at a constant L and angle of inclination, Rayleigh number increases with increasing of temperature potential [$\Delta T$]. Again increasing of $\Delta T$ increases the heat flux which in turns increases convective heat transfer co-efficient leading to the increase of $Nu_L$.

**Comparison:**

Figures 6.7 to 6.22 show the variation of average heat transfer co-efficient on aspect ratio for different $\Delta T$ and angles of inclination. The convective heat transfer coefficient for H = 25 mm is the higest and that for H = 10 mm is the lowest for same value of $\Delta T$ and $\Theta$. That is an increase in amplitude 'H' shows better heat transfer performance. This is due to the fact that better clearance between the adjacent ribs of corrugation may permit better clearance for inflow and outflow of convecting fluid.

Figures 6.39 and 6.40 shows the comparison of Nusselt number of the present study with the Nusselt number of the works of Elsherbiny [1977], Kabir [1988] and Feroz [1992]. For lower Rayleigh number i.e. for $Ra_L = 0.4 \times 10^6$. When the values of Nusselt number for square corrugation of H = 25 mm are compared with those of above works, it is shown that Elsherbiny's (Vee corrugated) values are higher by 41%, Kabir's (Sinusoidal corrugated) are higher by 26%, Feroz's (Trapezoidal corrugated) are higher by 16% and Feroz's (Rectangular corrugated) are higher by 10%.

From present study it is also shown that the value of Nusselt number for H = 25 mm is higher than that of H = 15 mm by 6% and of H = 10 mm by 15%.

It is also observed from these figures that for higher Rayleigh number ($Ra_L = 1.0 \times 10^6$) this difference in value of Nusselt number of present study is lower than other related works mentioned earlier.

Correlation:

In earlier studies of Kabir (1988) and Feroz (1992) correlations were formulated in the form of

$$Nu_L = C[Ra_L Cos\Theta]^n [A]^m.$$

They determined the exponents 'n' and 'm' by plotting $Nu_L$ vs $Ra_L Cos\Theta$ and $Nu_L/(Ra_L Cos\Theta)^n$ vs A respectively. The value of constant 'C' was determined from the graphical representation of $Nu_L$ vs $(Ra_L Cos\Theta)^n (A)^m$.

This graphical method for determining the value of exponents and constant has some inherent errors because the measurement of slope was done manually from the curves. So the above method was not used in this study. The values of exponents and constant were determined by a Computer Programming which uses the least square method of curve fitting to fit all the data. The values of 'C', 'n' and 'm' were found to be as follows

C = 0.295, n = 0.265, m = 0.442.

So all the experimental data for square corrugation were correlated by the following equation to within ± 20%.

$$Nu_L = 0.295 [Ra_L cos\Theta]^{0.265} [A]^{-0.442}.$$

Where, $3.294 \times 10^4 \leq Ra_L \leq 1.8814 \times 10^6$

$1.4 \leq A \leq 9.5$

$0^0 \leq \Theta \leq 75^0$

# CHAPTER − 7

# CONCLUSIONS AND RECOMMENDATIONS

This chapter includes the conclusions that can be drawn from the experimental investigation of natural convection of hot square corrugated plates to cold plates. The recommendations for which the present investigation can be extended are presented here.

## 7.1 Conclusions:

1. In all the three sets of square corrugation the natural convective heat transfer co-efficient [h] was found to be dependent on temperature potential [$\Delta$T], angle of inclination [$\Theta$] and aspect ratio [A].

2. It was found that the average natural convective heat transfer co-efficient increases with increasing of aspect ratio upto a certain limit and then has a tendency to decrease with further increasing of aspect ratio. This implies that for each set of corrugation there is a optimum value of aspect ratio for which the value of 'h' is maximum.

3. The dependency of average natural convective heat transfer coefficient [h] on temperature potential [$\Delta$T] is found to be more or less linear for all the three types of corrugation.

4. In all these three sets of corrugation the convective heat transfer co-efficient decreases with the increasing of angle of inclination.

5. From this investigation the maximum values of average natural convective heat transfer co-efficients were found to be 2.215 for H = 25mm, 2.143 for H = 15mm, and 2.059 for H = 10mm. All these values were obtained at horizontal position of the corrugated plates.

6. It was also observed that the average Nusselt number decreased with increasing of angle of inclination. The maximum values of average Nusselt number were experimentally found to be 7.613 for H = 25mm, 7.3465 for H = 15mm and 7.078 for H = 10mm. All these values were also found at horizontal position of the corrugated plates.

7. All the data for square corrugations were correlated by the following correlating equation to within ± 20%.

$$Nu_L = 0.295 (Ra_L \cos\Theta)^{0.265} (A)^{-0.442}$$

Where,

$3.294 \times 10^4 \le Ra_L \le 1.881 \times 10^6$

$1.40 \le A \le 9.50$

$0^0 \le \Theta \le 75^0$

$10^0 C \le \Delta T \le 35^0$

## 7.2 Recommendations:

1. The effect of Prandtl number on the natural convection heat transfer can be investigated by performing similar experiments with other fluids e.g., water, silicon oil, etc.

2. A comprehensive investigation of natural convection heat transfer of the similar type may be carried out over a wider range of Rayleigh number.

3. The entire investigation can be carried out by interferometric techniques for conforming the flow pattern of the convective fluid within the region.

4. An experimental investigation with very high temperature potential i.e. $\Delta T$ >> $35^0C$ and also the velocity field can be investigated.

5. Numerical simulation of natural convection heat transfer from hot corrugated plates to a cold flat plate can also be predicted.

6. The entire investigation can be repeated by using hot square corrugated plates with flush heat sources.

# REFERENCES

Arnold, J.N., Catton, I., and Edwards, D.K., 1976, "Experimental Investigation of Natural Convection in Inclined Rectangular Regions of Differing Aspect Ratios", J. Heat Transfer, Vol. 98, pp. 67-71.

Ayyaswamy, P.S., and Catton, I., 1974, "Natural Convection Flow in a Finite Rectangular Slot Arbitrarily Oriented with Respect to the Gravity Vector", International Journal of Heat and Mass Transfer, Vol. 17, pp. 173-184.

Ayyaswamy, P.S., and Catton, I., 1973, "The Boundary Layer Regime for Natural Convection in a Differentially Heated, Tilted Rectangular Cavity", J. Heat Transfer, Trans. ASME Series C, Vol. 95, pp. 543-545.

Buchberg, H., Catton, I., and Edwards, D.K., 1976, "Natural Convection in Enclosed Spaces: A Review of Application to Solar energy Collection", J. Heat Transfer, Vol. 98, No. 2, pp. 182-188.

Burmeister, L.C., 1983, "Convective Heat Transfer", John Wiley and Sons, Inc.

Channdrasekhar, S., 1961, "Hydrodynamic and Hydromagnetic Stability", Clarendon Press, Oxford.

Chinnappa, J.C.V., 1970, "Free Convection in Air Between a $60^0$ Vee-Corrugated Plate and Flat Plate", International Journal of Heat and Mass Transfer, Vol. 13, pp. 117-123.

Chu, T.Y., and Goldstein, R.J., 1973, "Turbulent Convection in a Horizontal Layer of Water", Journal of Fluid Mechanics, Vol. 60, pp. 141-159.

Chu, T.Y., and Goldstein, R.J., 1969, "Thermal Convection in a Horizontal Layer of Air", Prog. Heat and Mass Transfer, Vol. 2, pp. 55-75.

David, P. Dewitt, and Frank, P. Incropera, 1985, "Introduction to Heat Transfer".

De Graff, J.C.A., and Van Der Held, F.E.M., 1953, "The Relation Between the Heat Transfer and the Convection Phenomena in Enclosed Plane Air Layers", Appl. Sci. Res. A., Vol 3, pp. 393-409.

Difederico, I., and Foradoschi, F.P., 1966, "A Contribution to the Study of Free Convection in a Fluid layer heated from Below", International Journal of Heat and Mass Transfer, Vol. 9, pp. 1351-1360.

Dropkin, D., and Somerscales, F., 1966, "Experimental Investigation of the Temperature Distribution in a Horizontal Layer of Fluid Heated from below", International Journal of Heat and Mass Transfer, Vol. 9, pp. 1189-1204.

Dropkin, D., and Somerscales, F., 1965, "Heat Transfer by Natural Convection in Liquids Confined by Two parallel Plates which are Inclined at Various Angles with Respect to the Horizontal", Journal of Heat Transfer, Series C, Vol. 87, pp. 77-81.

Dropkin, D., and Globe, S.E., 1959, "Natural Convection in Liquids Confined by Two Horizontal Plates and Heated from Below", Journal of Heat Transfer, Vol. 87, Series C, pp. 24-28.

Eckert, E.R.G., and Carlson, W.O., 1969, "Natural Convection in an Air Layer Enclosed Between Two Vertical Plates with Different Temperatures", International Journal of Heat and Mass Transfer, Vol. 2, pp. 102-120.

Elsherbiny, S.M., Hollands, K.G.T., and Raithby, G.D., 1967, "Free Convection Across Inclined Air Layers with one Surface Vee-Corrugated", in Heat Transfer Solar Energy Systems, Howell, J.R., and Min, T., (eds.), American Society of Mechanical Engineerings, New York.

Emery, A., Chu, N.C., 1969, "Heat Transfer Across Vertical Layers", ASME Journal of Heat Transfer, Vol. 91, pp. 391.

Feroz, C.M., 1992, "Natural Convection from Hot Corrugated Plates to a Cold Flat Plate", M. Sc. Engineering (Mechanical) Thesis, BUET.

Gryzagoridis, J., 1971, "Natural Convection from a Vertical Plate in Low Grashof Number Range", International Journal of Heat and Mass Transfer, Vol. 14, pp. 162-164.

Hart, J., 1971, "Stability of the Flow in a Differentially heated Inclined Box", Journal of Fluid Mechanics, Vol. 47, pp. 547-576.

Herring, J.R., 1965, "Investigation of Problems in Thermal Convection", Journal Atoms. Sci. Vol. 20, p. 325.

Herring, J.R., 1964, "Investigation of Problems in Thermal Convection: Rigid Boundaries", Journal Atoms. Sci. Vol. 21, p. 227.

Hollands, K.G.T., Unny, T.E., Raithby, G.D. and Konicek, L., 1976, "Free Convective Heat Transfer Across Inclined Air Layers", Journal of Heat Transfer, Vol. 98, No. 2, pp. 189-193.

Hollands, K.G.T., Raithby, G.D. and Konicek, L., 1975, "Correlation Equations for Free Convection Heat Transfer in Horizontal Layers of air and Water", International Journal of Heat and Mass Transfer, Vol. 18, pp. 879-884.

Hollands, K.G.T., and Konicek, L., 1973, "Experimental Study of the Stability of Differentially Heated Inclined Air Layers", International Journal of Heat and Mass Transfer, Vol. 16, pp. 1467-1476.

Hollands, K.G.T., 1965, "Convectional Heat Transfer Between Rigid Horizontal Boundaries after Instability", Physics Fluids, Vol. 8, pp. 389-390.

Hollands, K.G.T., 1963, "Directional Selectivity, Emittance and Absorptance Properties of Vee-Corrugated Surfaces", Solar Energy, Vol. 7, pp. 108-116.

Holman, J.P., 1981, "Heat Transfer", Fifth Edition, McGraw-Hill Book Company.

Jakob, M., 1949, "Heat Transfer", Vol. 1, John Wiley and Sons, Inc. N.Y.

Jakob, M., 1946, Trans. ASMRE, Vol. 68, pp. 189.

Jeffreys, H., 1928, "Some Cases of Instability in Fluid Motion", Proc. Roy. Soc. (London), (A), vol. 118, p. 195.

Kabir Humayun, 1988, "An Experimental Investigation of Natural Convection Heat Transfer from a Hot Corrugated Plate to a Flat Plate", M.Sc. Engineering (Mechanical) Thesis, BUET.

Low, A.R., 1929, "On the Criterion for Stability of a Layer of Viscous Fluid Heated from Below", Proc. Roy. Soc. (London), (A), vol. 125, p. 180.

Malkus, W.V.R., 1963, "Outline of a Theory of Turbulent Convection", Theory and Fundamental Research in Heat Transfer, Edited by J.A. Clark, Pergamon Press, New York, pp. 203-212.

Mull W., and Reiher H., 1930, "Experimental Investigation of Free Convection Heat Transfer in Horizontal Air Layers", Gesundh-Ing. 28(1), pp. 1-28.

McAdams, W.H., 1949, "Heat Transmission", Third Edition, McGraw-Hill Book Company, Inc.

Ostrach, S., 1957, "Convective Phenomena in Fluids Heated from Below", Trans. ASME, Vol. 79, pp. 299-305.

O'Toole, J.L., and Siveston, P.L., 1961, "Correlations of Convective Heat Transfer in Confined Horizontal Layers", A.I.Ch.E. Chem. Engg. Prog. symp. Ser. Vol. 57(32), pp. 81-86.

Ozoe, H., Sayma, H., and Churchill, S.W., 1975, "Natural Convection in an Inclined Rectangular Channel at Various Aspect Ratios and Angles: Experimental Measurements", International Journal of Heat and Mass Transfer, Vol. 18, pp. 1425-1431.

Randall, K.R. et. al., "Interferometeric investigation of Convection in Slat-Flat Plate and Vee-Corrugated Solar Collectors", Solar Energy International Progress, pp. 447-460.

Rayleigh, L., 1916, "On Convection Currents in a Horizontal Layer of Fluid when the Higher Temperature is on the underside", Phil. Mag. Vol. 32, p. 529.

Rossby, H.T., 1969, "A Study of Benard Convection With and Without Rotation", Journal of Fluid Mechanics, Vol. 36(2), pp. 309-335.

Schluter, A., Lortz, D., Busse, F., 1965, "On the Stability of Steady Finite Amplitude Convection", Journal of Fluid Mechanics, vol. 23, pp. 129-144.

Schmidt, R.J., and Silveston, P.L., O.A., 1959, "Natural Convection in Horizontal Liquid Layers", Chem. Engg. Prog. Symp. Ser. 29, Vol. 55, pp. 163-169.

Schmidt, R.J., and Saunders, O.A., 1938, "On the Motion of Fluid Heated from Below", Proc. Roy. Soc. (London) (A), Vol. 165, pp. 216-218.

Sterling, C.V., and Scriven, L.E., 1964, Journal of Fluid Mechanics, Vol. 19, p. 321.

Thomson, J.J., 1882, Proc. Glasgow Phil. Soc., vol. 13, pp. 464.

# APPENDIX - A

## DESIGN OF THE TEST RIG

During the design of the test rig the following two aspects were considered:

[1]   Heat Transfer Calculations

[2]   Electrical Heater Design

**A1.   Heat Transfer Calculations:**

All the heat transfer calculations included estimation of the steady state heat transfer rates from different exposed heated surfaces of the experimental rig under different designed operating conditions as given below:

[1]   Calculation of rate of heat transfer from the hot corrugated plate to the cold flat plate by convection and radiation.

[2]   Calculation of rate of heat transfer from the exposed surfaces of the upper guard heater assembly to the ambient air by convection and radiation.

[3]   Calculation of rate of heat transfer from the exposed surfaces of the lower guards heater assembly to the ambient air by convection and radiation.

For proper design the above three items were estimated for two extreme design temperatures namely the maximum and minimum design temperatures. From the previous available experimental data it was observed that maximum heat transfer will occur when the rig is horizontal, and mean plate spacing is minimum and the temperature of the test rig is maximum. Similarly minimum heat transfer will occur when the rig is vertical, mean plate spacing is maximum and the temperature of the test rig is minimum.

## A1.1 Calculation of Rate of Heat Transfer from the Hot Corrugated Plate to the Cold Flat Plate:

Heat transfer from the hot corrugated plate to the cold flat plate takes place by two different modes (conduction is negligible); (a) natural convection and (b) radiation.

## A.1.1a     Calculation of Natural Convection Heat Transfer:

For design purpose it was assumed that the corrugated plate was a flat one. For computing heat transfer co-efficient approximately the following correlating equations by Jakob [1949] for horizontal [Fig. A.1] and vertical [Fig. A.2] positions of the test rig heated from below were used.

. For Horizontal position:

$$Nu_L = 0.195 \ [Gr_L]^{1/4}, \qquad 10^4 < Gr_L < 4 \ X \ 10^5 \qquad\qquad [1]$$

$$Nu_L = 0.068 \ [Gr_L]^{1/3}; \qquad\qquad Gr_L < 4 \ X \ 10^5 \qquad\qquad [2]$$

**For Vertical Position:**

$$Nu_L = 1, \qquad Gr_L < 2000 \qquad\qquad [3]$$

$$Nu_L = 0.18 \, [Gr_L]^{1/4} \, [H/L]^{-1/9}, \; 2 \times 10^3 < Gr_L < 2 \times 10^5 \qquad [4]$$

$$Nu_L = 0.065 \, [Gr_L]^{1/3} \, [H/L]^{-1/9}, \; 2 \times 10^5 < Gr_L < 11 \times 10^6 \qquad [5]$$

After knowing $Nu_L$, convective heat transfer co-efficient was found by using the following equation:

$$h = Nu_L.K/L \qquad\qquad [6]$$

And finally convective heat transfer rate was calculated by using the following equation:

$$q_{conv} = A_{COR}.h. \, [T_{COR} - T_{COLD}] \qquad\qquad [7]$$

### A.1.1b    Calculation of Radiation Heat Transfer:

For estimating the radiation heat transfer rate following assumptions were made:

– Interior surfaces i.e., the hot corrugated plate and cold flat plate behaved like black bodies.

– Heat Transfer by convection was not taken into account.

– Side walls of the test rig were adiabatic.

Generally radiation from a surface is due to reflection and emission. Since the interior surfaces as mentioned above were assumed to be black, the radiation emitted was absorbed without any reflection. Defining $q_{i-j}$ as the rate at which radiation was emitted by a black surface i and was intercepted by black surface j. [Figure A.3] i.e.

46

$$q_{i-j} = [A_i \ J_i] \ F_{ij} \tag{8}$$

Since radiosity equals emissive power for a black surface $[J_i = E_{bi}]$, hence

$$q_{i-j} = A_i \ F_{ij} \ E_{bi} \tag{9}$$

$$q_{j-i} = A_j \ F_{ji} \ E_{bi} \tag{10}$$

The net radiation exchanged between two black surfaces:

$$q_{ij} = q_{i-j} - q_{j-i}$$

or $\quad q_{ij} = A_i F_{ij} E_{bi} - A_j F_{ji} E_{bj} \tag{11}$

By reciprocity, $A_j F_{ji} = A_i F_{ij} \tag{12}$

According to Stefan − Boltzman law:

$$E_{bi} = \sigma \ T_i^4 \tag{13}$$

$$E_{bj} = \sigma \ T_j^4 \tag{14}$$

Now from equations [11], [12], [13] and [14]:

$$q_{ij} = A_i F_{ij} \ \sigma \ [T_i^4 - T_j^4] \tag{15}$$

Considering surfaces i and j as corrugated and flat plate respectively and assuming that the radiation emitted by the corrugated surface was intercepted by the cold flat plate $[F_{ij} = 1]$, the equation [15] took the following form:

$$q_{rad} = A_{cor} \ \sigma \ [T_{cor}^4 - T_{cold}^4] \tag{16}$$

From equation [16] the radiation heat transfer was estimated.

### A1.2 Calculation of Rate of Heat Transfer from the Exposed surfaces of the Upper Guard heater Assembly to the Ambient Air by Convection and Radiation:

When the experimental rig was kept horizontal, the exposed surfaces of the upper guard heater assembly consisted of two pairs of parallel vertical plane surfaces facing outward having dimensions of 660mm X 127mm and 579mm X 127mm.

When the experimental rig was kept vertical, one of the pairs of dimensions 660mm X 127mm of the exposed surfaces of the upper guard heater assembly

became horizontal; one facing upward and another facing downward. But the other pair of the exposed heated surfaces of dimension 579mm X 127mm remained vertical facing outward.

For design the following correlations were used to estimate the rate of heat transfer from the exposed surfaces of the upper guard heater assembly:

[i]    For computing convective heat transfer co-efficient approximately the following correlating equation recommended by Gyrzagoridis [1971] for vertical heated surfaces of height H [Figure A.4] was used.

$$Nu_H = 0.555 \ [Gr_H Pr]^{1/4}, \ 10 < Gr_H < 10^9$$    [17]

where,

$Nu_H$ and $Gr_H$ are based on length of the vertical surface.

[ii]   For computing convective heat transfer co-efficient approximately for heated horizontal surfaces [Figure A.5 and A.6] of characteristic length Lc = $\sqrt{}$(Area of the plate) = $A_p$ the following correlating equations recommended by McAdams [1949] were used.

$$Nu_{Lc} = 0.54 [Gr_{Lc}.Pr]^{1/4}, 10^5 < Gr_{Lc} < 2 \ X \ 10^7, [For \ upward \ facing].$$    [18]

$$= 0.14 \ [Gr_{Lc}.Pr]^{1/3}, \ 2 \ X \ 10^7 < Gr_{Lc} < 3 \ X \ 10^{10}$$

$$Nu_{Lc} = 0.27 \ [Gr_{Lc}.Pr]^{1/4}, \ 3 \ X \ 10^5 < Gr_{Lc} < 3 \ X \ 10^7$$

[For downward facing]    [19]

Where, $Nu_{Lc}$ and $Gr_{Lc}$ are based on the characteristic length $L_c$ of the plane as mentioned above.

The radiation heat transfer from these exposed heated surfaces were estimated by the following equation:

$$q_{rad} = A_s . \varepsilon_s . \sigma . [T_s^4 - T_s^4] \qquad (20)$$

### A1.3 Calculation of Rate of Heat Transfer from the Exposed Surfaces of the Lower Guard heater Assembly to the Ambient Air by Convection and Radiation:

When the experimental rig was kept horizontal, the exposed surfaces of the lower guard heater assembly consisted of two pairs of parallel vertical plane surfaces facing outward having dimension of 660mm X 64mm and 579mm X 64mm and the bottom surface 660mm X 579mm facing downward.

When the experimental rig was kept vertical, one of the pairs of surface having the dimensions 660mm X 64mm of the lower guard heaters assembly became horizontal; one facing upward and another facing downward. But the other pair of the exposed heated surfaces of dimensions 579mm X 64mm remaind vertical facing outward. The bottom face became vertical.

For estimating both convective and radiative heat transfer rate from the exposed surfaces of the lower guard heater assembly the correlating caution were the same as described in the preceeding section [A.1.2].

For both the lower and the upper guard heater assembly the sum of the heat convected and radiated from the exposed surfaces must be equal to the amount of heat conducted from guard heaters through asbestos and wooden strip layers. But during the design the exposed surface temperature [$T_s$] of the guard heaters assembly was not known. So $T_s$ was assumed and estimation of conduction heat transfer was made. Then by using this surface temperature the amount of

convective and radiative heat transfer were calculated. The iterative solution was continued until the conduction heat transfer rate became equal to the sum of convective and radiative heat transfer. The equation used for estimating conduction heat transfer rate is given below:

$$q_{cond} = A_s . \Sigma_{j=1}^{2} K_j / L_j [T_s - T_s]$$ (21)

$K_1$ = The thermal conductivity of asbestos cloth = 0.192 $w/m^0k$

$K_2$ = The thermal conductivity of wooden strip = 0.130 $w/m^0k$

$L_1$ = The thickness of the asbestos cloth = 12mm

$L_2$ = The thickness of the wooden strip = 12mm

$T_s$ = Temperature of the guard heating element = $T_{COR}$


Now by substituting the above values into eqn. [21] the conduction heat transfer rate was found to be:

$$q_{cond} = 26.833 A_s [T_g - T_s]$$ (22)

The present experimental investigation was carried out with a rectangular rig that was made by Kabir [1988]. So the results of the heat transfer calculations for rig design were taken from Kabir's work.


## A2.   Heater Design:


The total number of heaters were six in the experimental setup. Among the heaters one heater was used in the experimental test section and the other five heaters acted as guard heaters. Each of these heaters had separate controlling variac through which power input to the heaters were controlled during experiment. Power required for each heater was estimated from heat transfer calculations shown in A1.

The details of the heater design are given below:

Power [P] taken by the electric heater of resistance R can be determined by the following equation:

$$P = I_{safe}^2 \times R \qquad [23]$$

If r be the resistance of the heating wire per meter of length, then for a heater of power P the length of the heating wire will be:

$$L = R/r \qquad [24]$$

By knowing $I_{safe}$ and power [P] taken by each electric heater the required resistance [R] was calculated from eqn. [23]. For a particular heating wire, internal resistance "r" is fixed. so, by putting the values of R and r into eqn. [24] required length for each heater was determined.

The ratings of the heating wires were as follows:

Type 1:     Resistance, r = 39.37 ohms/m

            Current carrying capacity = 0.75 amps.

Type 2:     Resistance, r = 26.25 ohms/m

            Current carrying capacity = 1.5 amps.

The particulars of the heating arrangement that were used are given in following tabular forms:

| Heater No. and Name | Maximum Power Requirement (Watt) | Type | Length of wire (cm) | Location | Variac Connected with Heater | |
|---|---|---|---|---|---|---|
| | | | | | Safe Installed Capacity (Watt) | Safe Voltage (Volt) |
| Experimental hot corrugated plate heater. | 12.50 | 1−Nicrome Wire | 97.40 | Experimental test section Fig. 4.3 | 22.5 | 30 |
| Outer side guard heater. | 83.40 | 1−Nicrome Wire | 376.60 | Longitudinal sides of the test section Fig. 4.3 | 22.5 | 30 |
| Outer end guard heater. | 20.79 | 1−Nicrome Wire | 93.87 | Lateral sides of the test section Fig. 4.3 | 90 | 120 |
| Upper outer guard heater. | 97.60 | 2−Nicrome Wire | 165.24 | Upper guard heater ring Fig. 4.4 | 180 | 120 |
| Bottom guard heater | 113.02 | 1−Nicrome Wire | 510.34 | Lower guard heater ring Fig. 4.4 | 90 | 120 |
| Lower outer guard heater | 43.17 | 1−Nicrome Wire | 194.93 | Lower guard heater ring Fig. 4.5 | 45 | 60 |

# APPENDIX - B

## CONDUCTION CORRECTION

One dimensional fourier conduction equation is;

$q" = K.\Delta T_c/\Delta x$ [For one layer of conductive zone]  [1]

$= T_c/\Sigma(\Delta x_i/k_i)$ [For two or more layers of conductive zone]  [2]

According to the present investigation it is observed that under steady state heat conduction the resistance to the heat conduction will consist of the resistance offered by the upper asbestos cloth layer and upper corrugated plate [G.I. Sheet].

The thermal conductivity of asbestos cloth, $K_1 = 0.157$ W/m$^0$k.

The thermal conductivity of G.I. sheet $K_2 = 70$ W/m$^0$k.

The thickness of asbestos cloth, $X_1 = 2.15052 \times 10^{-3}$m.

The thickness of G.I. Sheet, $X_2 = 7.9375 \times 10^{-4}$m.

( The above vlues were taken from M. Sc. Engineering thesis of Feroz, 1992 )

It is assumed that there is no temperature difference at the interface of the lower corrugated plate and the interface of the lower guard heater box. So that the heat only goes up toward the cold plate. It is also assumed that the temperature at the bottom surface of the lower corrugated plate is equal to the temperature at the interface of the two asbestos cloth.

Now by substituting the above values into equation [2] the conduction correction in temperature measurements were found to be:-

$\Delta T_c = 0.0137089$ q"  [3]

Where, q" will be taken as electrical heat input [W/m$^2$] per unit projected surface area of the experimental section of the hot corrugated plate.

# APPENDIX - C

## DETERMINATION OF EMISSIVITY OF THE CORRUGATED SURFACE

As the accuracy in predicting the radiation heat transfer from the experimental hot corrugated plate to the cold flat plate largely depends on the precise determination of the long wave emissivity and hemispherical emissivity of the corrugated surface, so the emissivity of square corrugated plates were determined as accurate as possible.

Both the three sets of square corrugated plates were painted by dull black plastic paint. Hollands [1963] developed the method of determination of the hemispherical emissivities of the Vee-corrugated surfaces using the emissivity of the plane surface. When a plane G. I. sheet is uniformly painted to dull black with black paint, its emissivity can be taken as the emissivity of the black paint. From table 3.6 of "Journal of Solar Energy", H.P. Gary; Vol. 1, John Wiley and Sons Ltd. [1982] the emissivity of the black paint was found to be 0.94. The emissivity of the G. I. corrugated [painted black] plate was assumed to be the same as that of plane G.I. sheet [painted black]. Considering this value of the emissivity, the hemispherical emissivity of square corrugated plate having opening angle of $90^0$ was found to be 0.95 [using figure C.2].

## APPENDIX - D

### CORRELATIONS

D.1 Correlations of natural Convection Heat Transfer in an Inclined Rectangular Region:

Difedevico and Foraboschi [1966] carried out experimental investigation on natural convection heat transfer in an inclined rectangular region with different convecting fluids and developed correlation in the following form:

$$Nu = C \ [R_a]^n \ [Pr]^m \qquad\qquad [1]$$

Kabir [1988] carried out an experimental investigation of natural convection heat transfer across air layer from a hot sinusoidal corrugated plate to a flat plate enclosed in a rectangular region inclined at various angle with respect to horizontal for various aspect ratios [A] and developed the following correlation:

$$Nu_L = 0.0132 \ [Ra_L cos\theta]^{0.51} . \ [A]^{-0.35} \qquad\qquad [2]$$

Where,

$$5.56 \times 10^3 \leq Ra_L \leq 2.34 \times 10^6$$

Feroz [1992] carried out an experimental investigation of natural convection heat transfer across hot trapezoidal and rectangular corrugated plates to a cold flat plate enclosed in a rectangular region included at various angle with respect to horizontal for various aspect ratios [A] and developed the following correlations

$$Nu_L = 0.0112 \ [Ra_L \cos\theta]^{0.521} . \ [A]^{-0.4546} \qquad [3]$$

$$Nu_L = 0.0102 \ [Ra_L \cos\theta]^{0.530} . \ [A]^{-0.4423} \qquad [4]$$

Where,

$$9.84 \times 10^4 \leq Ra_L \leq 2.29 \times 10^6$$

$$0 \leq \theta \leq 75^0$$

$$2.60 \leq A \leq 5.22$$

$$10^0C \leq \Delta T \leq 35^0C$$

## D.2 Correlation of Natural Convection Heat Transfer from a Hot Corrugated Plate to a Cold Flat Plate:

The present study was an experimental investigation of natural convection from hot square corrugated plates to a cold flat plate. Only square corrugated plates of different amplitudes were used. The required correlation was derived by considering the effect of the followings factors:

## D.2a Effect of Fluid Properties:

The most commonly used dimensionless parameters which include the effect of fluid properties in natural convection are:

$$Pr = \mu \ C_p/k \qquad and$$

$$Ra_L = g.\beta.\Delta T.L^3/\nu.\alpha$$

The present experimental investigation was carried out with only one convecting fluid [air], so Pr was assumed as constant property in the correlating equation. Therefore Nusselt number [Nu], which measures the thermal convective property of the fluid mainly depends on Rayleigh number

[$Ra_L$]. It was experimentally found that Nusselt number increases with the increasing of Rayleigh number. For analysis of natural convection from inclined surface because of buoyancy force, $Ra_L$ is generally substituted by its vertical component i.e. $Ra_L \cos\Theta$. So $Ra_L \cos\Theta$ should include the contribution of the fluid property in natural convection. Let correlation of the following form be assume:

$$Nu_L \propto [Ra_L \cos]^D \qquad [5]$$

In this case all the data of three sets of corrugation were solved by Fortran Programme of curve fitting. From the best fit curve of linear regression model the correlation obtained was,

$$NuL \propto (Ra_L \cos\Theta)^{0.165}$$

## D.2b  Effect of Spacing between Hot and Cold Plates:

Elsherbiny [1977], Kabir [1988] and Feroz [1992] suggested the following dimensionless group to describe the contribution of plate spacing between hot corrugated plate and cold flat plate in natural convection in a rectangular enclosure heated from below:

$$A = L/H \qquad [6]$$

In equation [6] "L" is mean plate spacing and "H" is amplitude of corrugation. It was experimentally observed that average convective heat transfer coefficient for both types of corrugation increases upto a certain limit with the increase of aspect ratio [A]. So, this dimensionless number also should include the contribution of spacing between hot and cold plates in free convection.

By including this dimensionless group the correlating equation was also obtained by similar Fortran programme of curve fitting. From the best fit curve the correlating equation containing aspect ratio `A` was found to be

$$Nu_L = 0.295 \ [Ra_L \cos\Theta]^{0.265} \ [A]^{-.443}$$

where

$$3.294 \ X \ 10^4 \ \leq \ Ra_L \ \leq \ 1.8814 \ X \ 10^6$$

$$1.4 \ \leq \ A \ \leq \ 9.5$$

$$0^0 \ < \ \Theta \ \leq \ 75^0$$

The graphical representation of the correlation is shown in figure 6.42)
The correlation correlates almost all data to ± 20%.

# FIGURES

All dimensions are in millimeter unless otherwise mentioned.
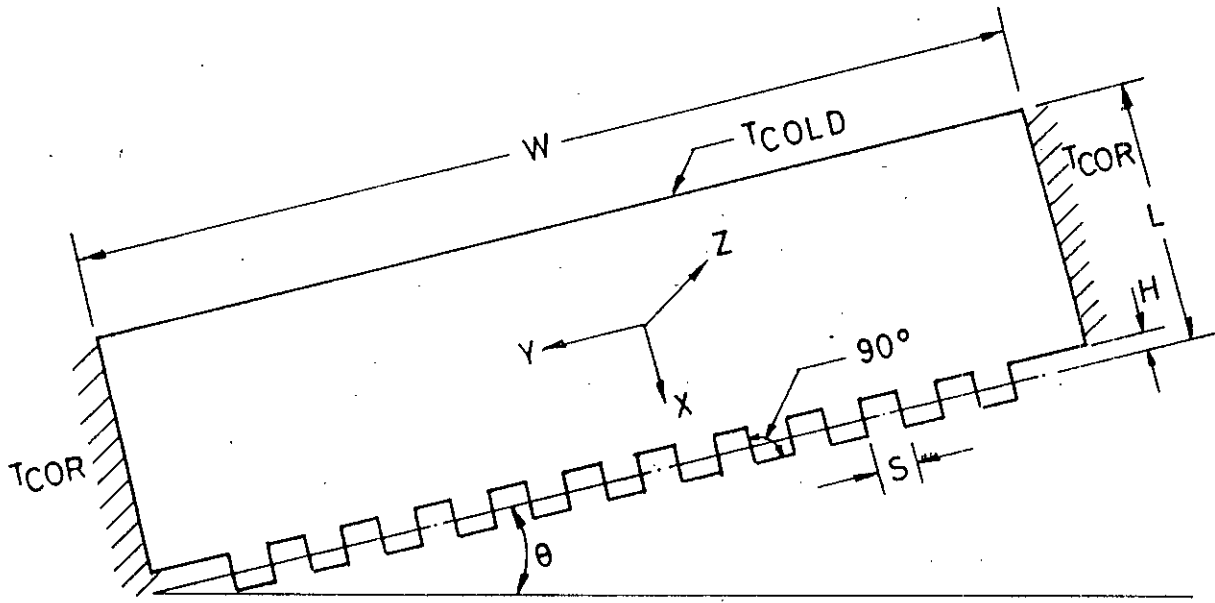
$\theta = 0°-75°$

L $= 35-95$ mm

H $= 10, 15, 25$ mm

S $= 20, 30, 50$ mm

W $= 63.5$ cm

FIG. 3.1 SKETCH OF THE INCLINED AIR LAYER BOUND BY
SQUARE CORRUGATED PLATE AND FLAT PLATE

1.  EXPERIMENTAL HOT PLATE
2.  COLD PLATE
3.  CONSTANT HEAD WATER DRUM
4.  TEST SECTION
5a. VARIAC FOR HEATER-5
5b. VARIAC FOR HEATER-6
5c. VARIAC FOR HEATER-3
5d. STABILIZER FOR HEATER-1
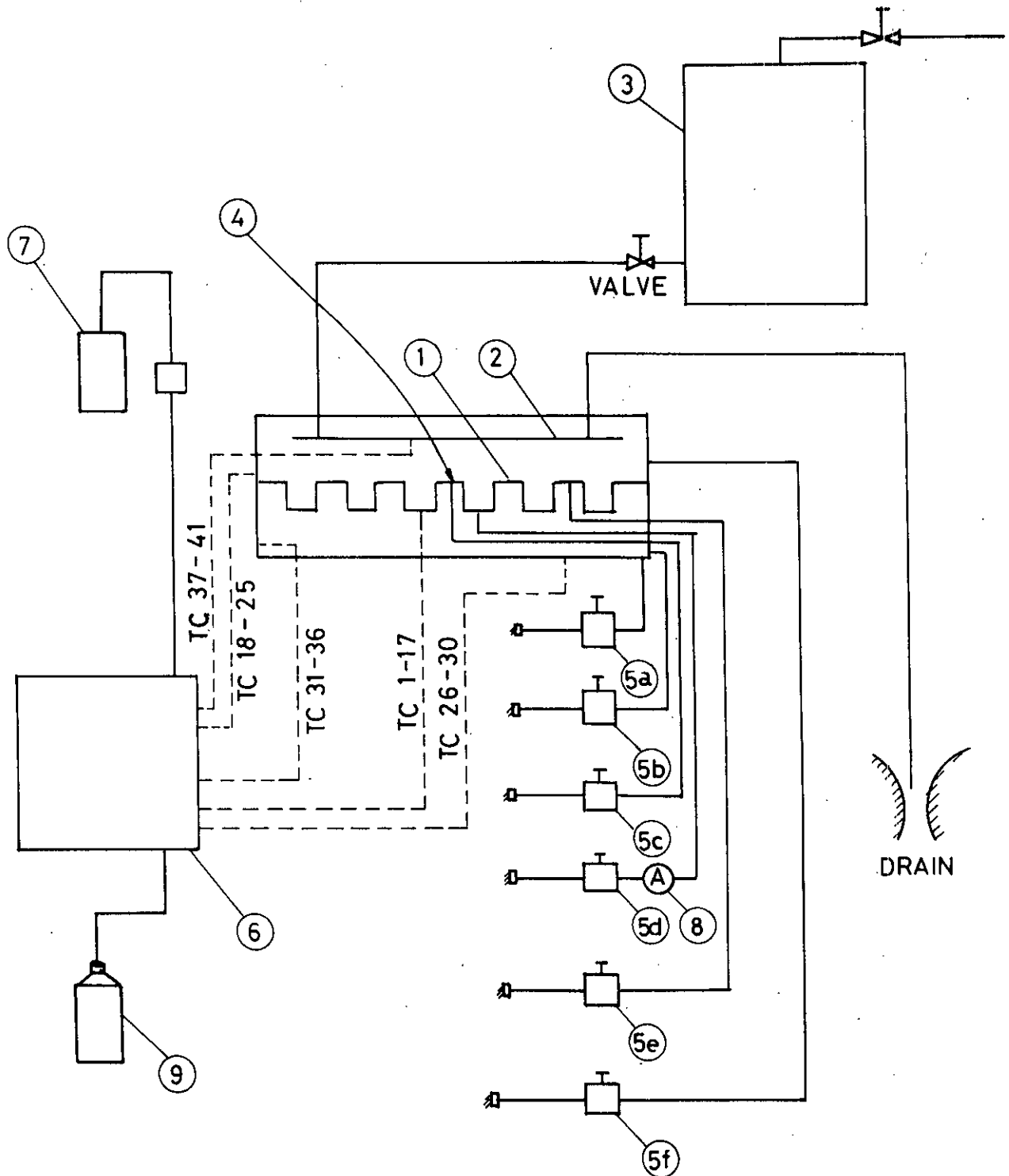
5e. VARIAC FOR HEATER-2
5f. VARIAC FOR HEATER-4
6.  THERMOCOUPLE SELECTOR SWITCH
7.  DIGITAL MILIVOLT METER
8.  DIGITAL AMMETER
9.  COLD JUNCTION

FIG : 4.1 SCHEMATIC DIAGRAM OF THE EXPERIMENTAL SET-UP.
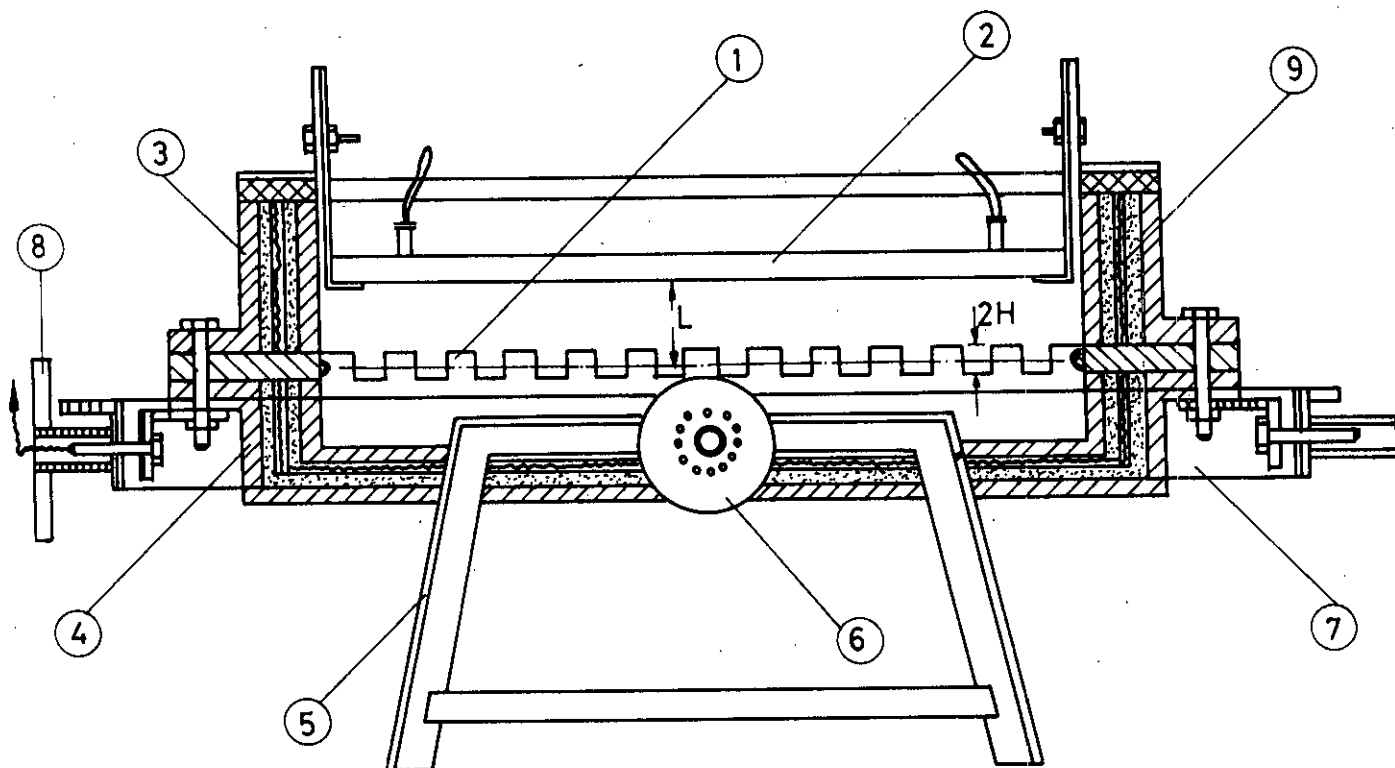
1. HOT PLATE ASSEMBLY
2. COLD PLATE
3. UPPER GUARD HEATER
4. LOWER GUARD HEATER
5. END RIG HOLDER
6. ALIGNMENT PLATE
7. SIDE RIG HOLDER
8. ALIGNMENT INDICATOR
9 NICHROME HEATERS

FIG. 4.2 DETAILS OF THE TEST SECTION FOR   SQUARE   CORRUGATION
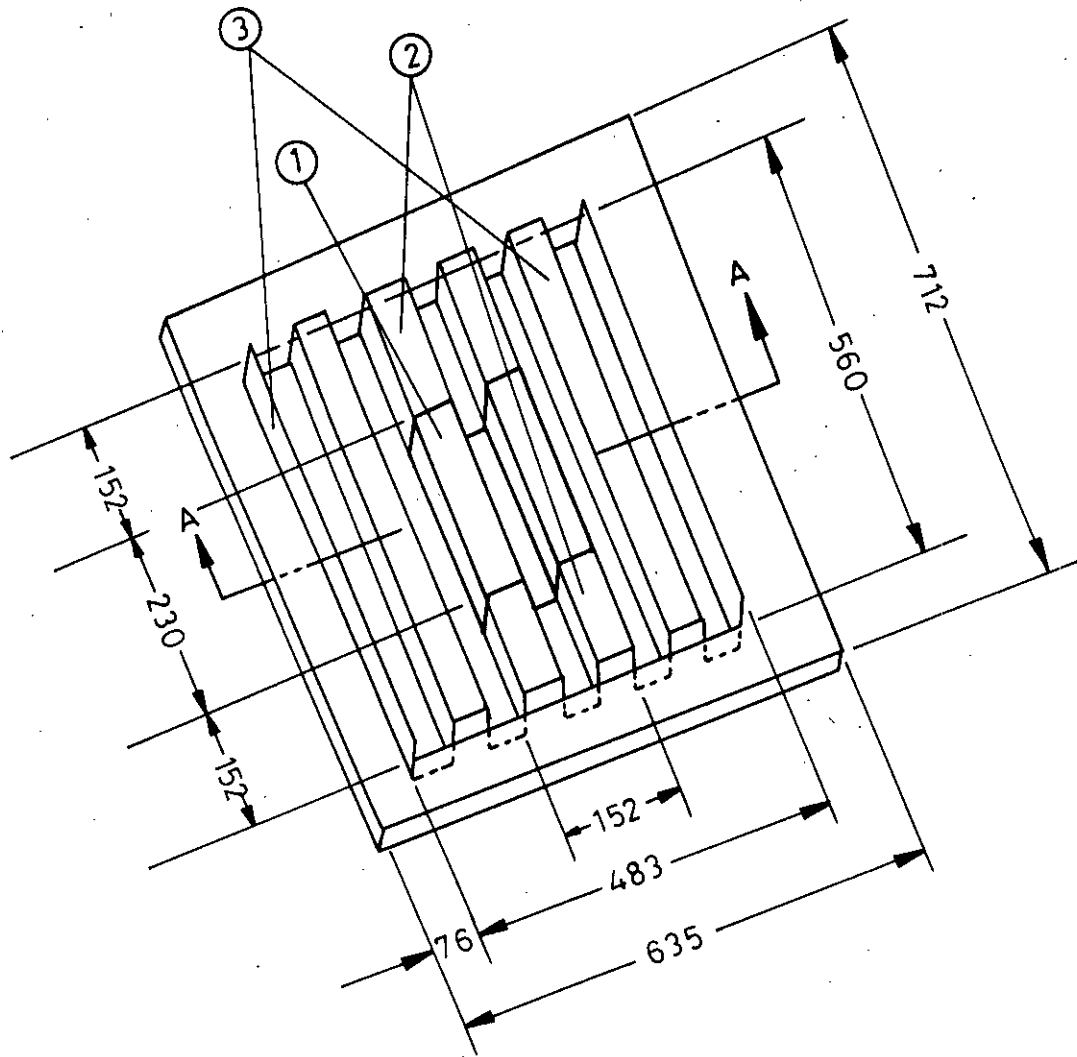
1. EXPERIMENTAL HOT PLATE.
2. OUTER END GUARD HEATER.
3. OUTER SIDE GUARD HEATER.

SANDWICHED HEATER
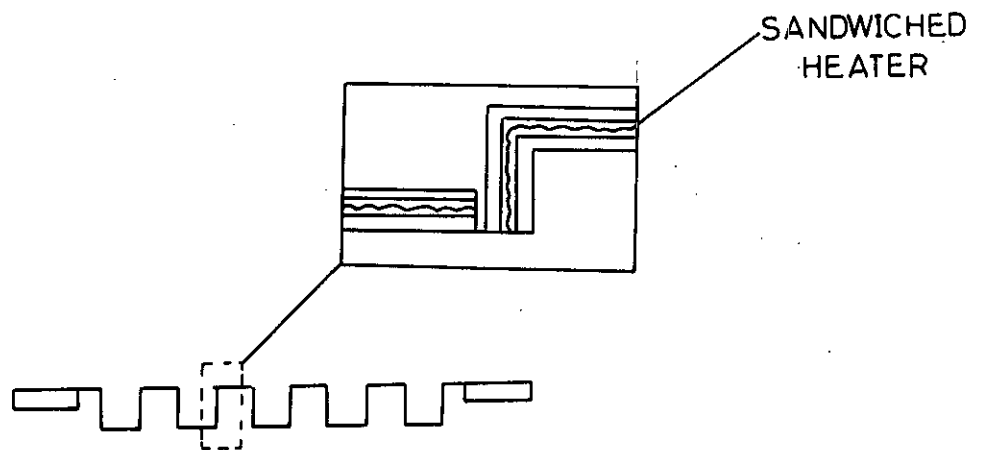
FIG:4.3 DETAILS OF HOT PLATE ASSEMBLY.

63
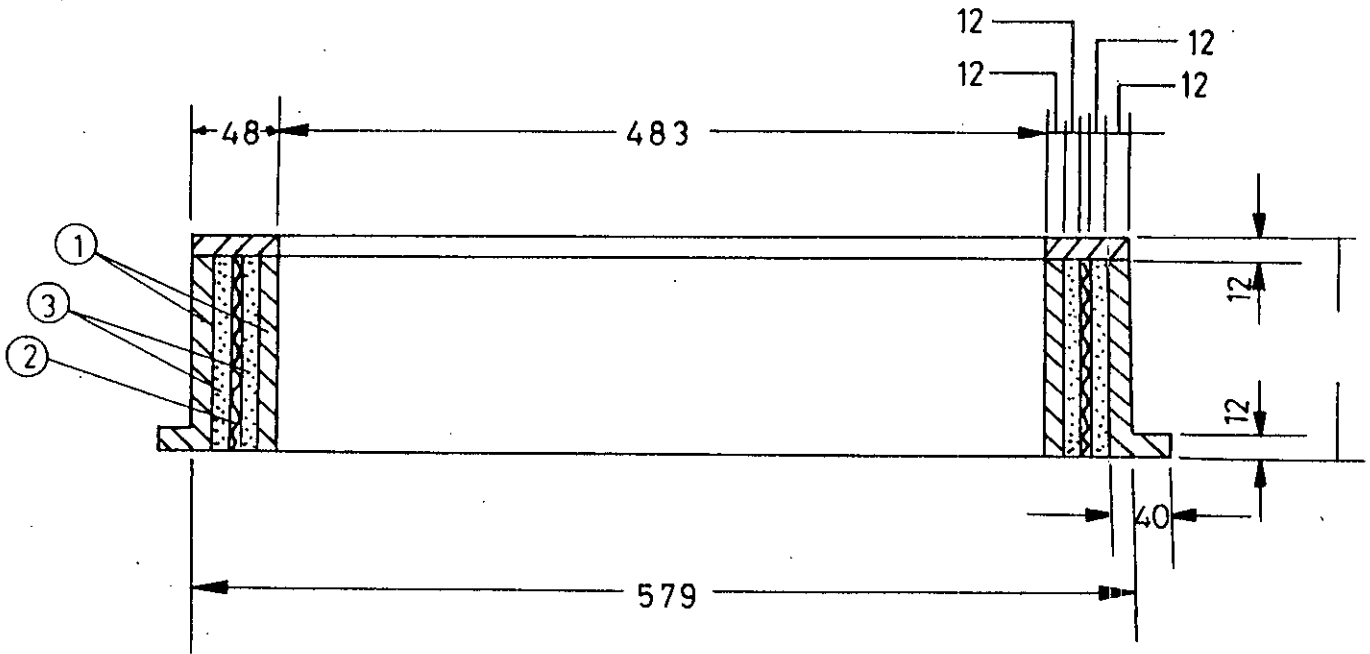
1. INNER AND OUTER WOODEN RING.
2. UPPER OUTER GUARD HEATER.
3. INNER AND OUTER ASBESTOS RING.

FIG.44 DETAILS OF UPPER GUARD HEATER RING.
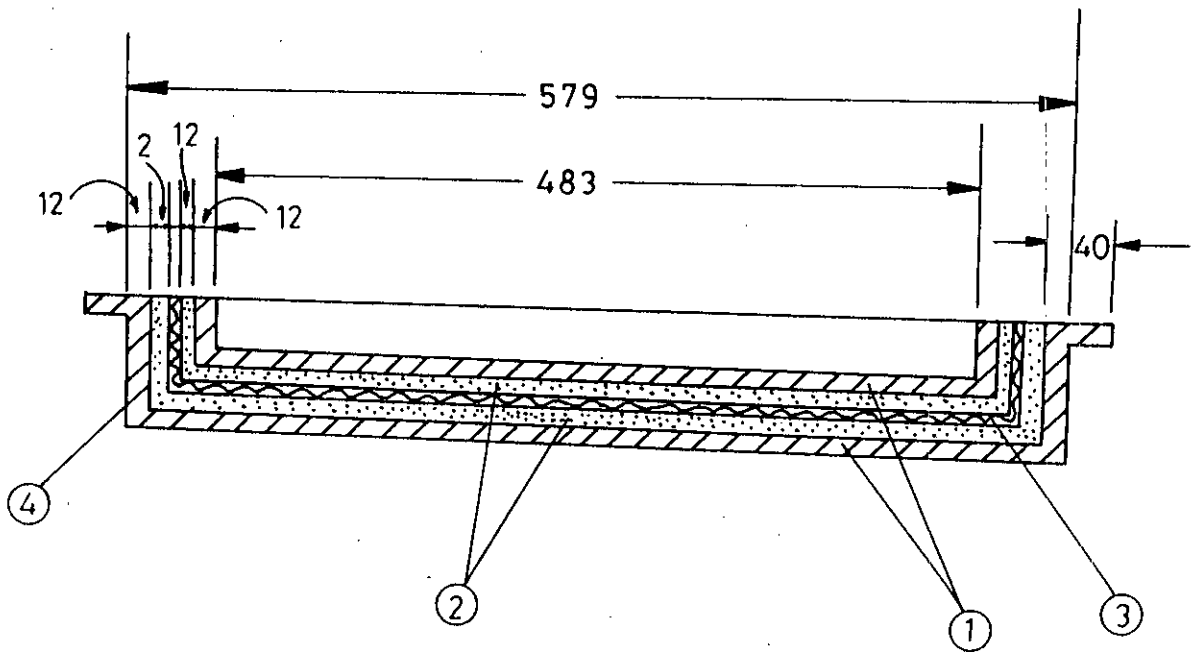
1. INNER AND OUTER WOODEN BOX.
2. ASBESTOS    INSULATION.
3. BOTTOM  GUARD  HEATER.
4. LOWER  OUTER GUARD  HEATER. RING

FIG:4.5 DETAILS OF LOWER  OUTER  GUARD  HEATER BOX.
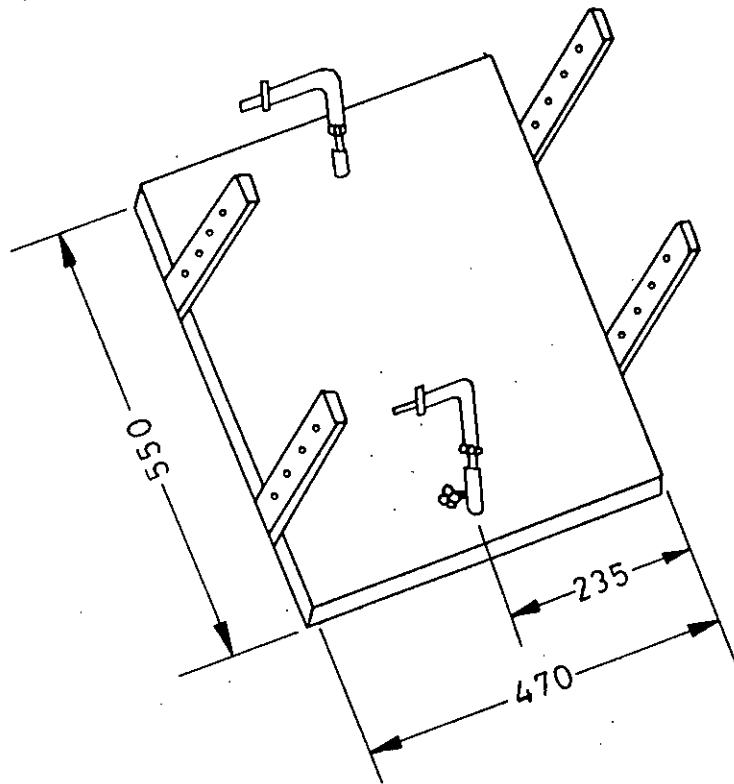
FIG:4.6 DETAILS OF THE COLD PLATE ASSEMBLY
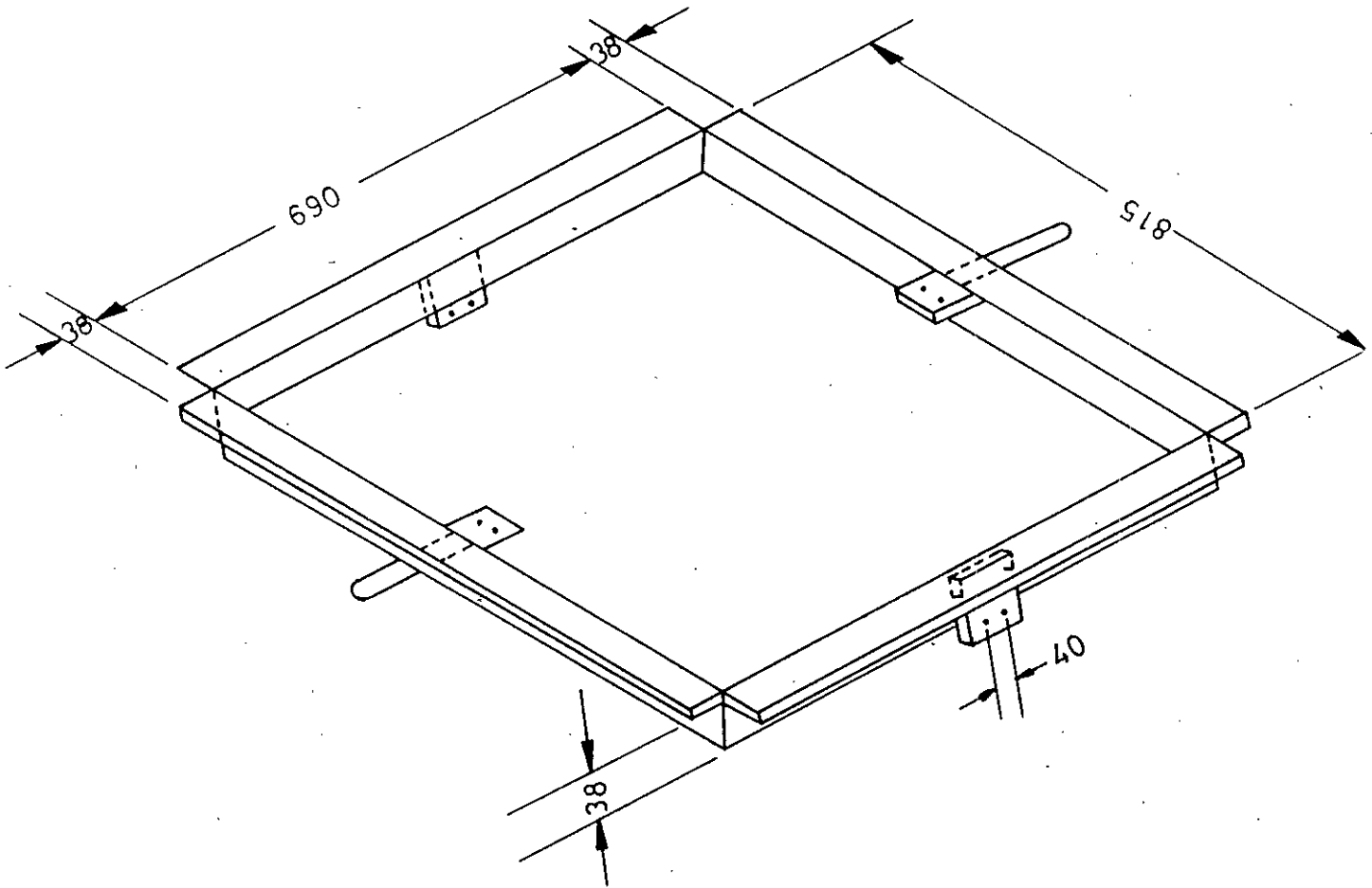
FIG: 4.7   THE   RECTANGULAR   SUPPORTING   FRAME
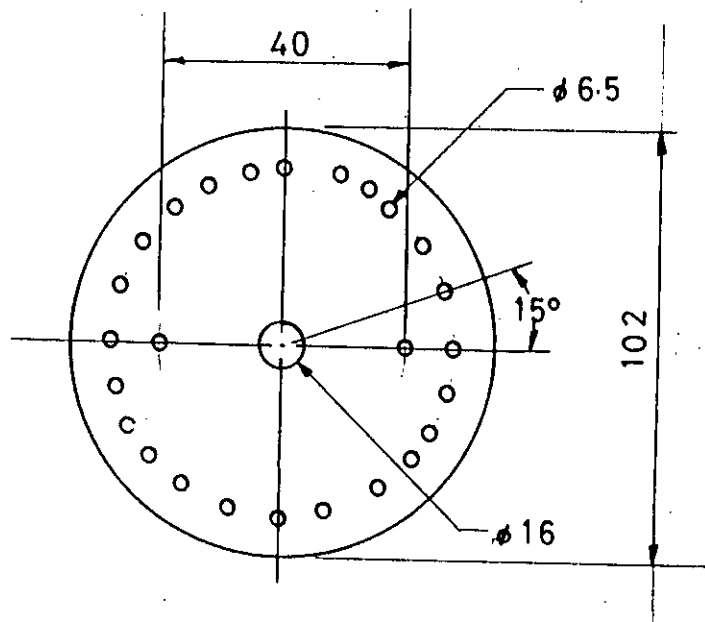
FIG.4.8 ALIGNMENT PLATE
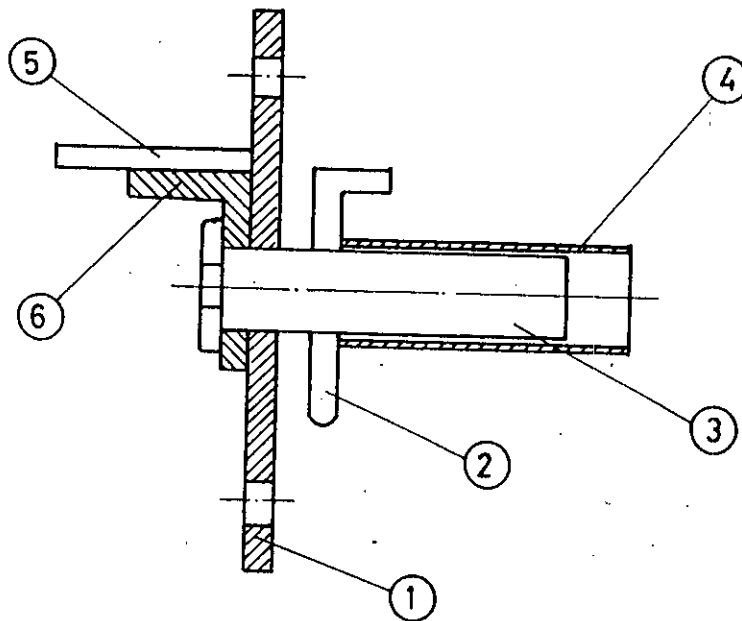


1. ALIGNMENT PLATE

2. SUPPORTING STAND

3. SUPPORTING BOLT

4. SUPPORTING BOLT HOLDER

5. SUPPORTING FRAME

6. OVER HANGING SIDE SUPPORT

FIG.4.9 CONNECTING ASSEMBLY OF RECTANGULAR SUPPORTING FRAME AND SUPPORTING STAND.

68
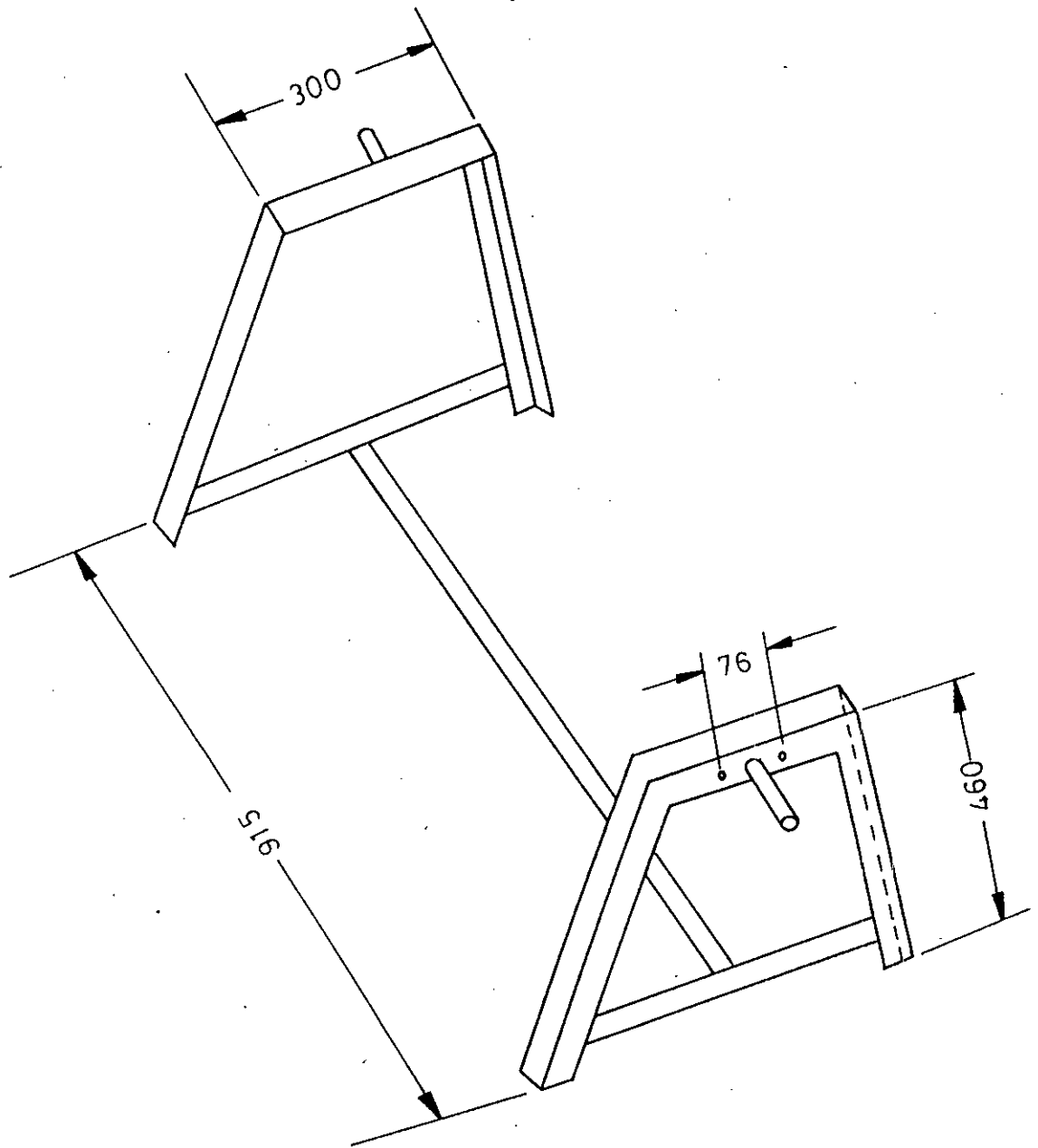
FIG:4.10 THE SUPPORTING FRAME
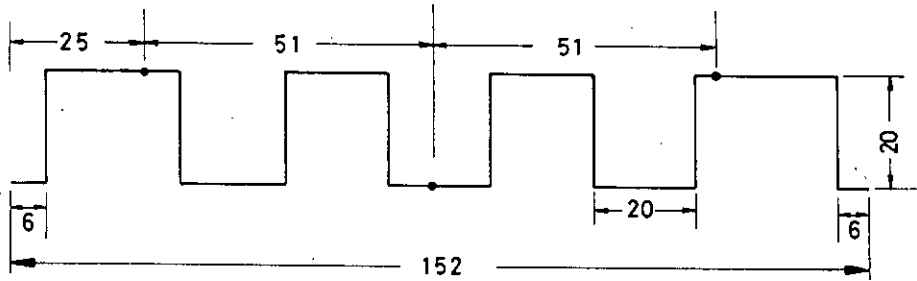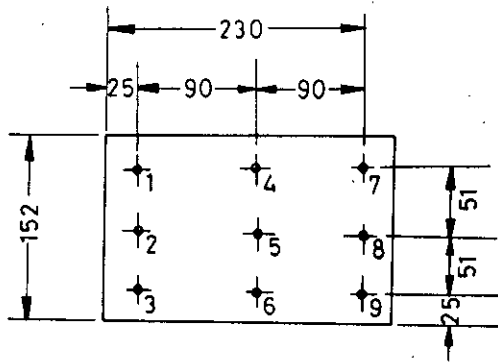
POSITION OF THERMOCOUPLES IN THE TEST SECTION OF THE HOT
SQUARE CORRUGATED PLATE OF H = 10MM.
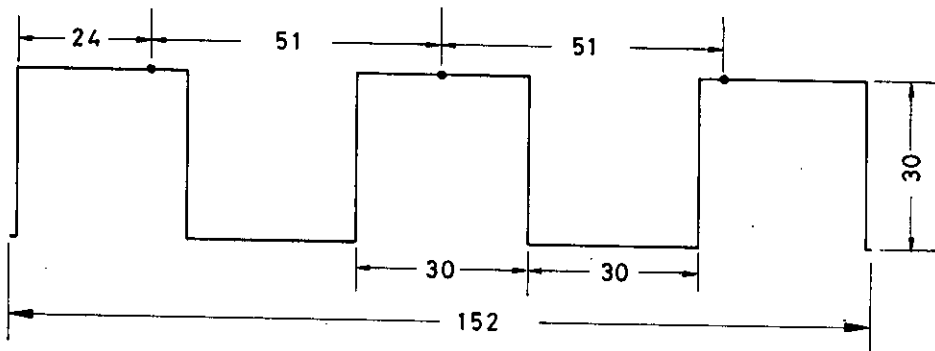
POSITION OF THERMOCOUPLES IN THE TEST SECTION OF THE HOT
SQUARE CORRUGATED PLATE OF H = 15MM.
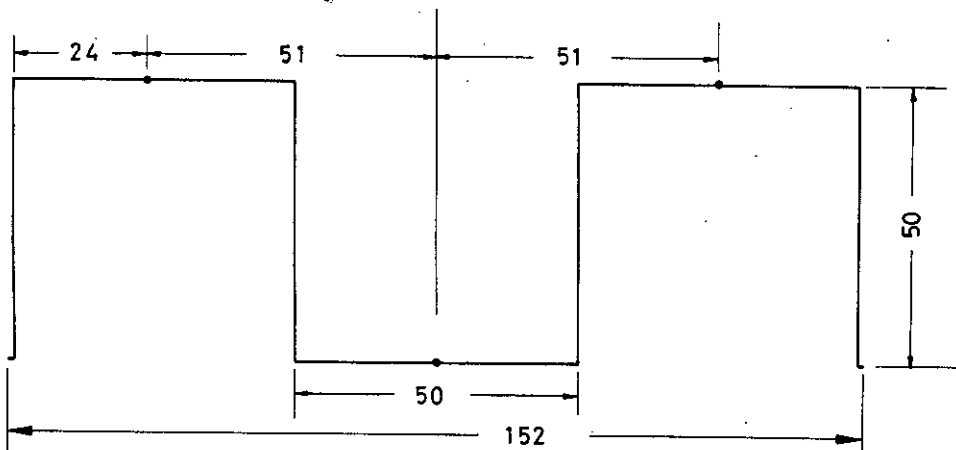
POSITION OF THERMOCOUPLES IN THE TEST SECTION OF THE HOT
SQUARE CORRUGATED PLATE OF H = 25MM.

FIG:5.1 POSITION OF THERMOCOUPLES IN THE TEST
SECTION OF THE HOT PLATE

70
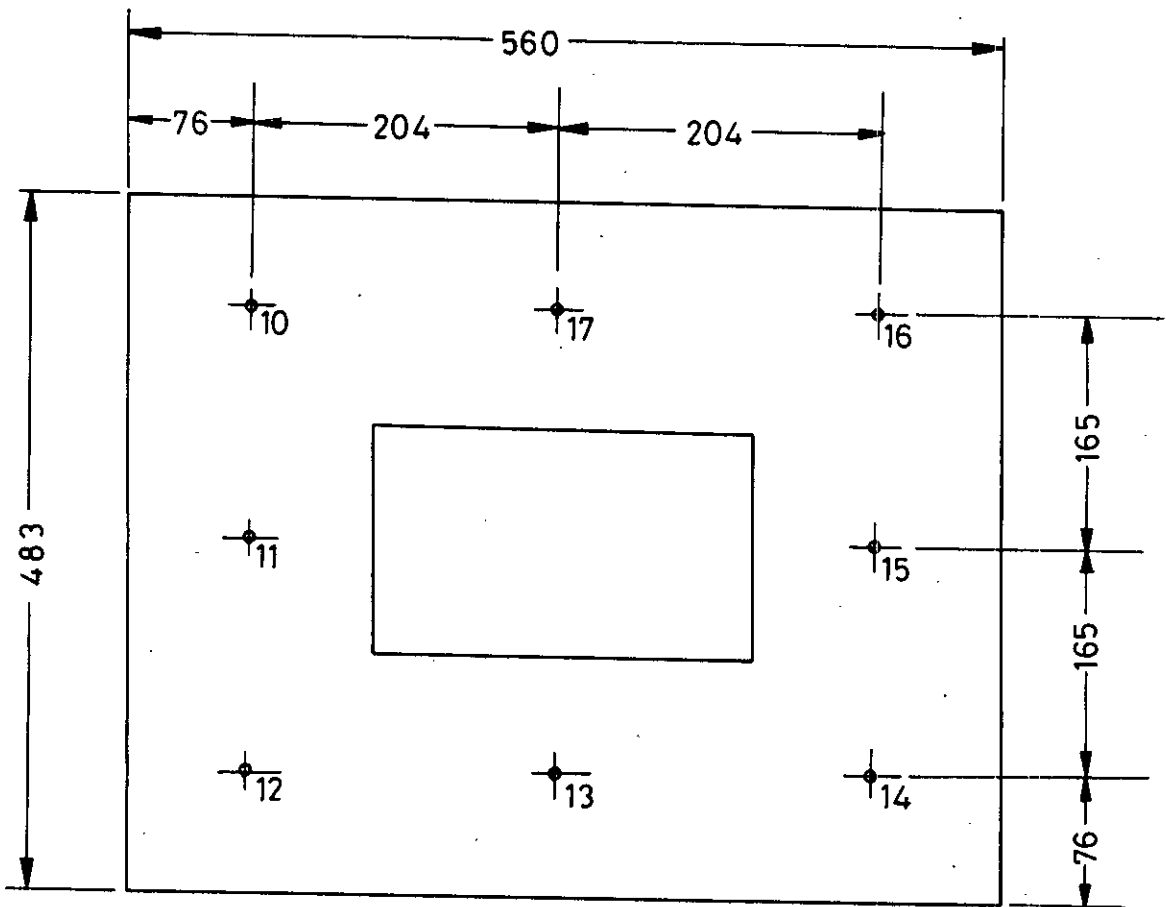
FIG:52 POSITION OF THERMOCOUPLES IN OUTER END AND
SIDE GUARD HEATER SECTIONS

71
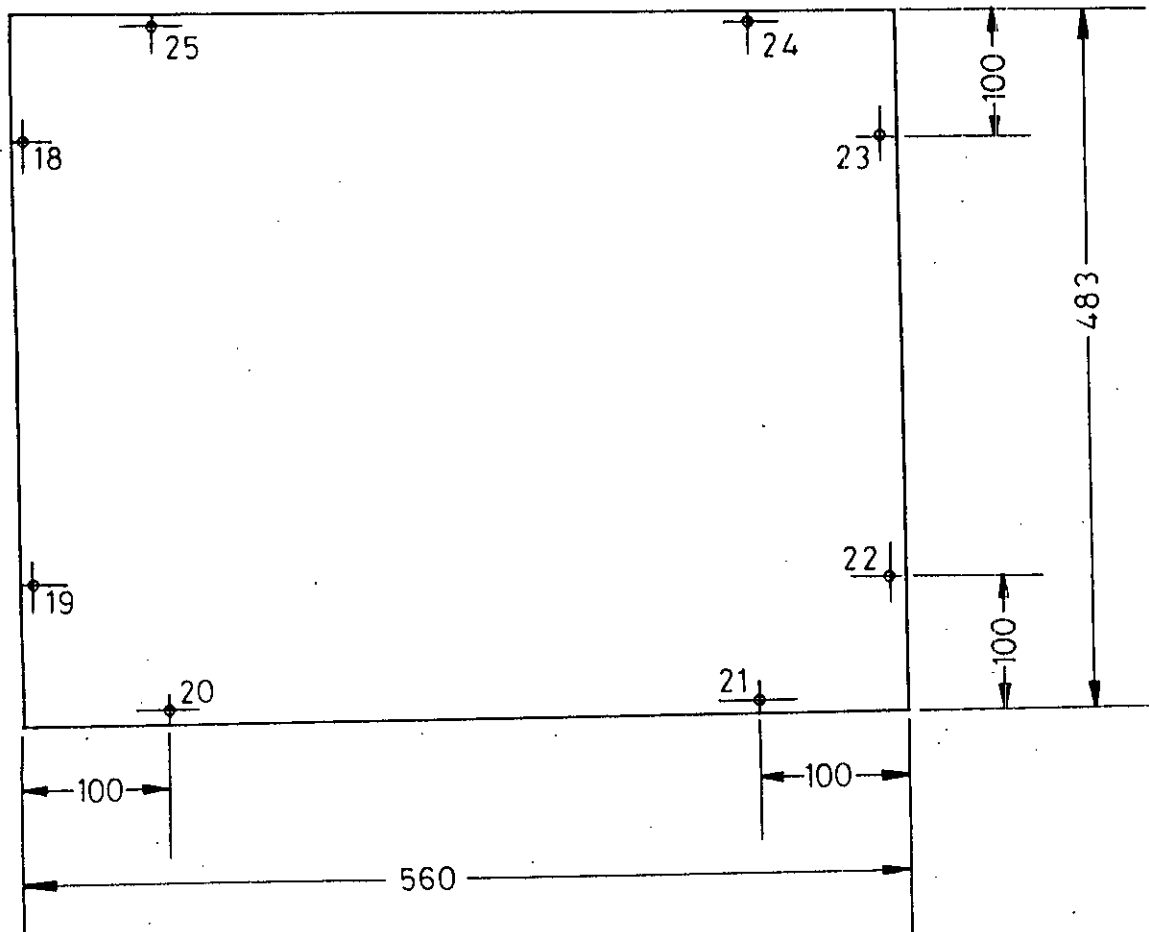
FIG:5.3 POSITION OF THERMO COUPLES IN UPPER
OUTER GUARD HEATER RING.
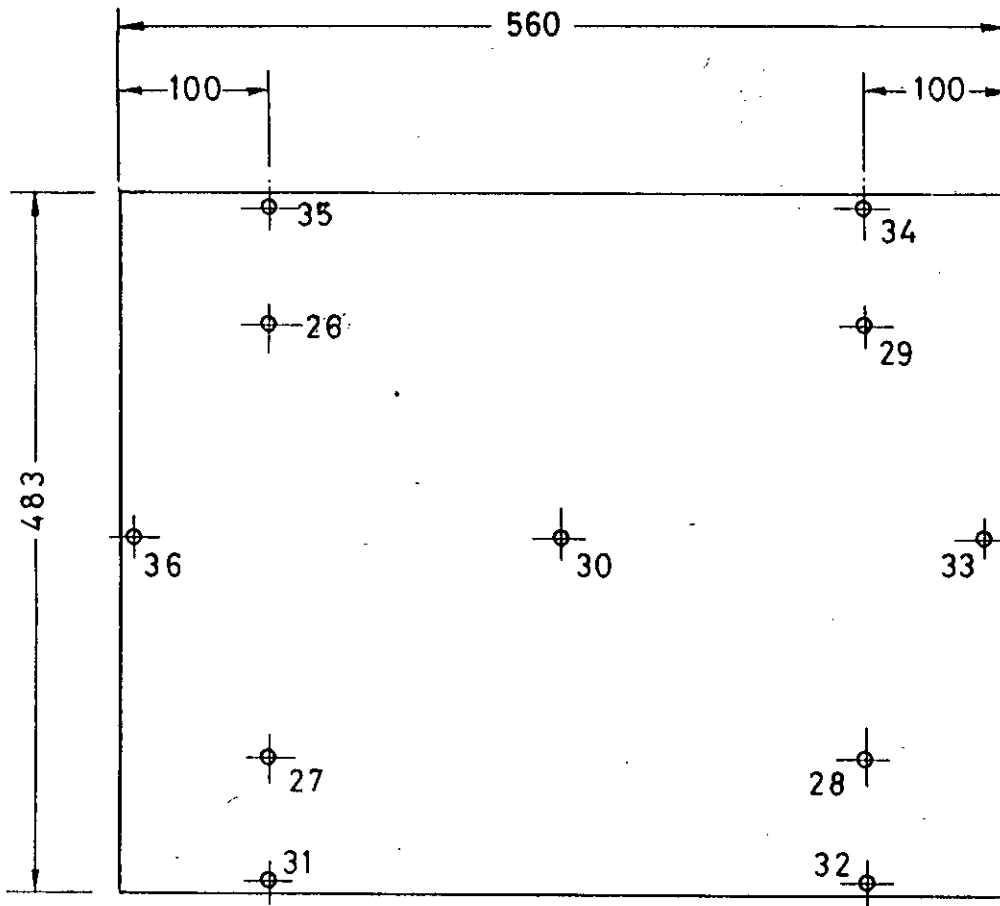
FIG.5.4 POSITION OF THERMOCOUPLES IN LOWER OUTER-GUARD HEATER BOX
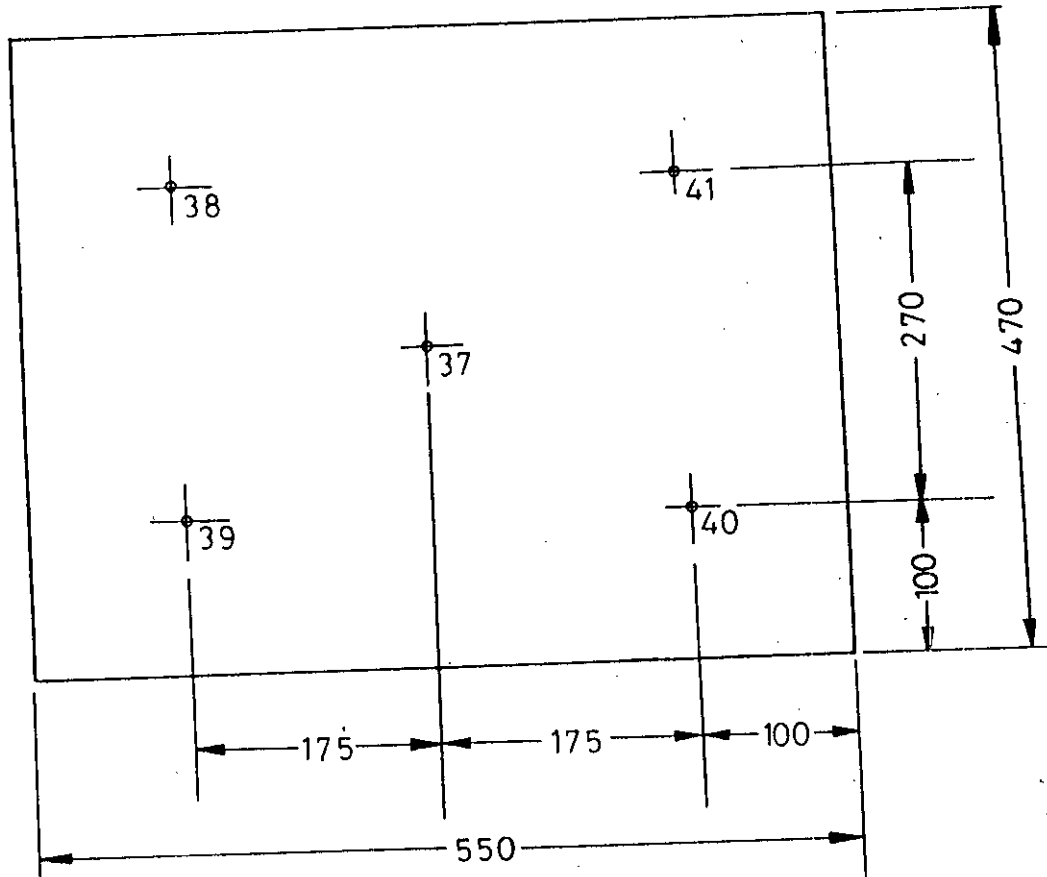
FIG:5.5 POSITION OF THERMO COUPLES IN
COLD FLAT PLATE.
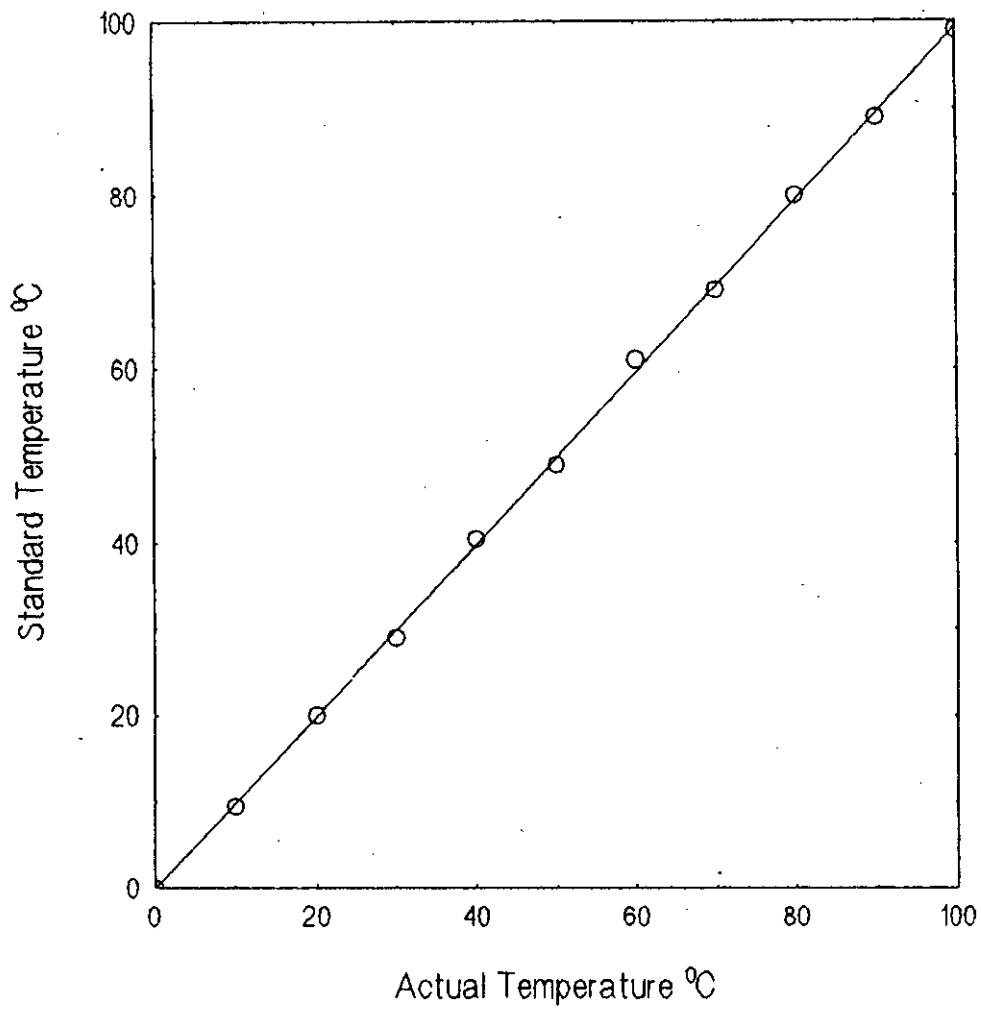
FIG. 5.6:  THERMOCOUPLE    CALIBRATION    CURVE    FOR
THERMOCOUPLE  NO. 5.
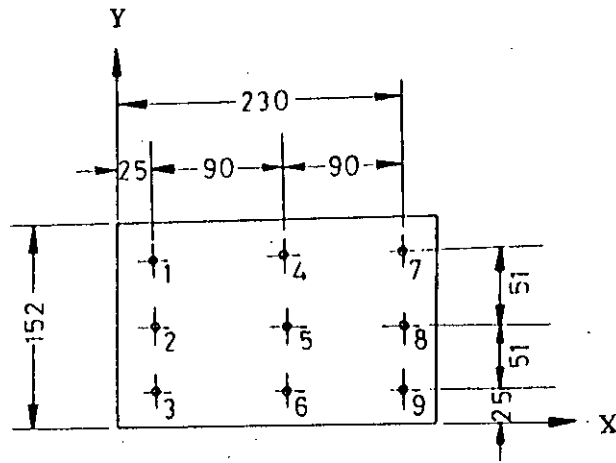
POSITION OF THERMOCOUPLES IN THE TEST
SECTION OF THE HOT PLATE

H = 10mm, θ = 0°
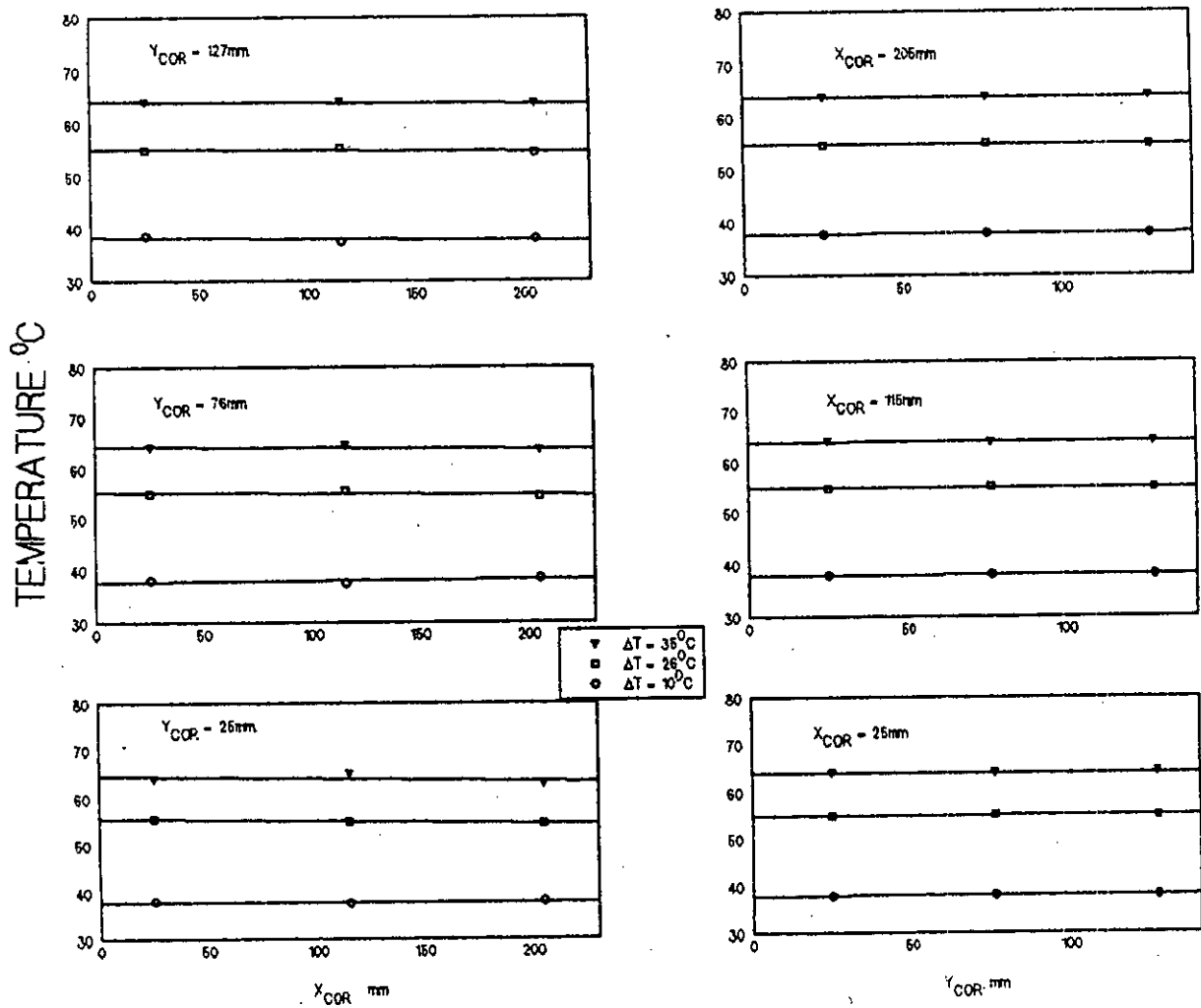


FIG. 6.1:   TEMPERATURE DISTRIBUTION OVER THE TEST SECTION
OF THE HOT SQUARE CORRUGATED PLATE OF
H = 10MM.
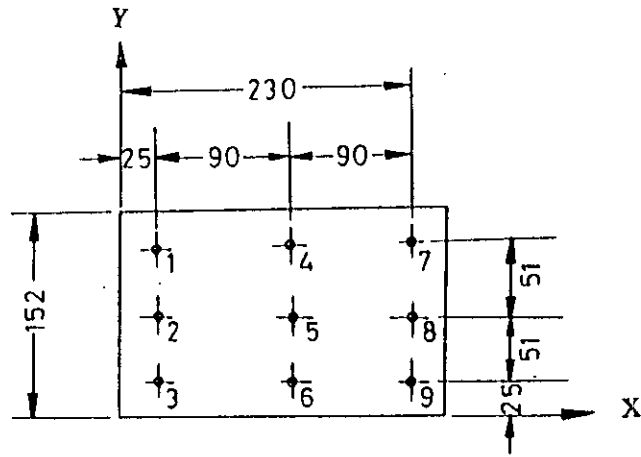
POSITION OF THERMOCOUPLES IN THE TEST
SECTION OF THE HOT PLATE

$H = 15mm, \theta = 45^0$
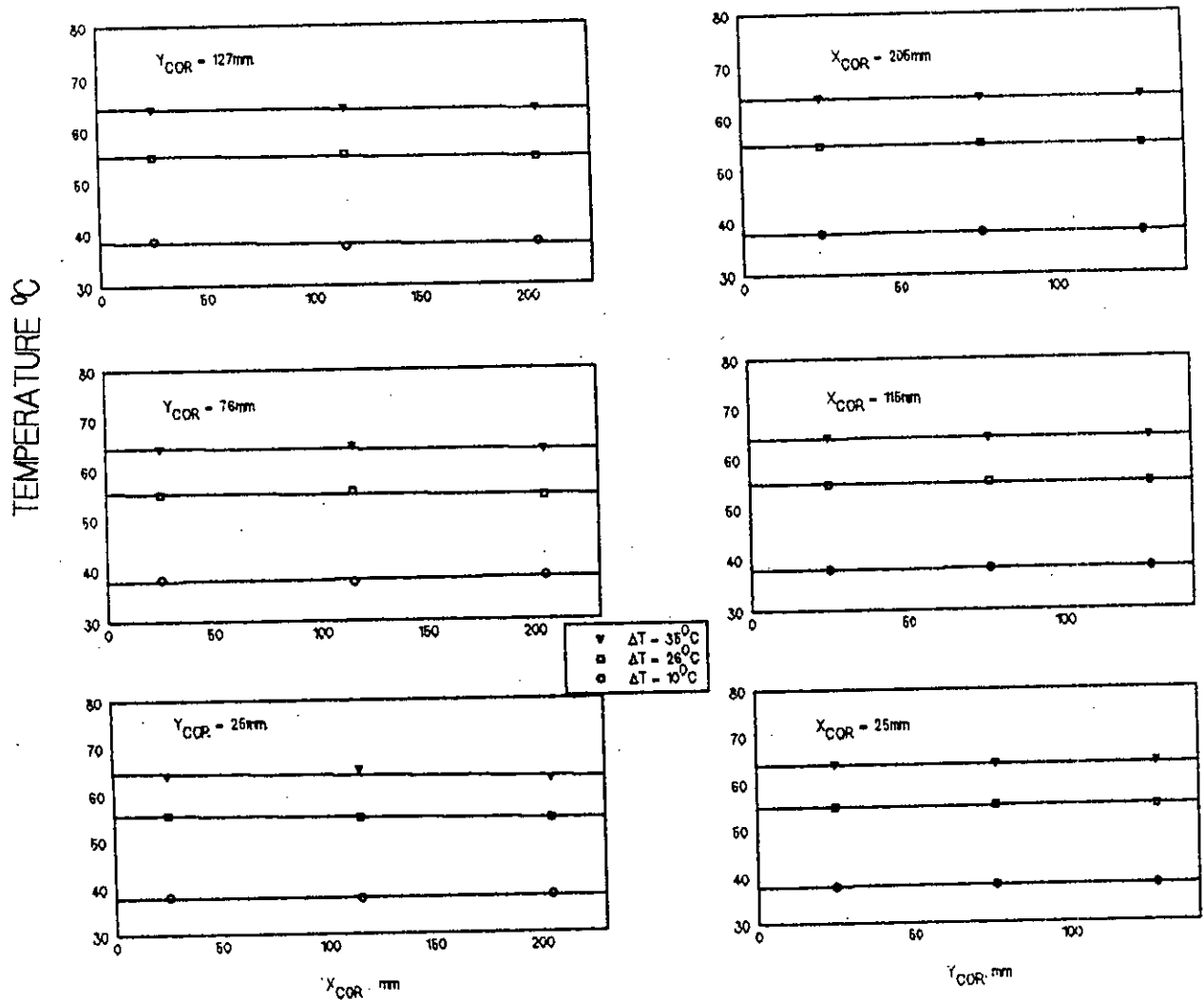


FIG. 6.2:  TEMPERATURE DISTRIBUTION OVER THE TEST SECTION
OF THE HOT SQUARE CORRUGATED PLATE OF
H = 15MM.
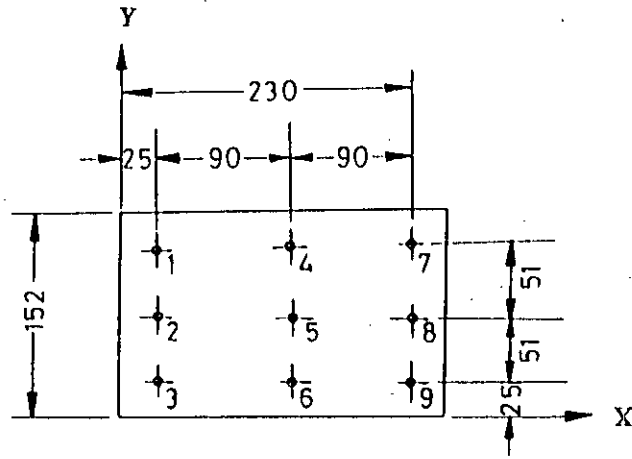
POSITION OF THERMOCOUPLES IN THE TEST
SECTION OF THE HOT PLATE

$H = 25mm, \theta = 75^0$
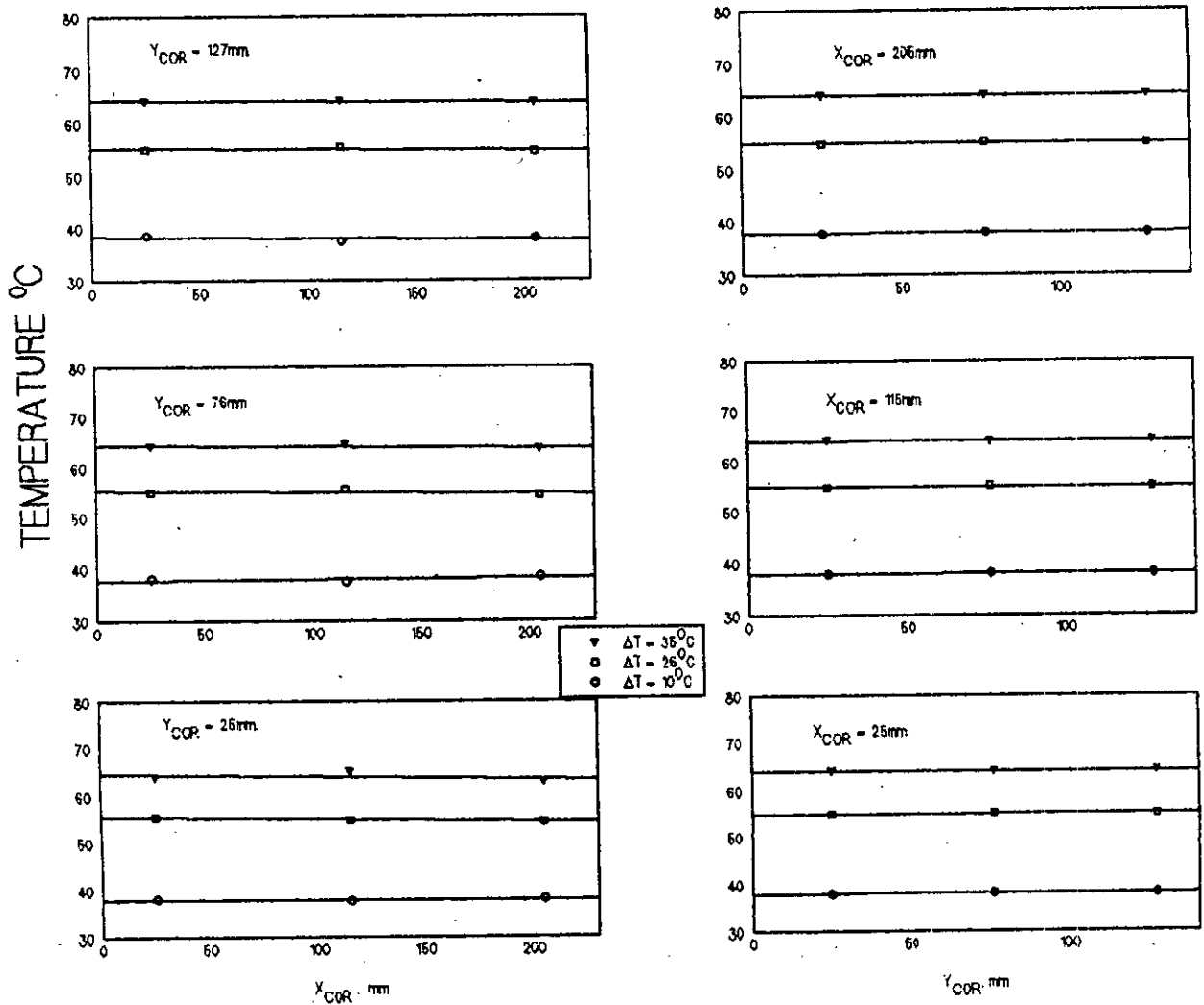


FIG. 6.3:    TEMPERATURE DISTRIBUTION OVER THE TEST SECTION
OF THE HOT SQUARE CORRUGATED PLATE OF
H = 25MM.

78
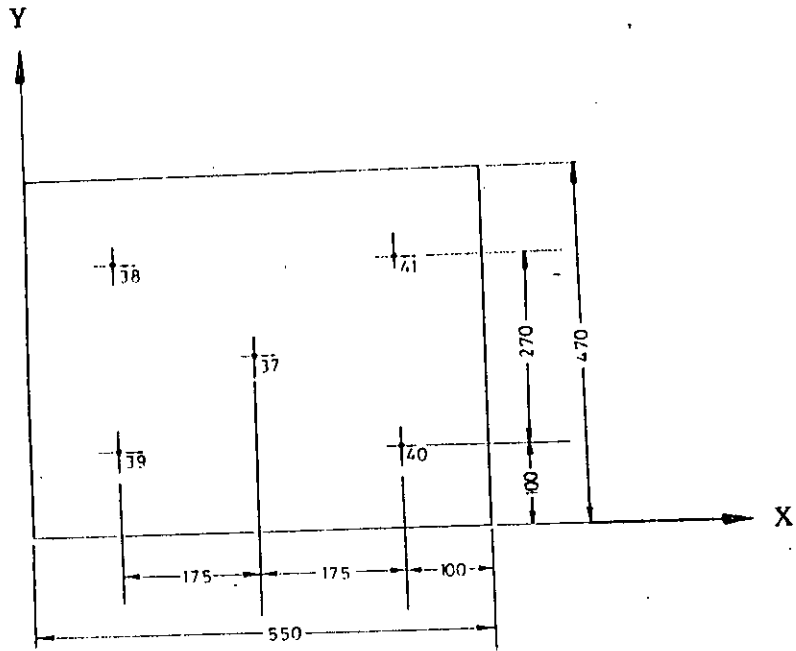
POSITION OF THERMO COUPLES IN
COLD FLAT PLATE.

H = 10mm, θ = 0⁰
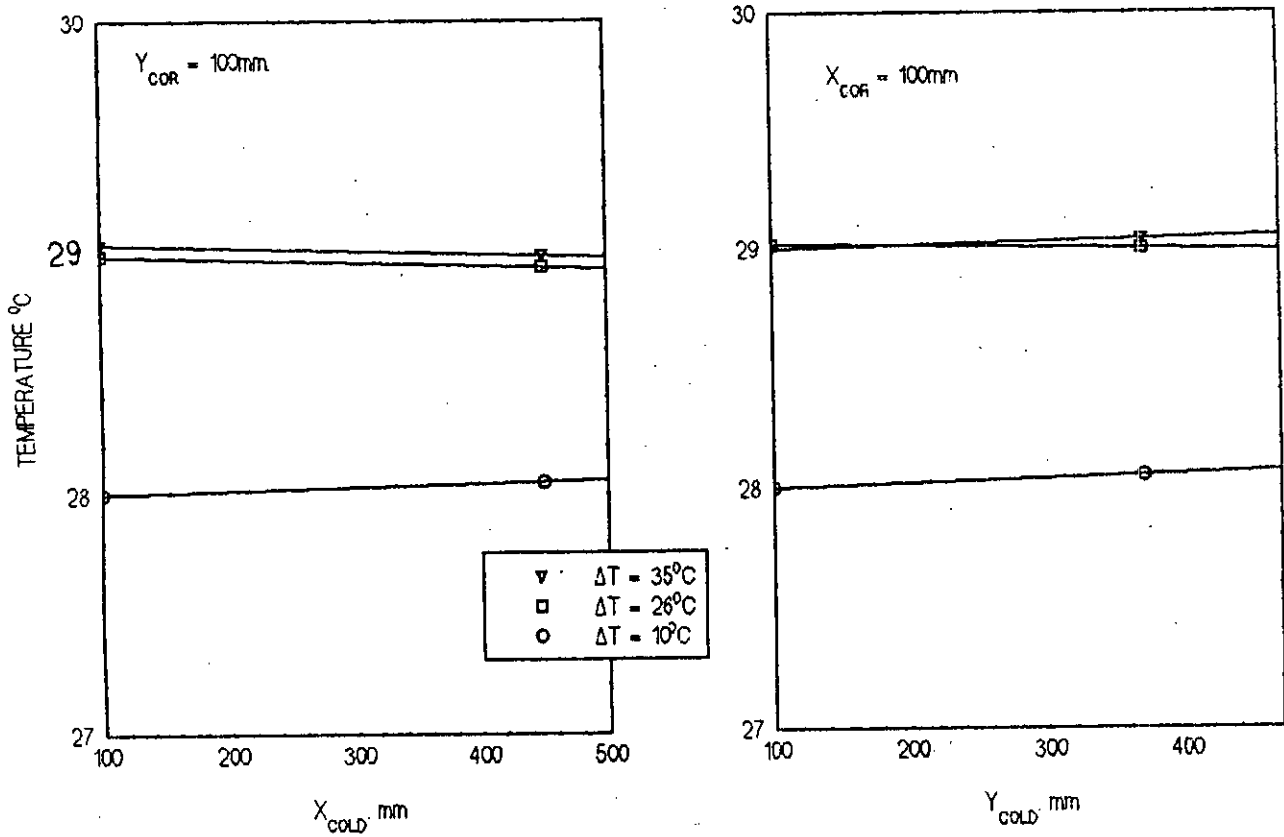


FIG. 6.4: TEMPERATURE DISTRIBUTION OVER THE COLD FLAT
PLATE FOR H = 10MM.

79

POSITION OF THERMO COUPLES IN COLD FLAT PLATE.

$H = 15mm, \theta = 45^0$

$Y_{COR} = 100mm$

$X_{COR} = 100mm$

TEMPERATURE $^0C$

$X_{COLD}$ mm

$Y_{COLD}$ mm

| | |
|---|---|
| ∇ | $\Delta T = 35^0C$ |
| ▫ | $\Delta T = 26^0C$ |
| ○ | $\Delta T = 10^0C$ |
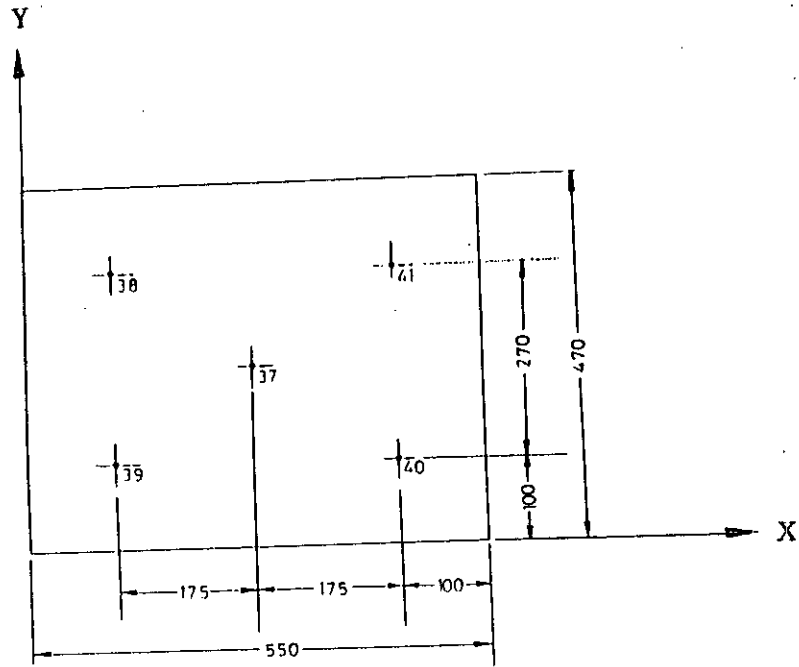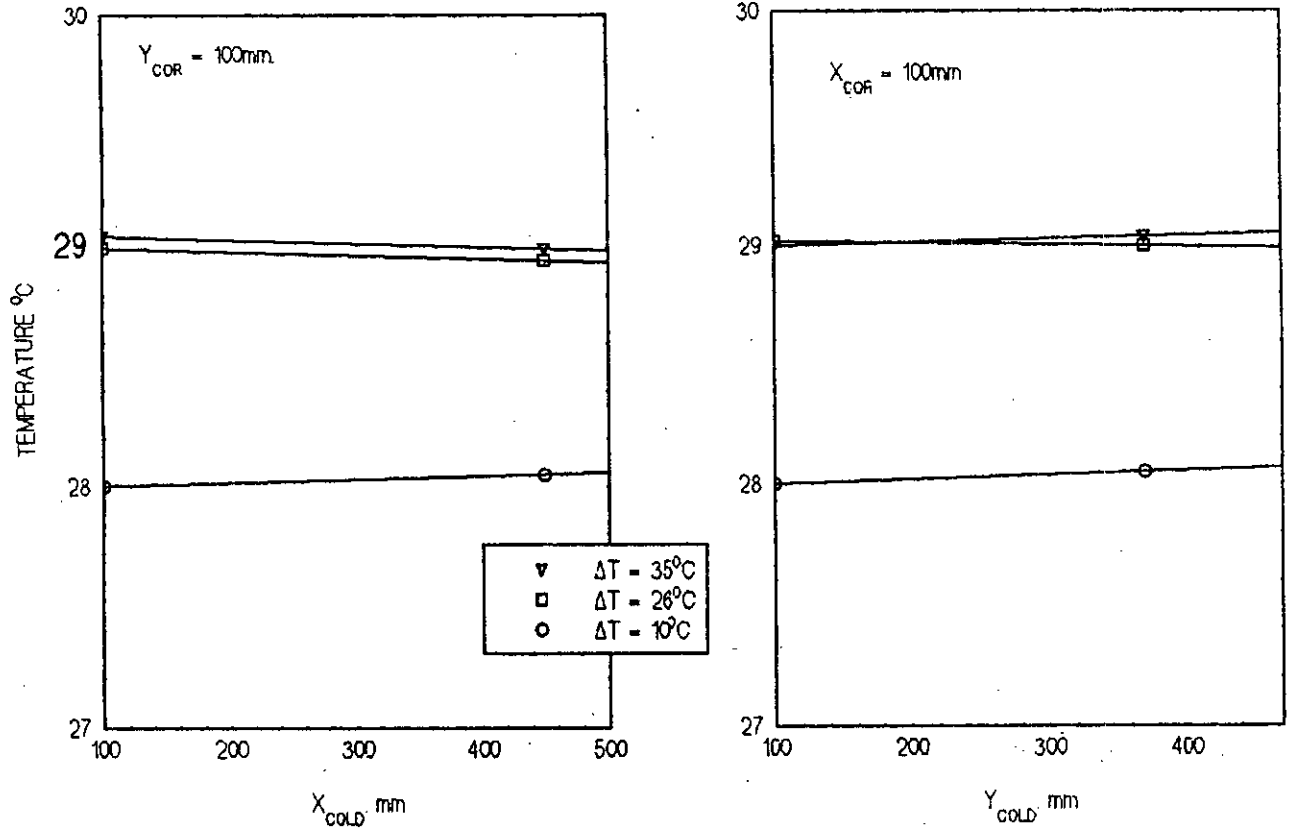
FIG. 6.5: TEMPERATURE DISTRIBUTION OVER THE COLD FLAT PLATE FOR H = 15MM.

80
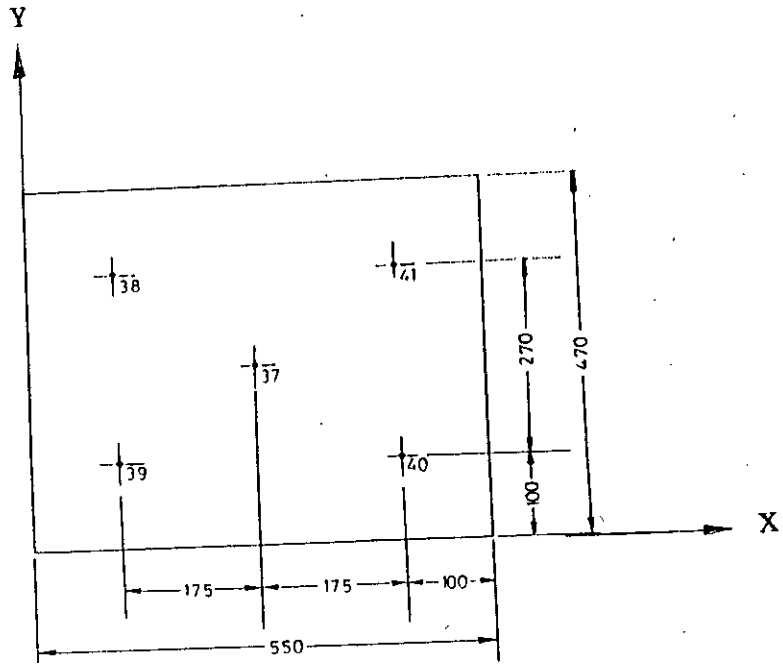
POSITION OF THERMO COUPLES IN
COLD FLAT PLATE.

$$H = 25mm., \theta = 75^0$$
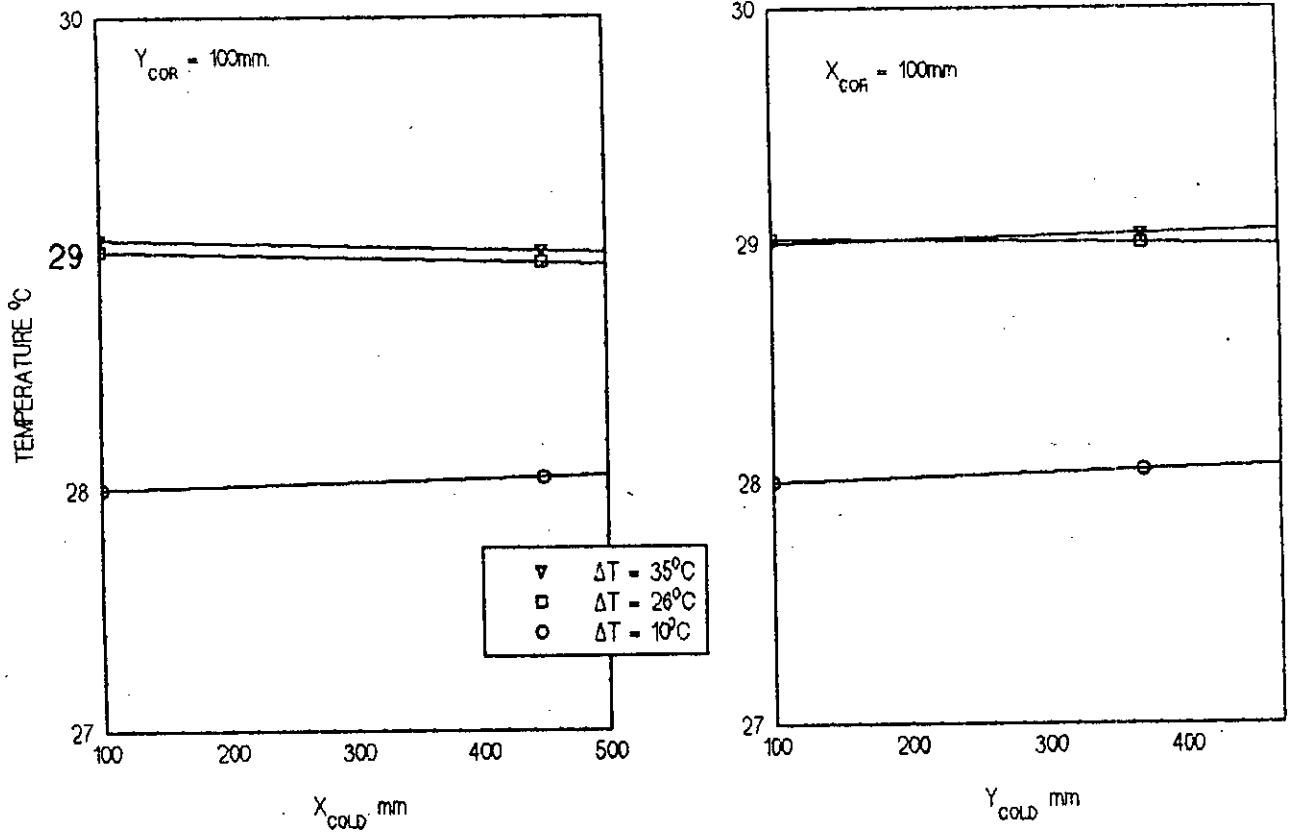


FIG. 6.6:    TEMPERATURE  DISTRIBUTION  OVER  THE  COLD  FLAT
PLATE FOR H = 25MM.

81
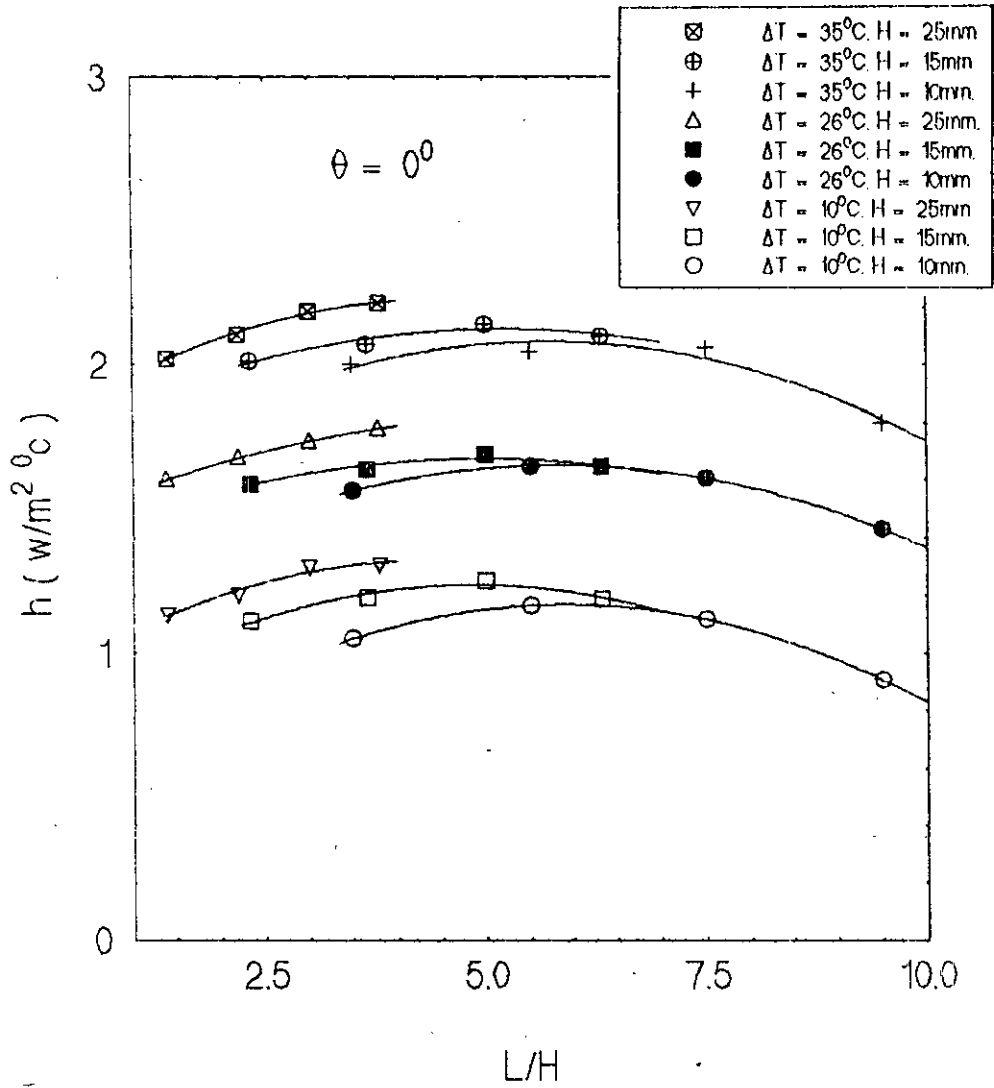
FIG. 6.7: EFFECT OF ASPECT RATIO (A) ON AVERAGE HEAT TRANSFER COEFFICIENT FOR $\theta = 0^0$.

82
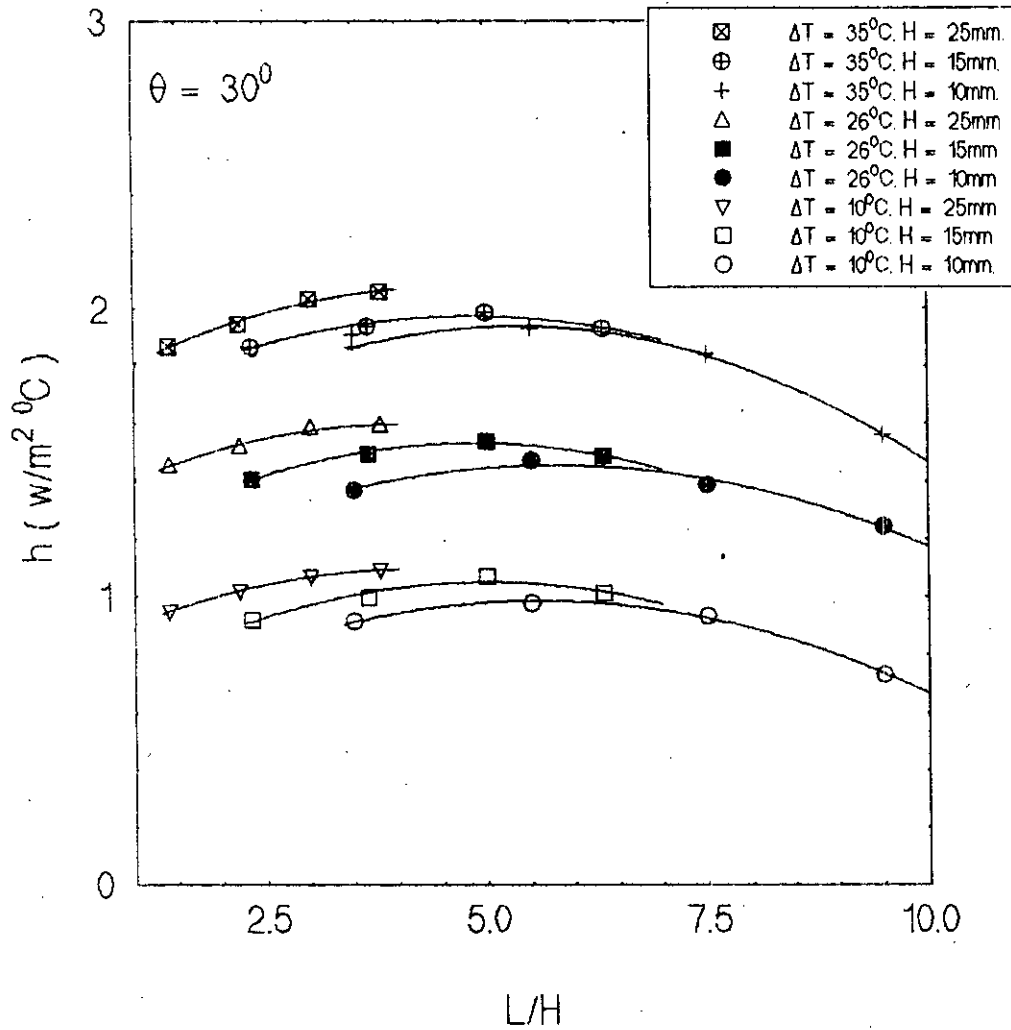
FIG. 6.8: EFFECT OF ASPECT RATIO (A) ON AVERAGE HEAT TRANSFER COEFFICIENT FOR $\theta = 30^0$.
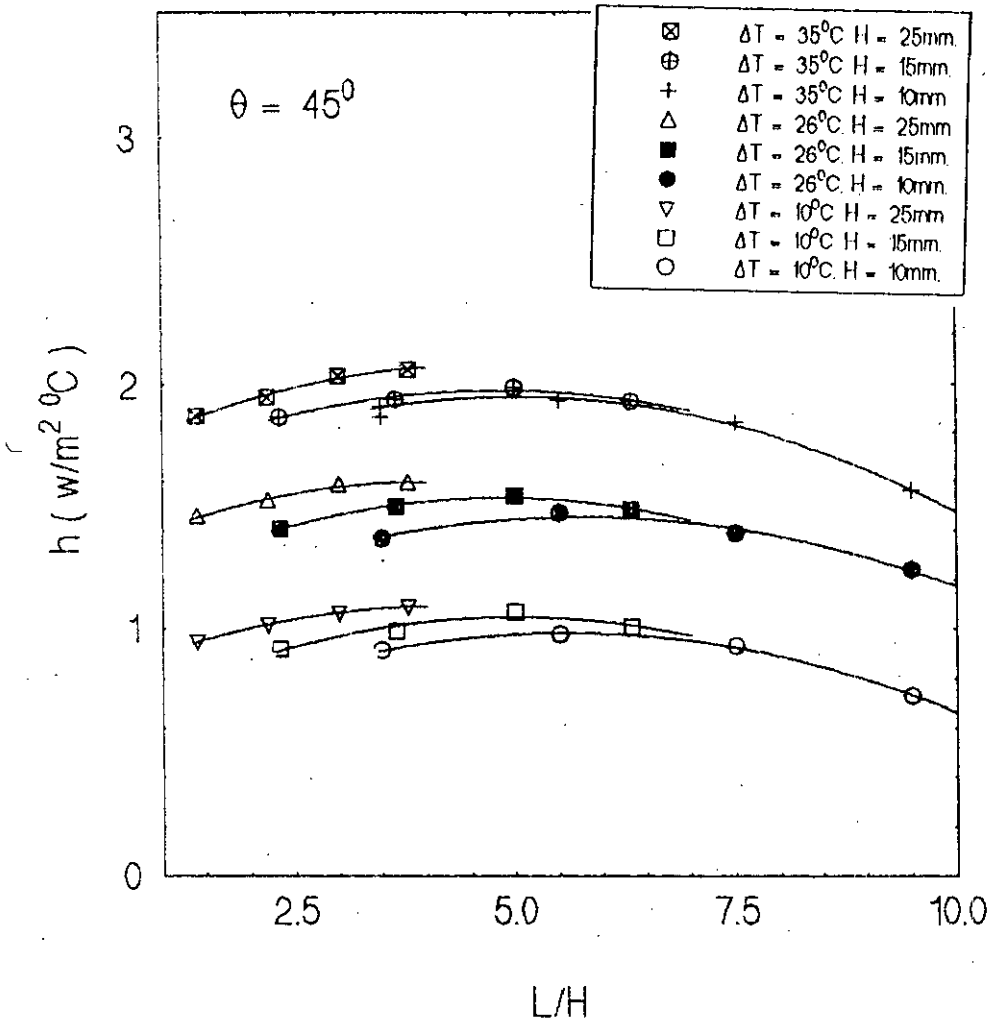
FIG. 6.9: EFFECT OF ASPECT RATIO (A) ON AVERAGE HEAT
TRANSFER COEFFICIENT FOR $\theta = 45^0$.

θ = 75⁰

Legend:
- ⊠  ΔT = 35°C. H = 25mm
- ⊕  ΔT = 35°C. H = 15mm
- +  ΔT = 35°C. H = 10mm
- △  ΔT = 26°C. H = 25mm
- ■  ΔT = 26°C. H = 15mm
- ●  ΔT = 26°C. H = 10mm
- ▽  ΔT = 10°C. H = 25mm
- □  ΔT = 10°C. H = 15mm
- ○  ΔT = 10°C. H = 10mm

y-axis: $h \ (\ w/m^2 \ ^0C\ )$ with values 0, 0.5, 1.0, 1.5

x-axis: L/H with values 2.5, 5.0, 7.5, 10.0
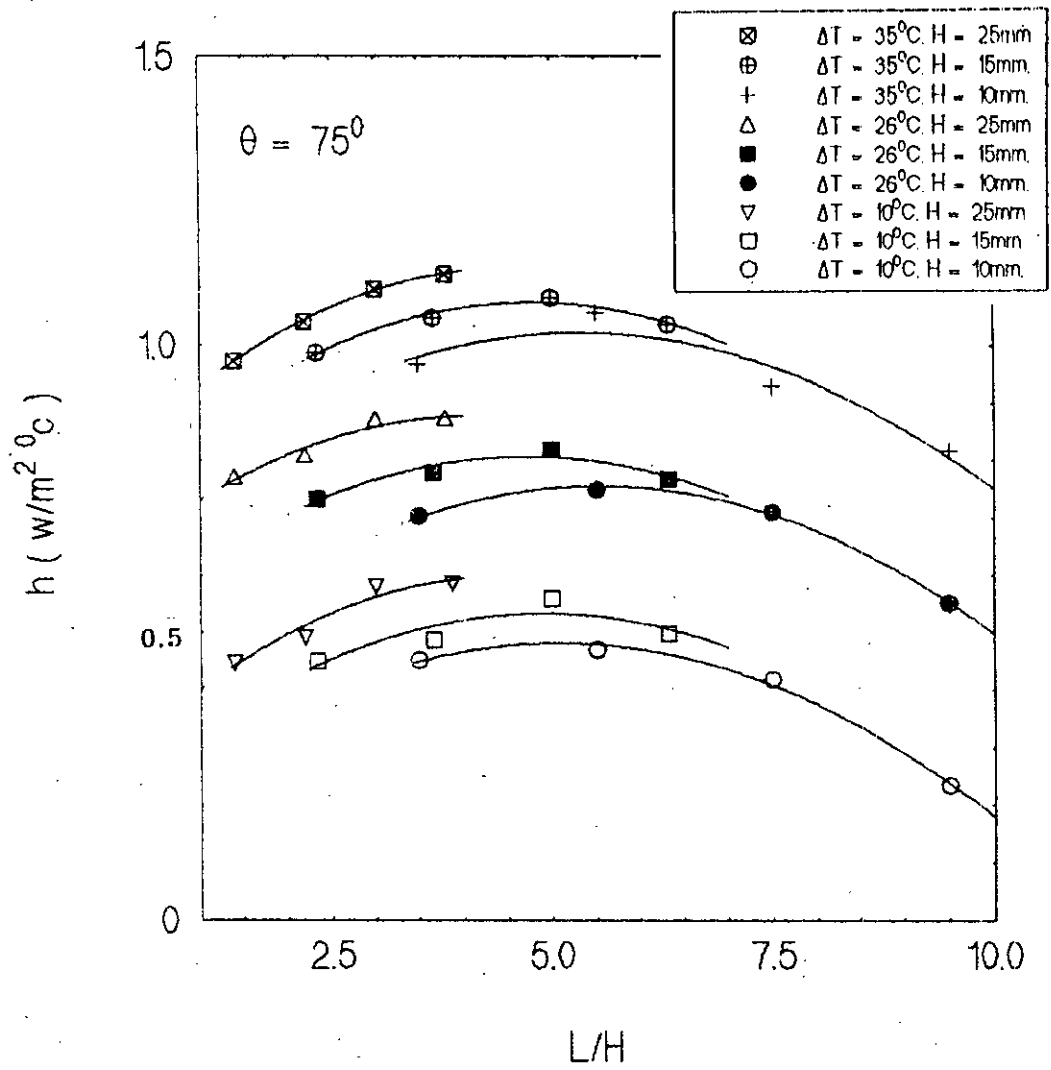
FIG. 6.10.    EFFECT OF ASPECT RATIO (A) ON AVERAGE HEAT
TRANSFER COEFFICIENT FOR θ = 75⁰.

85
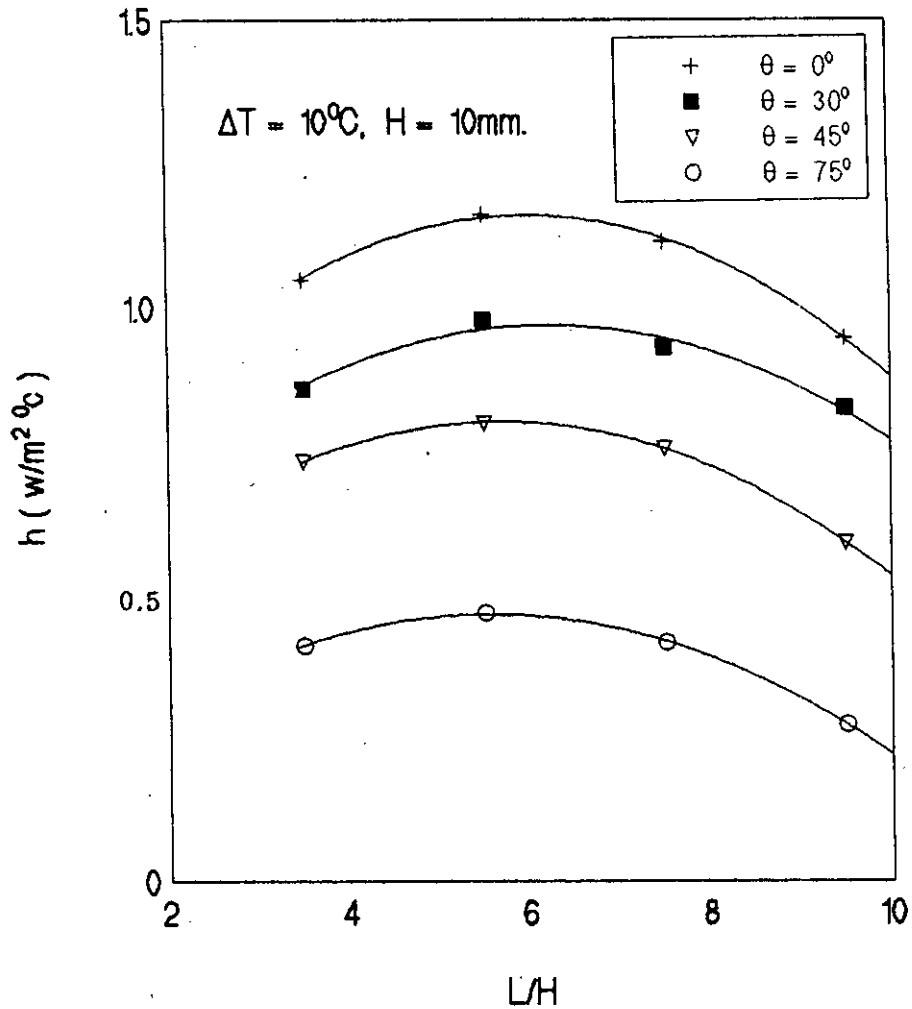
FIG. 6.11:   EFFECT OF ASPECT RATIO (A) ON AVERAGE HEAT
TRANSFER COEFFICIENT FOR DIFFERENT ANGLES OF
INCLINATION.
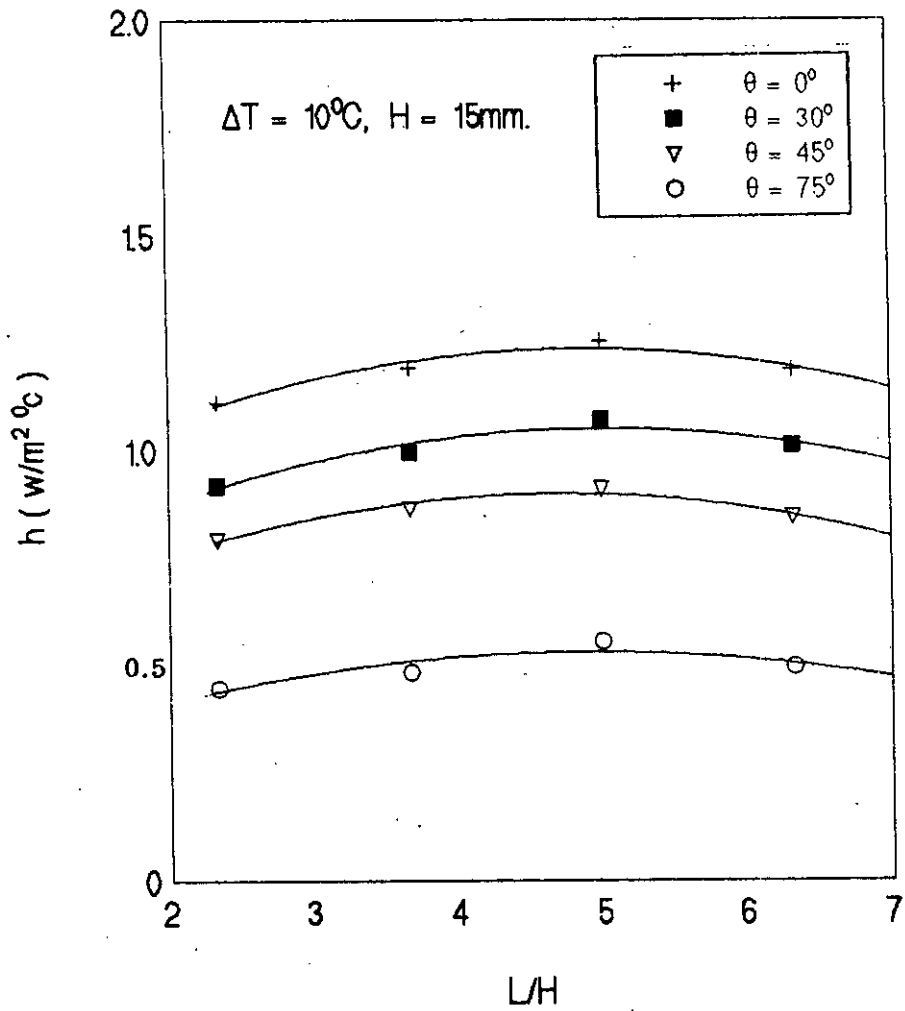
FIG. 6.12: EFFECT OF ASPECT RATIO (A) ON AVERAGE HEAT TRANSFER COEFFICIENT FOR DIFFERENT ANGLES OF INCLINATION.
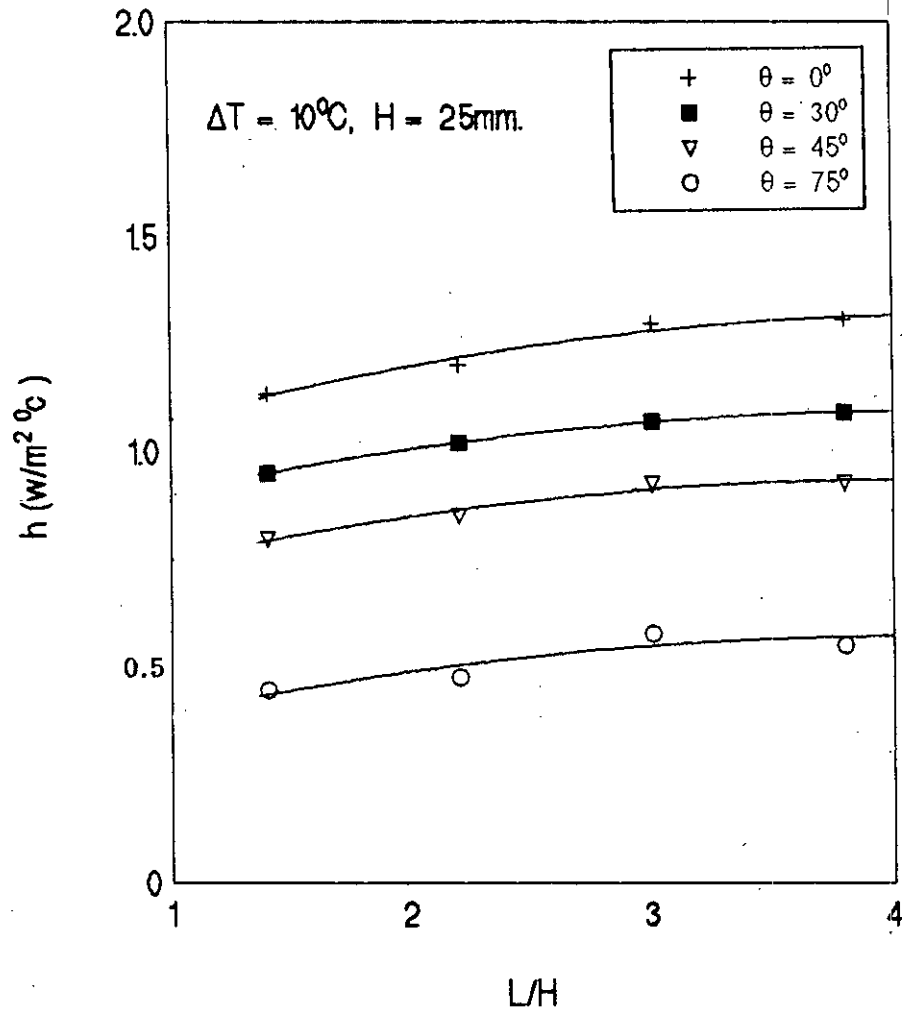
FIG. 6.13: EFFECT OF ASPECT RATIO (A) ON AVERAGE HEAT TRANSFER COEFFICIENT FOR DIFFERENT ANGLES OF INCLINATION.
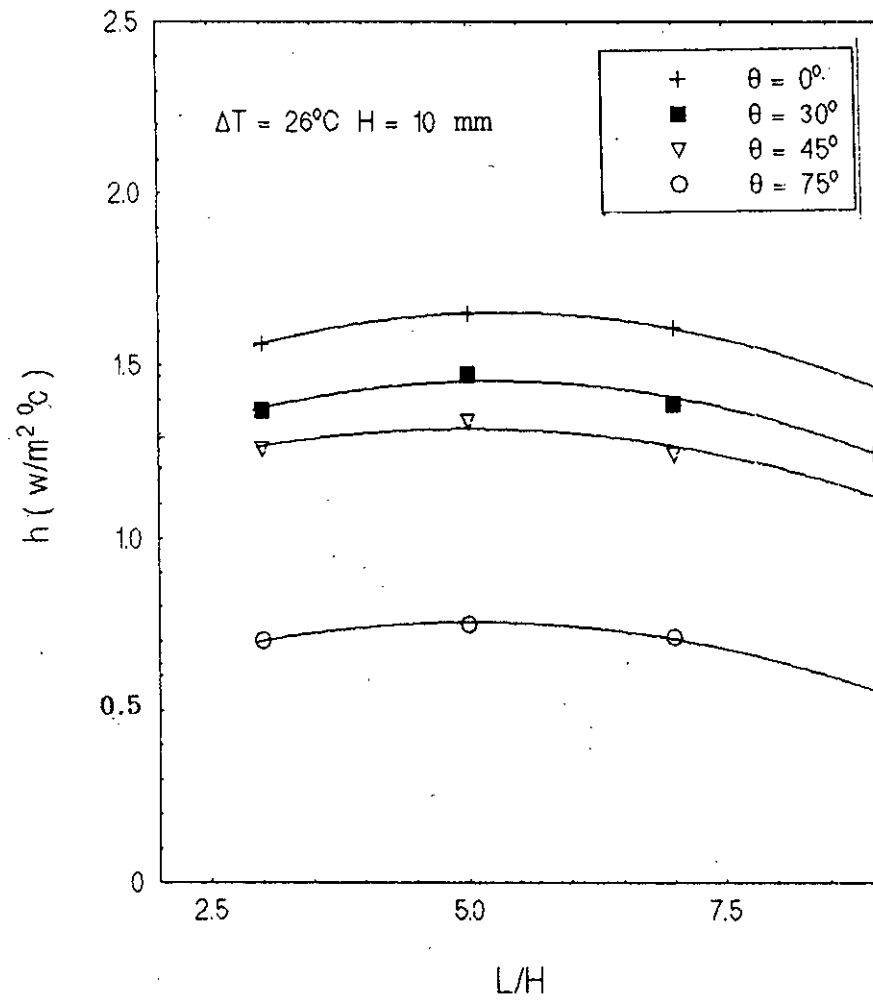
FIG. 6.14: EFFECT OF ASPECT RATIO (A) ON AVERAGE HEAT TRANSFER COEFFICIENT FOR DIFFERENT ANGLES OF INCLINATION.
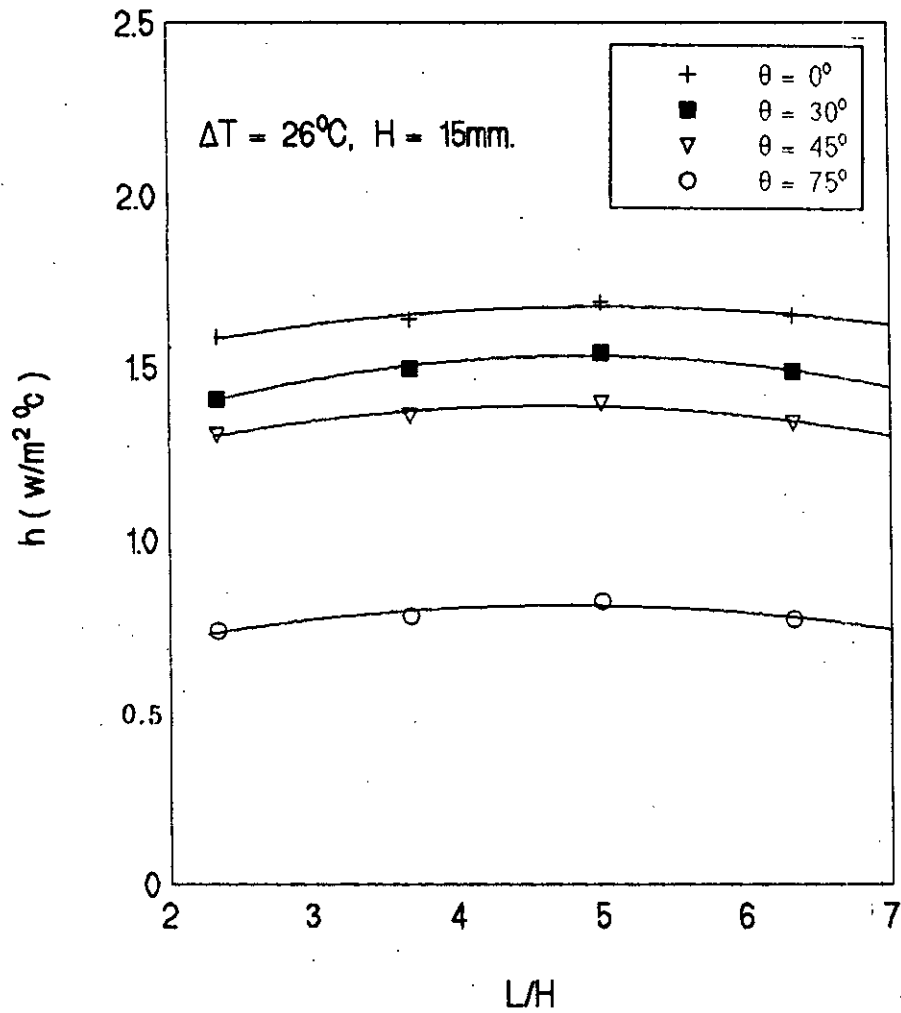
FIG. 6.15:    EFFECT OF ASPECT RATIO (A) ON AVERAGE HEAT
TRANSFER COEFFICIENT FOR DIFFERENT ANGLES OF
INCLINATION.
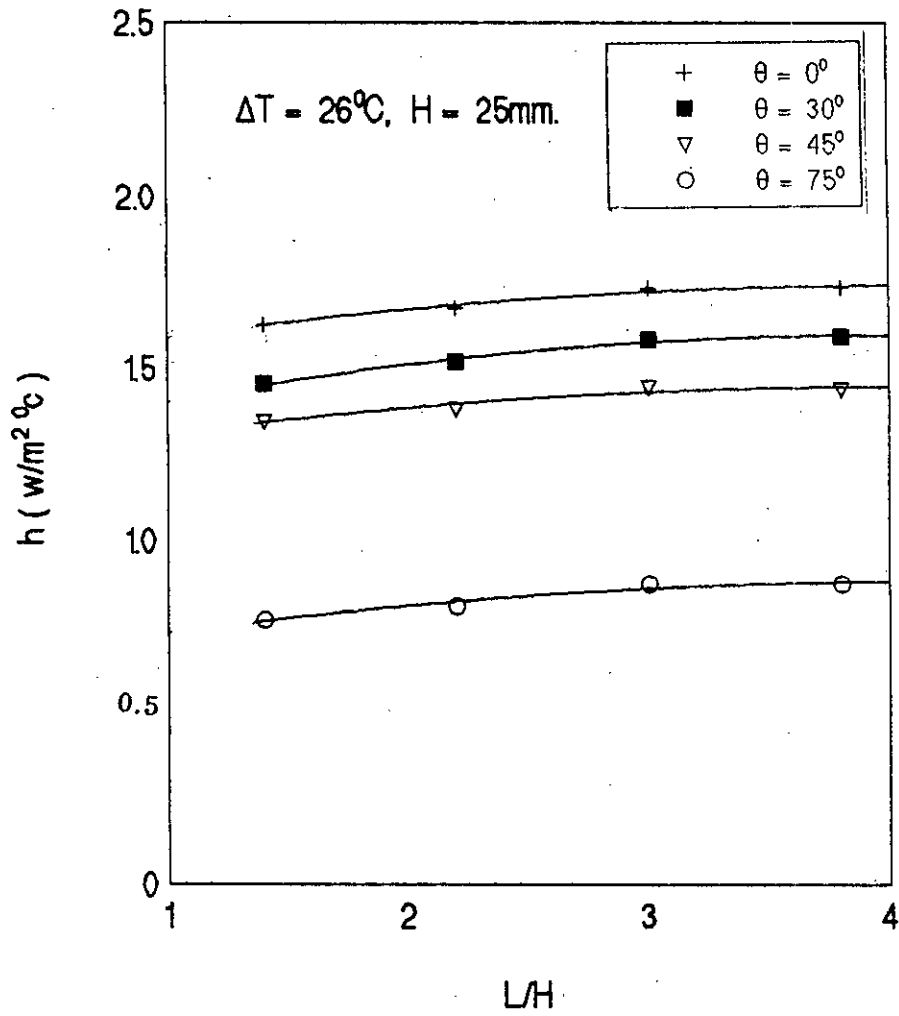
FIG. 6.16: EFFECT OF ASPECT RATIO (A) ON AVERAGE HEAT
TRANSFER COEFFICIENT FOR DIFFERENT ANGLES OF
INCLINATION.
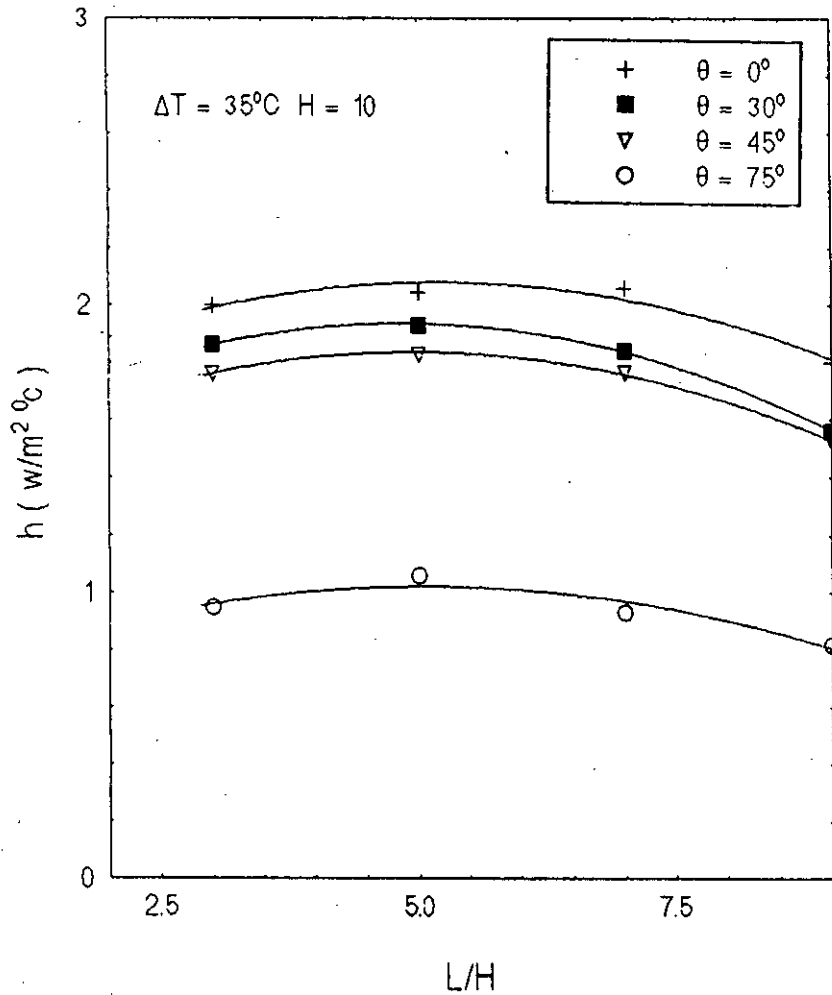
FIG. 6.17: EFFECT OF ASPECT RATIO (A) ON AVERAGE HEAT TRANSFER COEFFICIENT FOR DIFFERENT ANGLES OF INCLINATION.
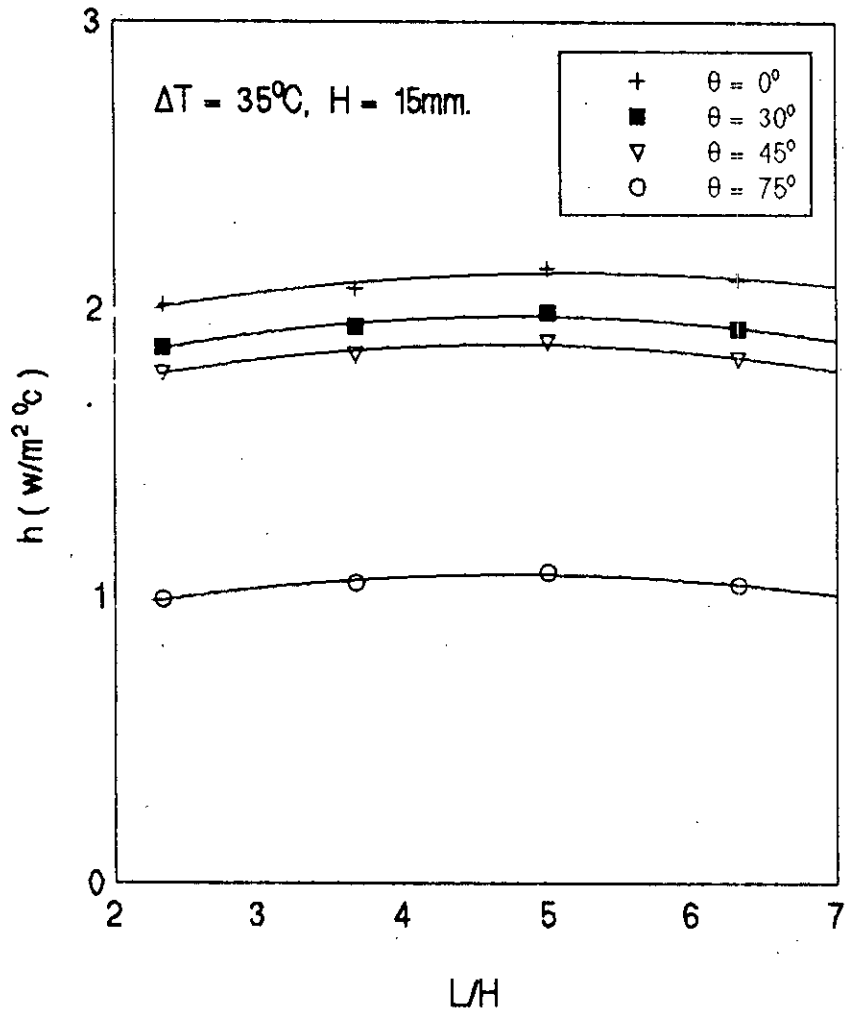
FIG. 6.18: EFFECT OF ASPECT RATIO (A) ON AVERAGE HEAT TRANSFER COEFFICIENT FOR DIFFERENT ANGLES OF INCLINATION.
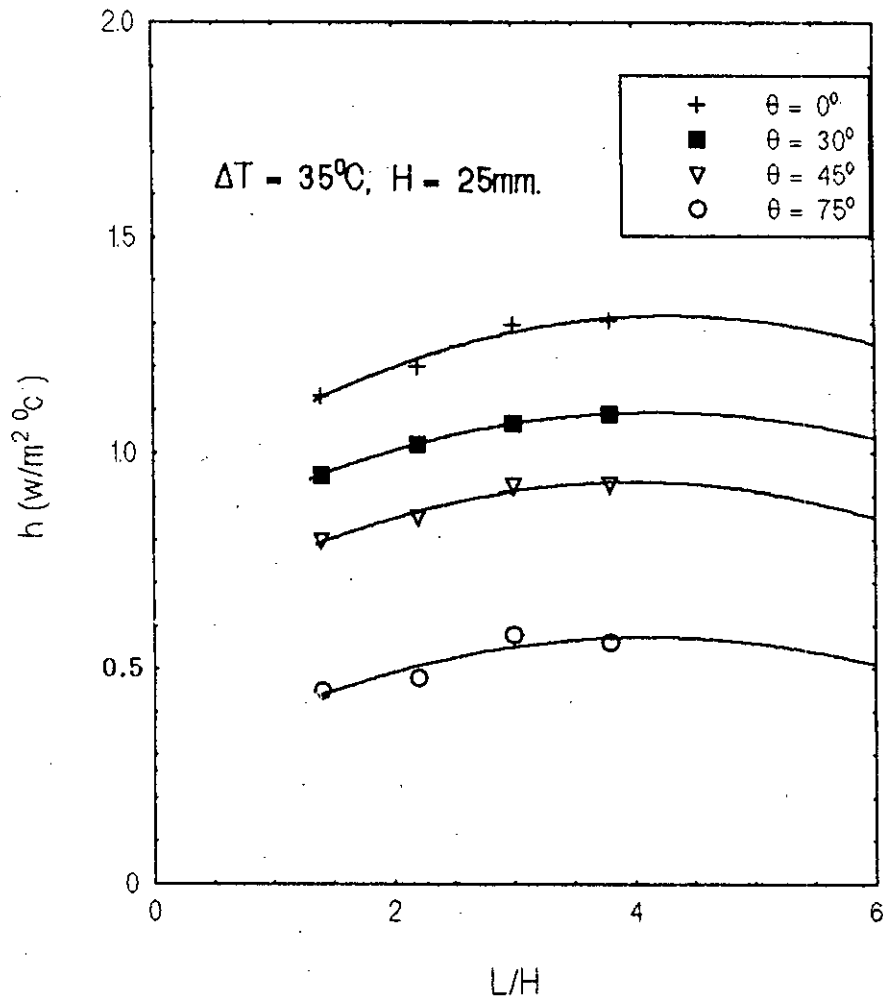
FIG. 6.19: EFFECT OF ASPECT RATIO (A) ON AVERAGE HEAT TRANSFER COEFFICIENT FOR DIFFERENT ANGLES OF INCLINATION.
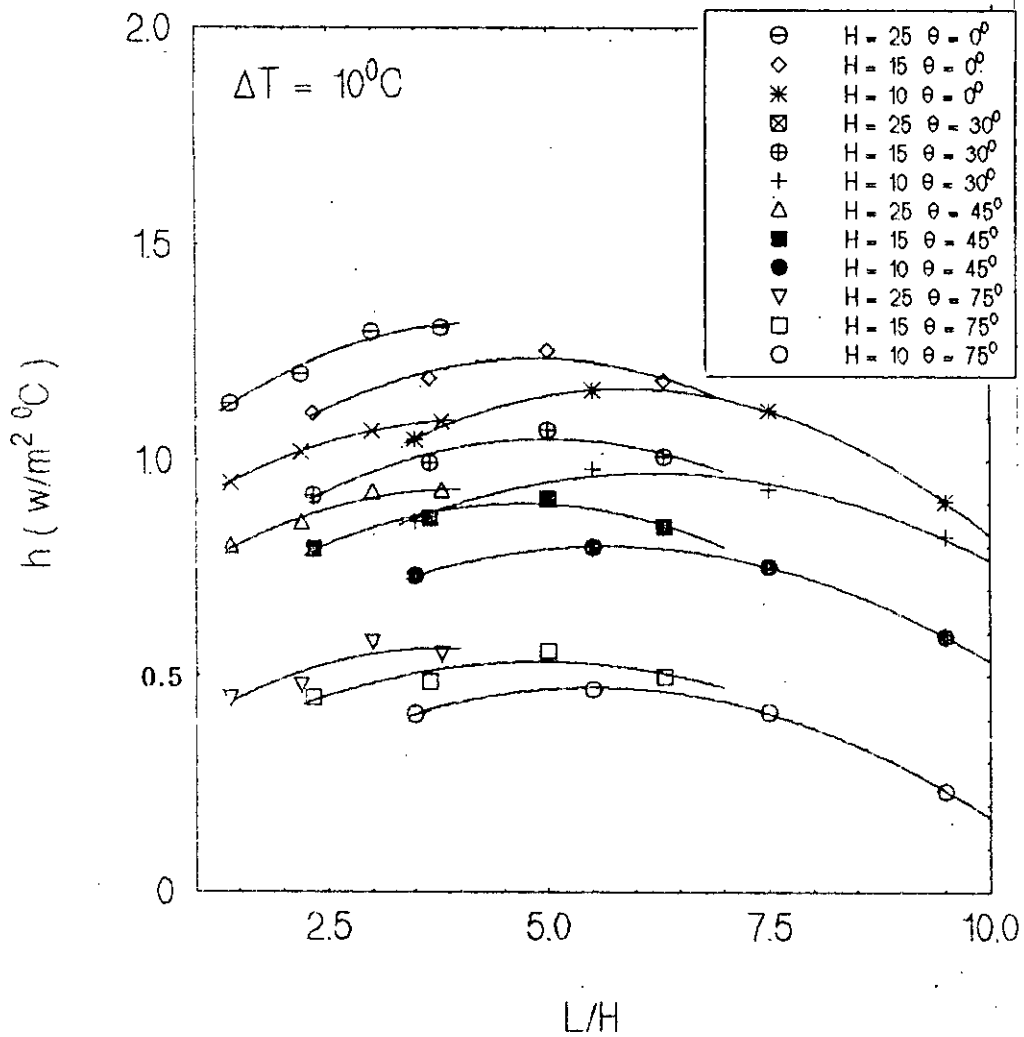
FIG. 6.20: EFFECT OF ASPECT RATIO ON AVERAGE HEAT TRANSFER COEFFICIENT FOR $\Delta T = 10^0 C$.
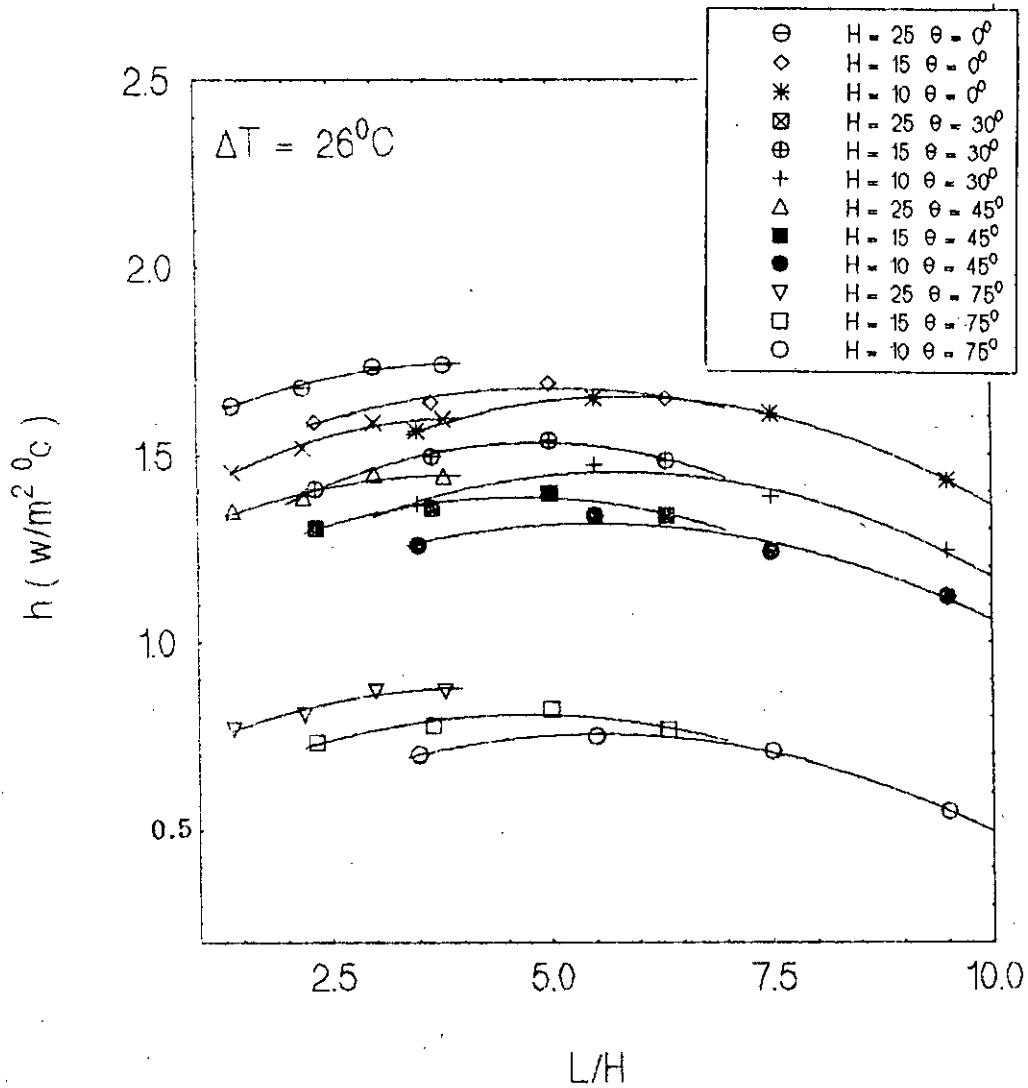
FIG. 6.21: EFFECT OF ASPECT RATIO ON AVERAGE HEAT TRANSFER COEFFICIENT FOR $\Delta T = 26^0C$.

96
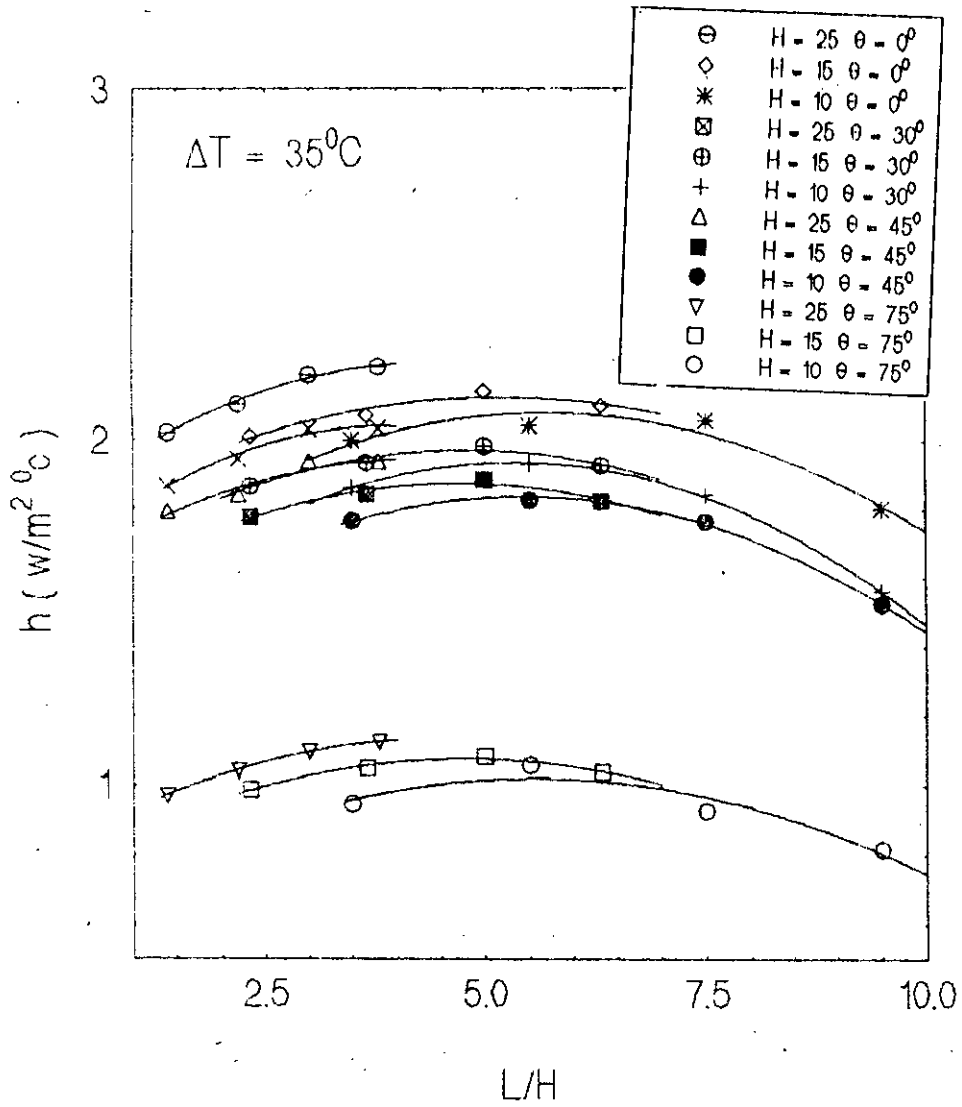
FIG. 6.22: EFFECT OF ASPECT RATIO ON AVERAGE HEAT TRANSFER COEFFICIENT FOR $\Delta T = 35^{0}$C.

97
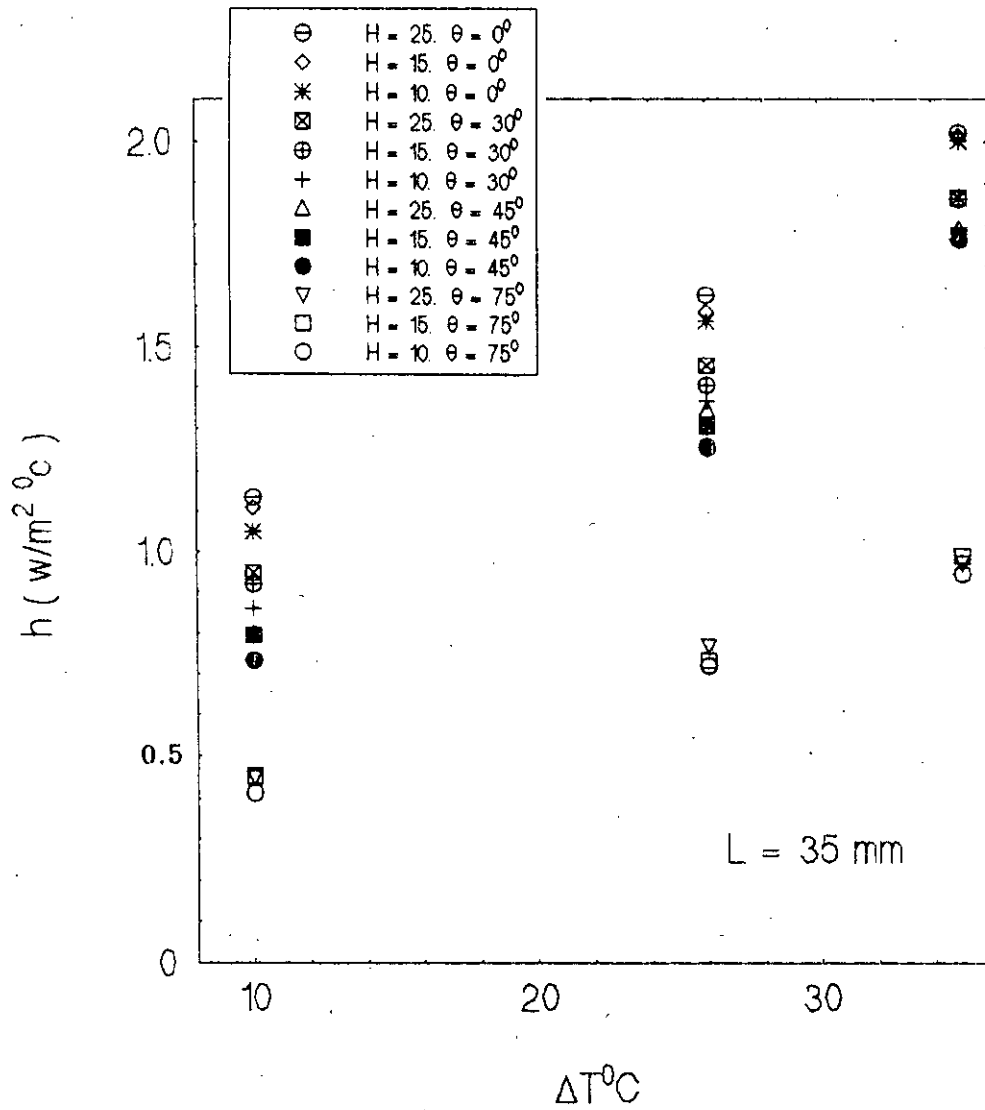
FIG. 6.23: EFFECT OF TEMPERATURE POTENTIAL (ΔT) ON AVERAGE HEAT TRANSFER COEFFICIENT FOR L = 35MM.
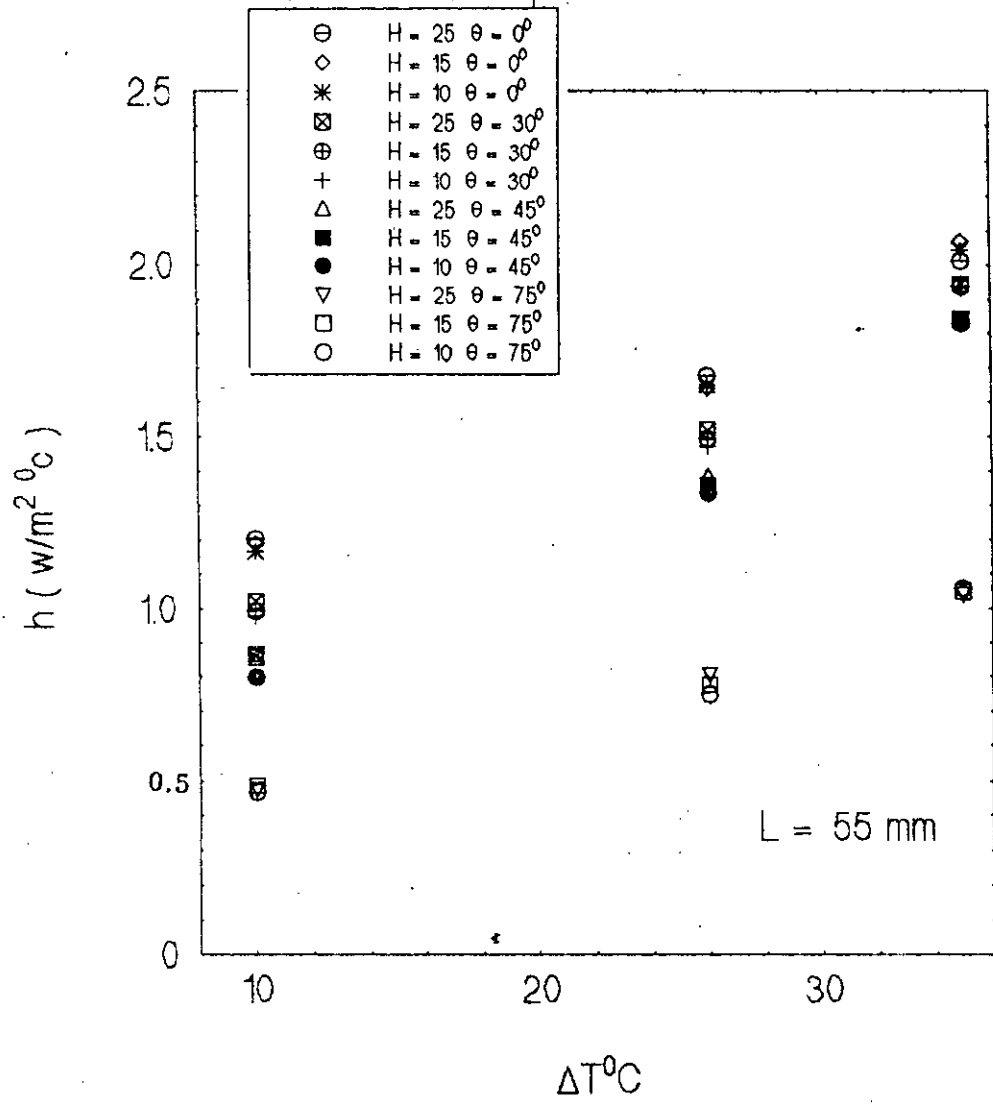
FIG. 6.24:   EFFECT OF TEMPERATURE POTENTIAL (ΔT) ON
AVERAGE HEAT TRANSFER COEFFICIENT FOR
L = 55MM.
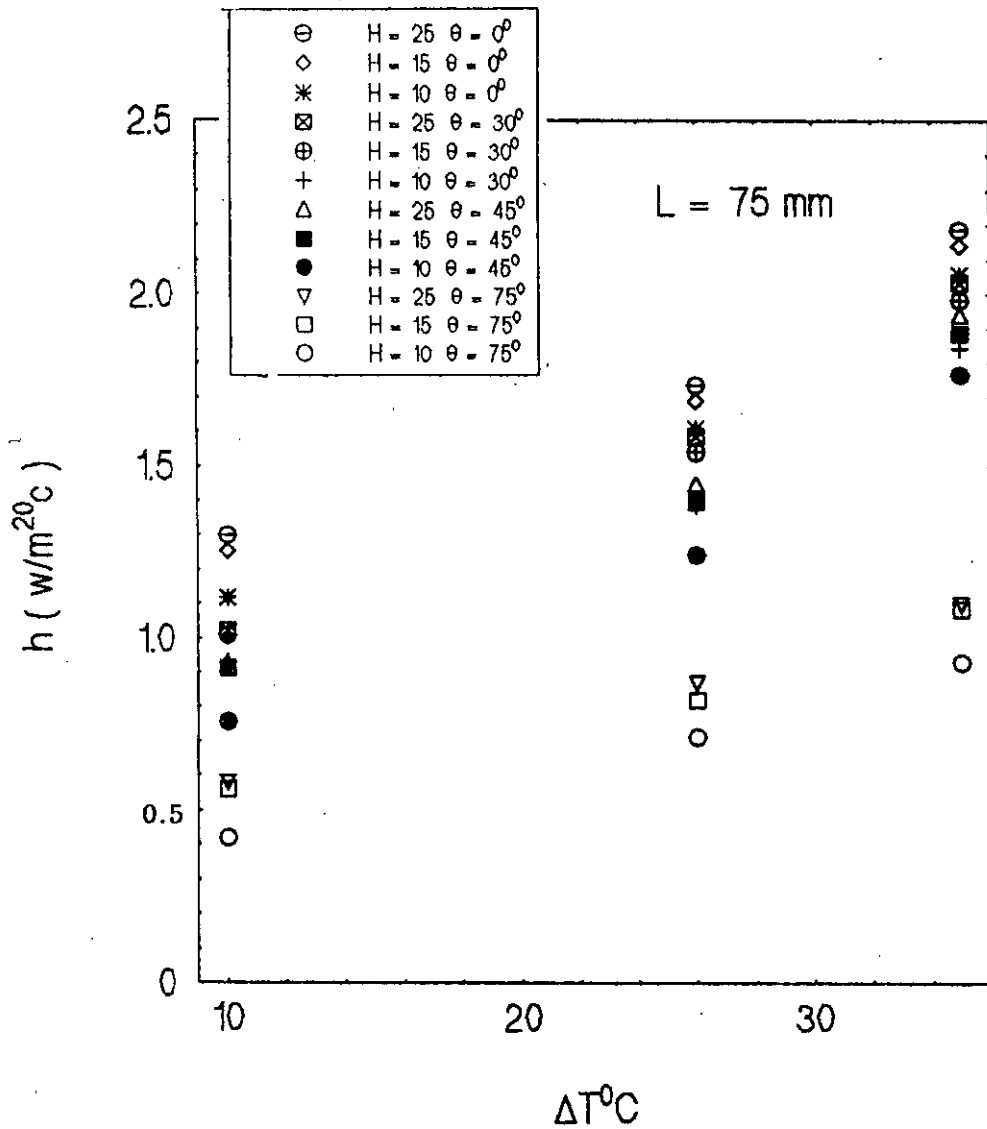
FIG. 6.25: EFFECT OF TEMPERATURE POTENTIAL (ΔT) ON AVERAGE HEAT TRANSFER COEFFICIENT FOR L = 75MM.

L = 95mm.

h ( w/m²⁰C )

2.5

2.0

1.5

1.0

0.5

0

| | | |
|---|---|---|
| ⊖ | H = 25 | θ = 0° |
| ◇ | H = 15 | θ = 0° |
| ✳ | H = 10 | θ = 0° |
| ⊠ | H = 25 | θ = 30° |
| ⊕ | H = 15 | θ = 30° |
| + | H = 10 | θ = 30° |
| △ | H = 25 | θ = 45° |
| ■ | H = 15 | θ = 45° |
| ● | H = 10 | θ = 45° |
| ▽ | H = 25 | θ = 75° |
| □ | H = 15 | θ = 75° |
| ○ | H = 10 | θ = 75° |

10        20        30

ΔT⁰C
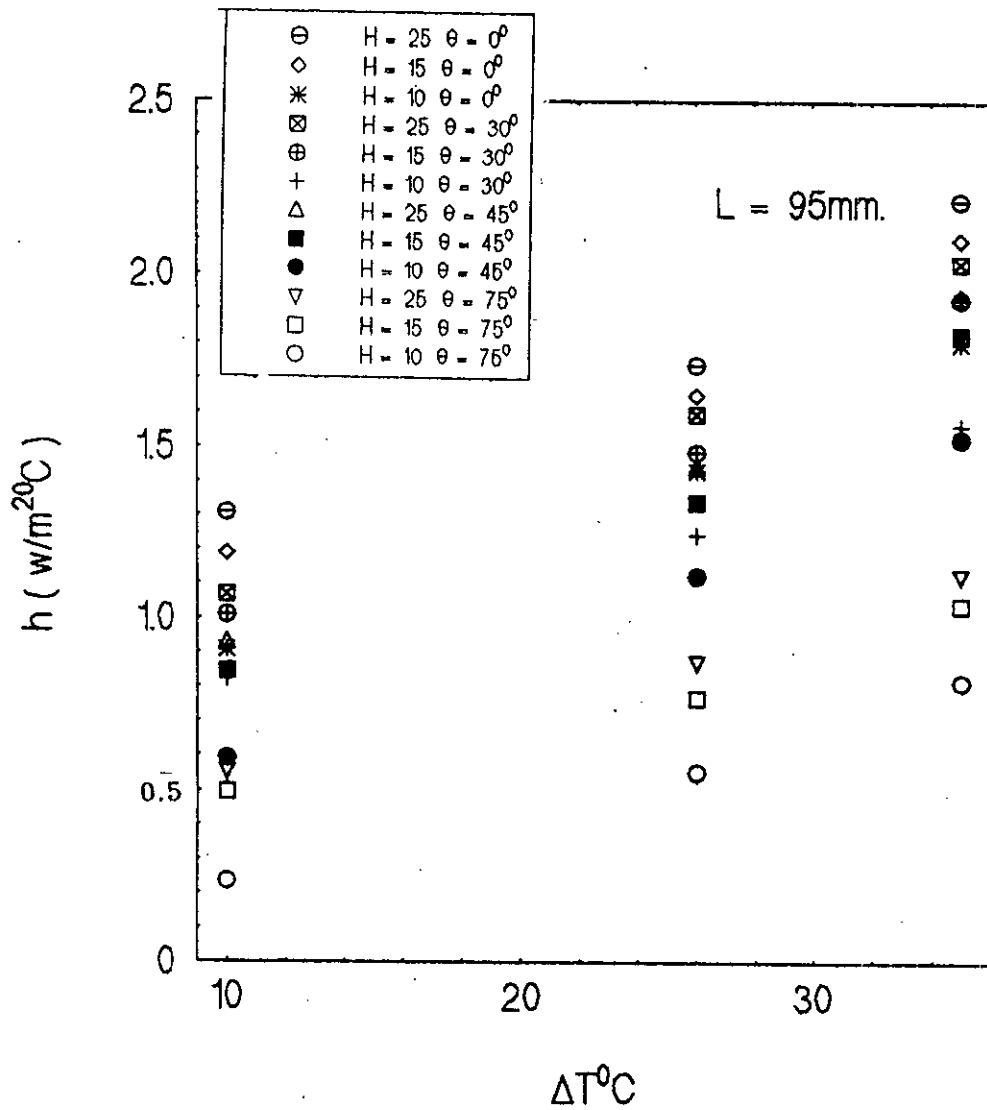
FIG. 6.26: EFFECT OF TEMPERATURE POTENTIAL (ΔT) ON AVERAGE HEAT TRANSFER COEFFICIENT FOR L = 95MM.

101
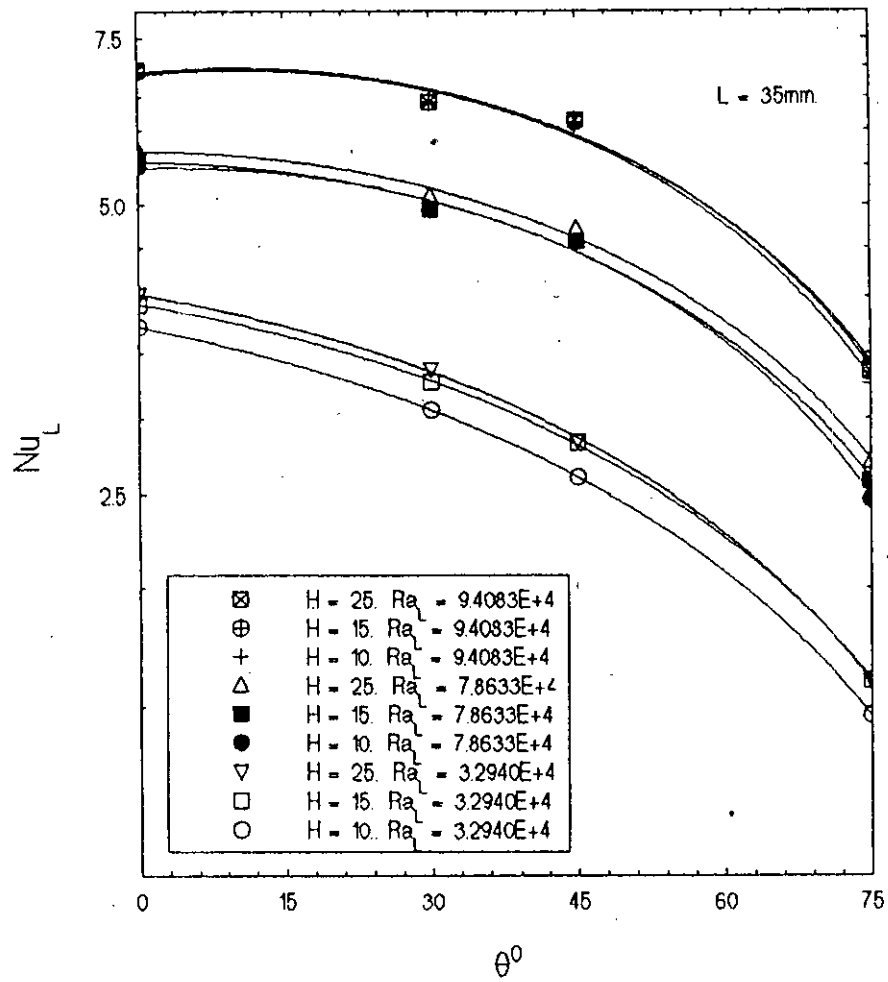
FIG. 6.27: EFFECT OF ANGLE OF INCLINATION ON NUSSELT NUMBER FOR L = 35MM

102
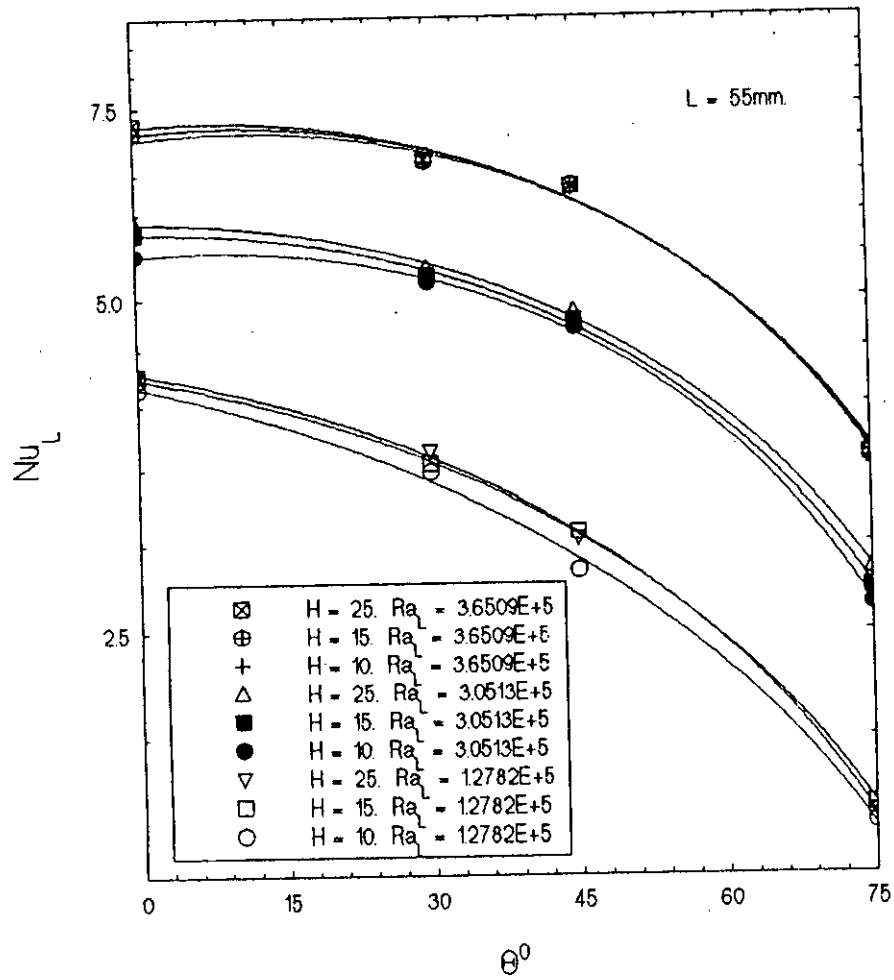
FIG. 6.28: EFFECT OF ANGLE OF INCLINATION ON NUSSELT NUMBER FOR L = 55MM

103
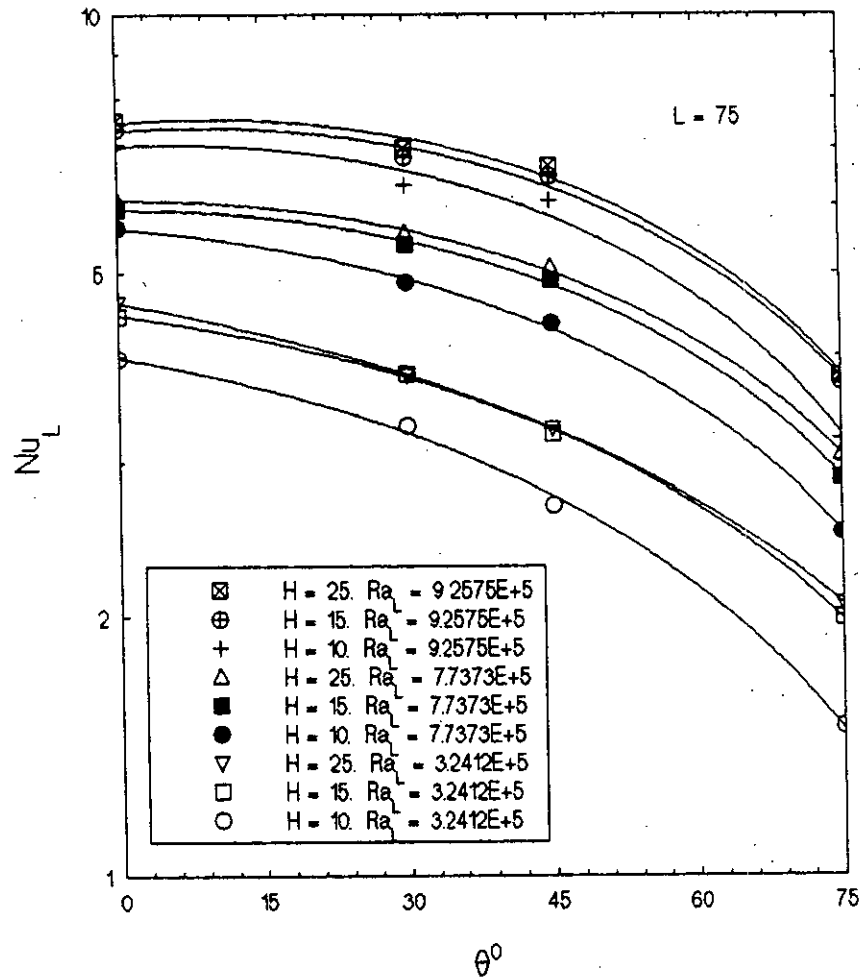
FIG. 6.29: EFFECT OF ANGLE OF INCLINATION ON NUSSELT NUMBER FOR L = 75MM
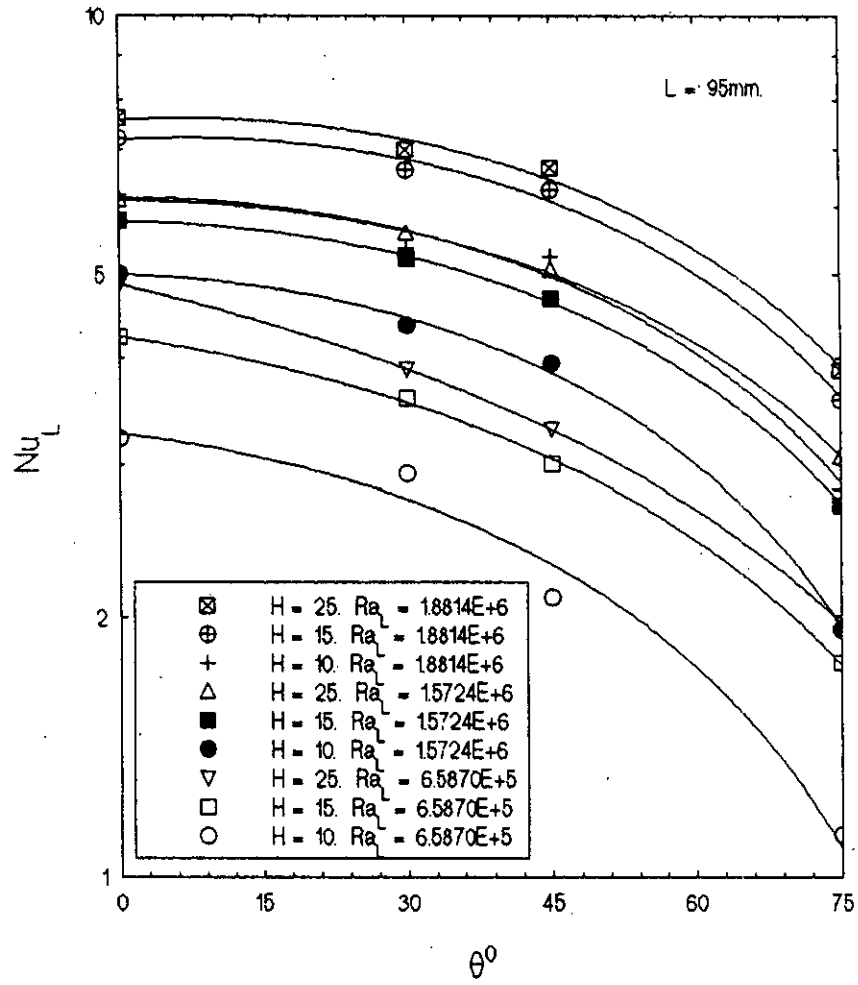
FIG. 6.30:   EFFECT   OF   ANGLE   OF   INCLINATION   ON   NUSSELT
NUMBER   FOR   L   =  95MM
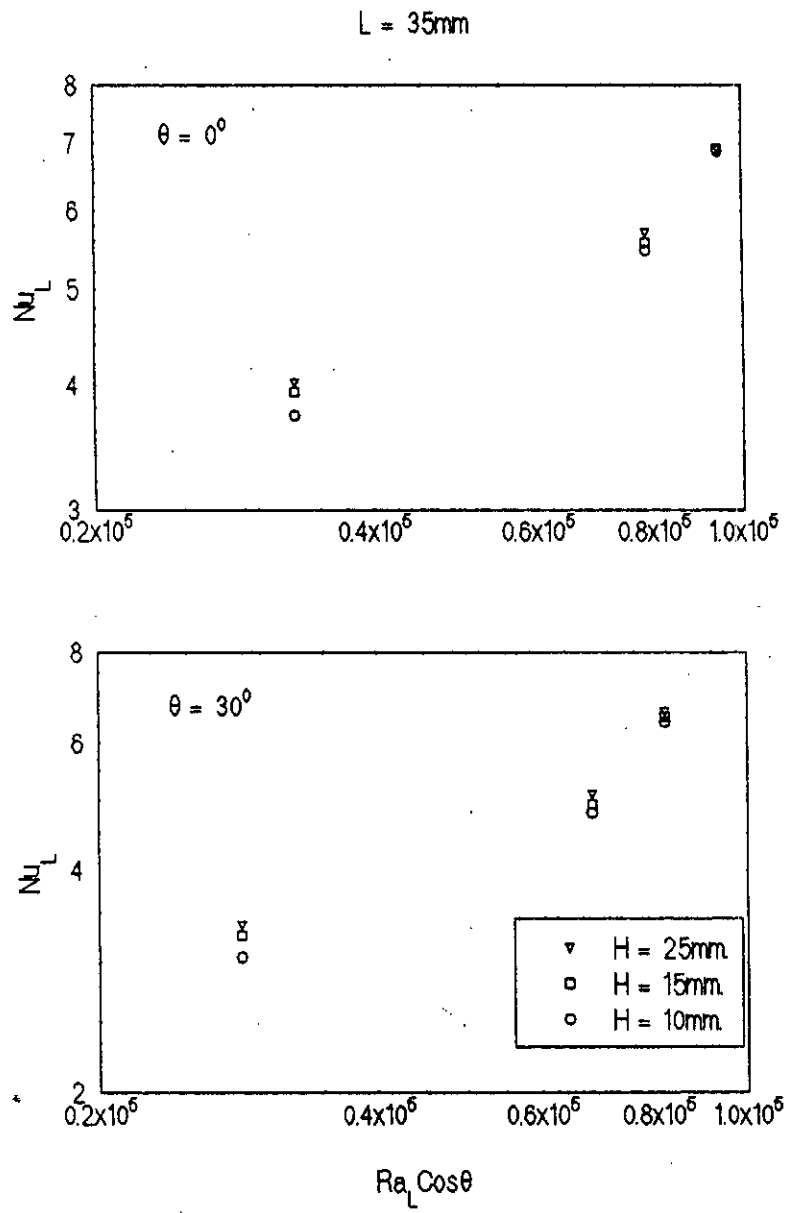
FIG. 6.31: PLOT OF AVERAGE NUSSELT NUMBER VS $RA_L COS\theta$ FOR L = 35MM
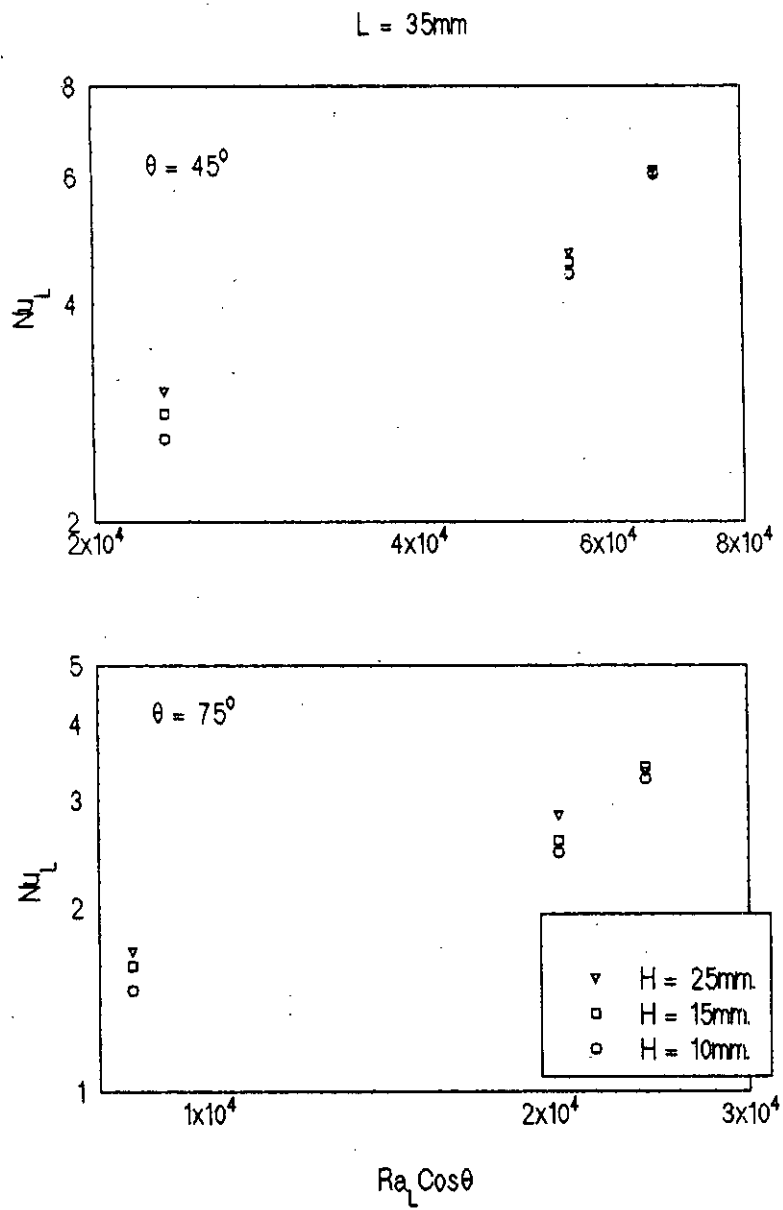
FIG. 6.32: PLOT OF AVERAGE NUSSELT NUMBER VS $RA_L COS \theta$ FOR L = 35MM
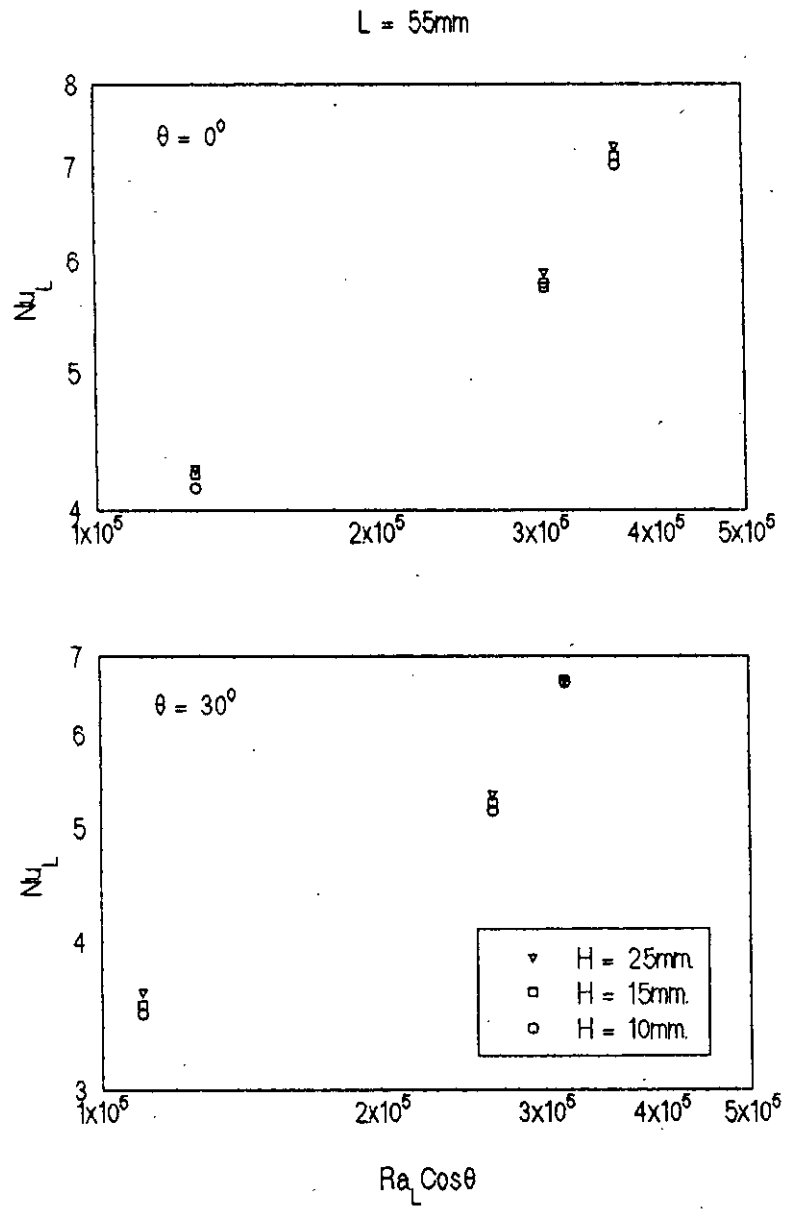
FIG. 6.33:  PLOT OF AVERAGE NUSSELT  NUMBER  VS $RA_L COS\theta$ FOR
L  = 55MM
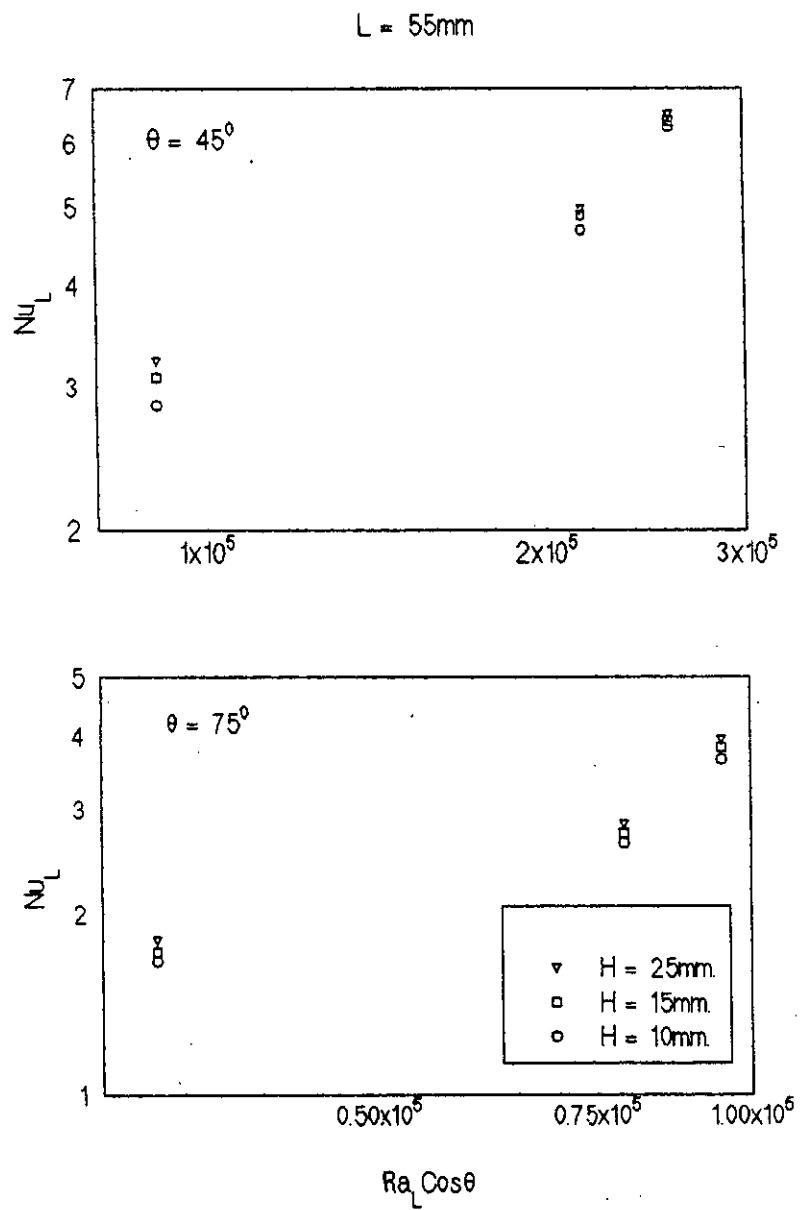
FIG. 6.34:   PLOT OF AVERAGE NUSSELT  NUMBER  VS $RA_L COS\theta$ FOR
L  = 55MM
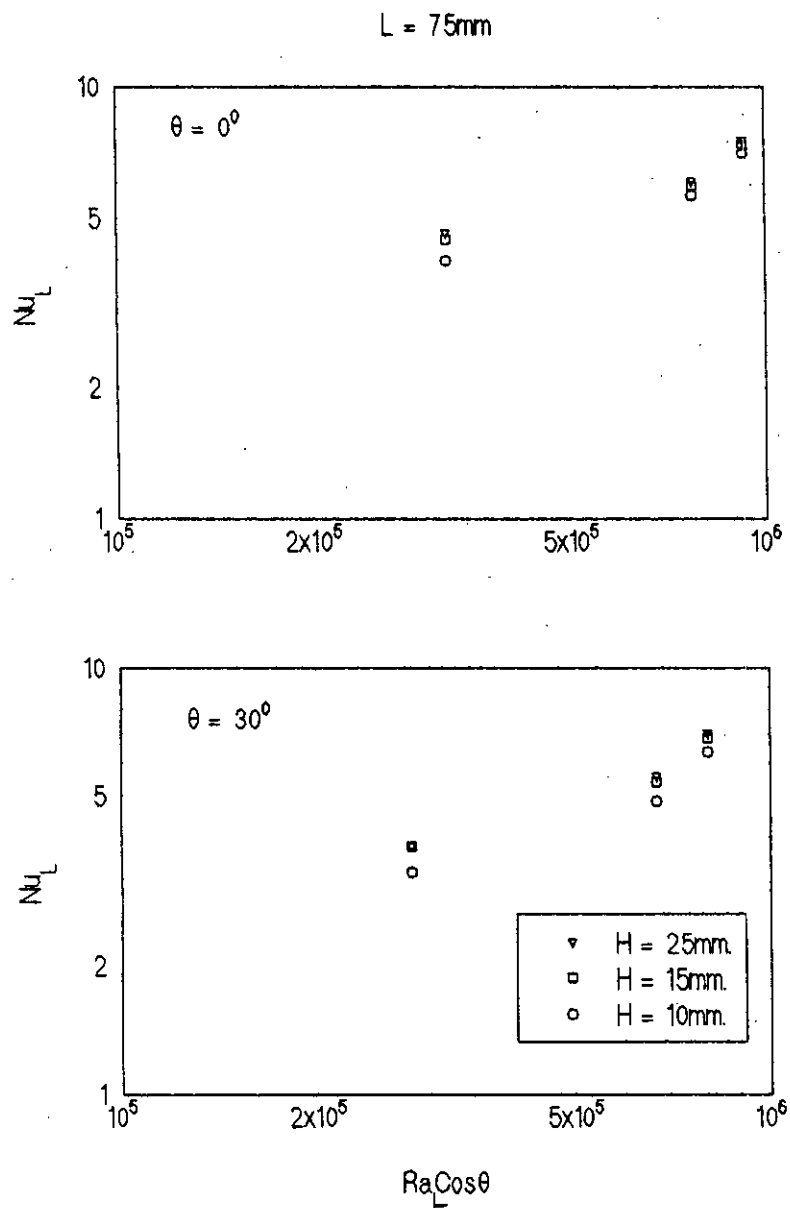
FIG. 6.35: PLOT OF AVERAGE NUSSELT NUMBER VS $RA_L COS\theta$ FOR L = 75MM
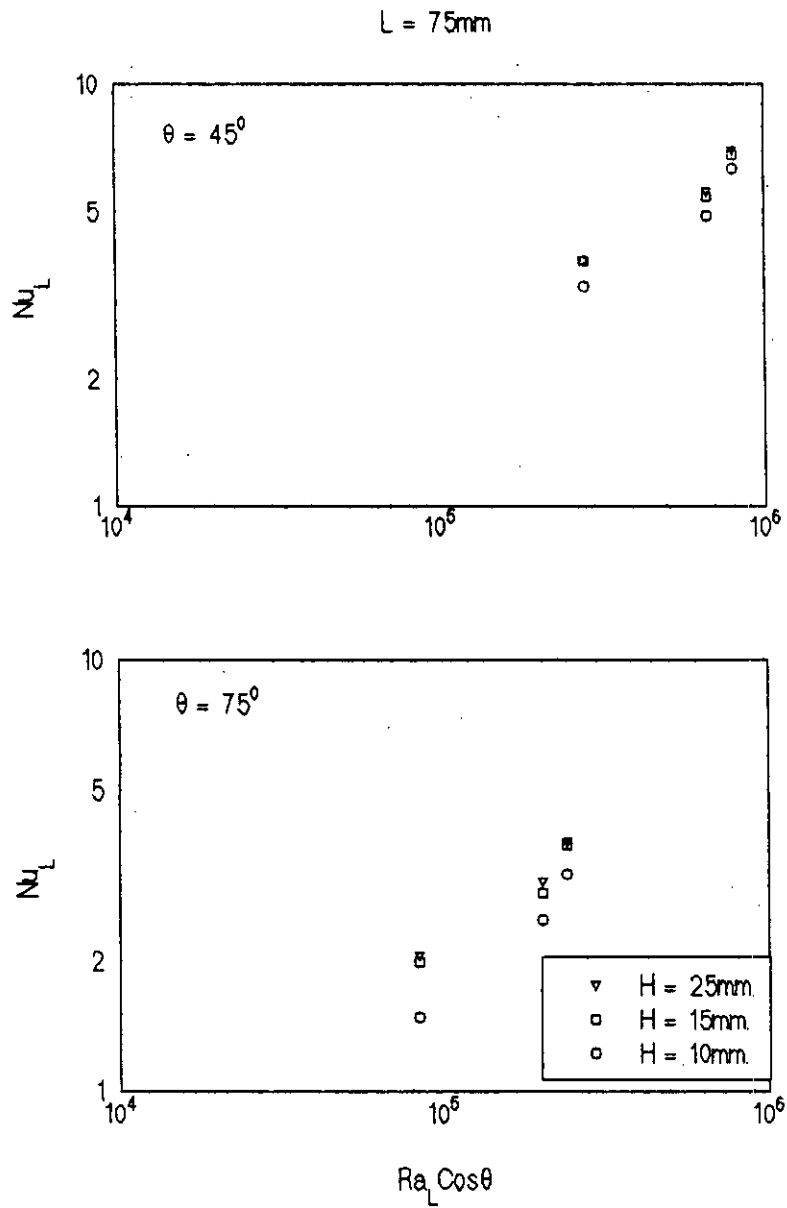
FIG. 6.36: PLOT OF AVERAGE NUSSELT NUMBER VS $RA_L COS\theta$ FOR L = 75MM

111

L = 95mm

θ = 0°

θ = 30°

$Nu_L$

$Ra_L Cos\theta$

H = 25mm.
H = 15mm.
H = 10mm.
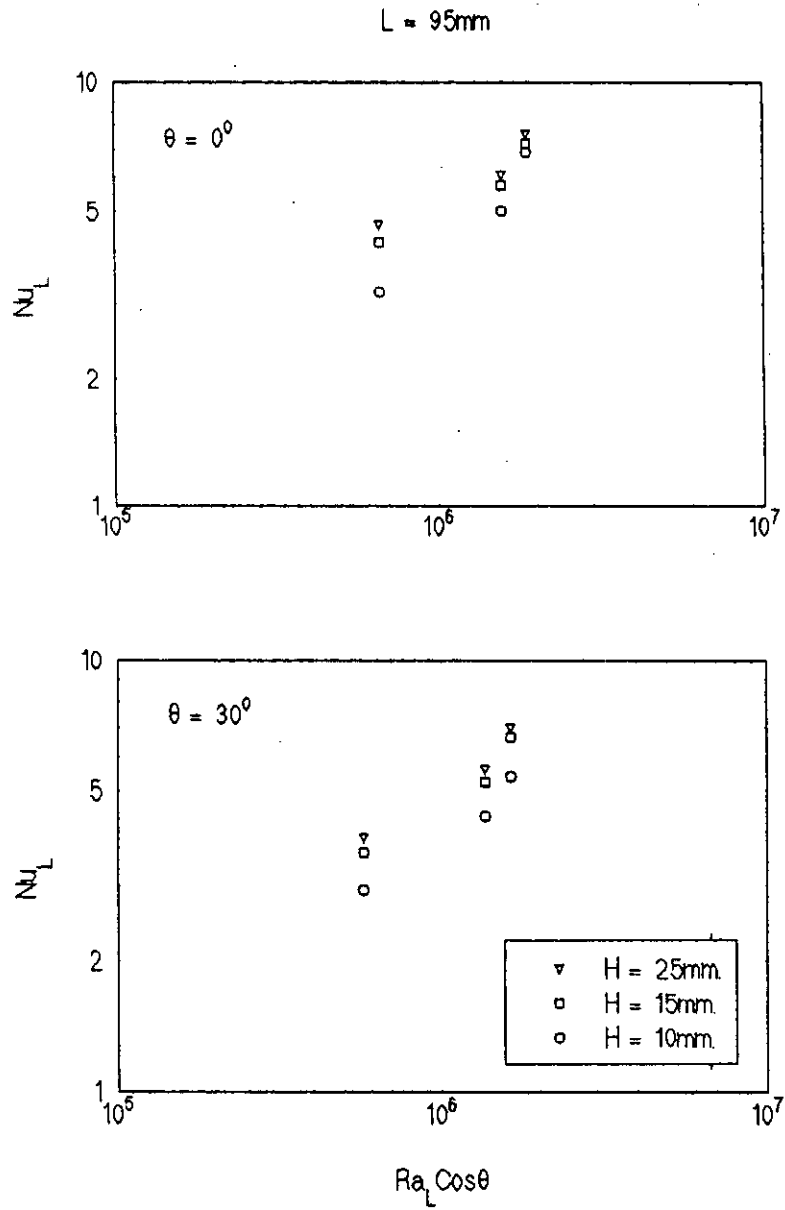
FIG. 6.37:   PLOT OF AVERAGE NUSSELT  NUMBER  VS $RA_L COS\theta$ FOR
L = 95MM

112
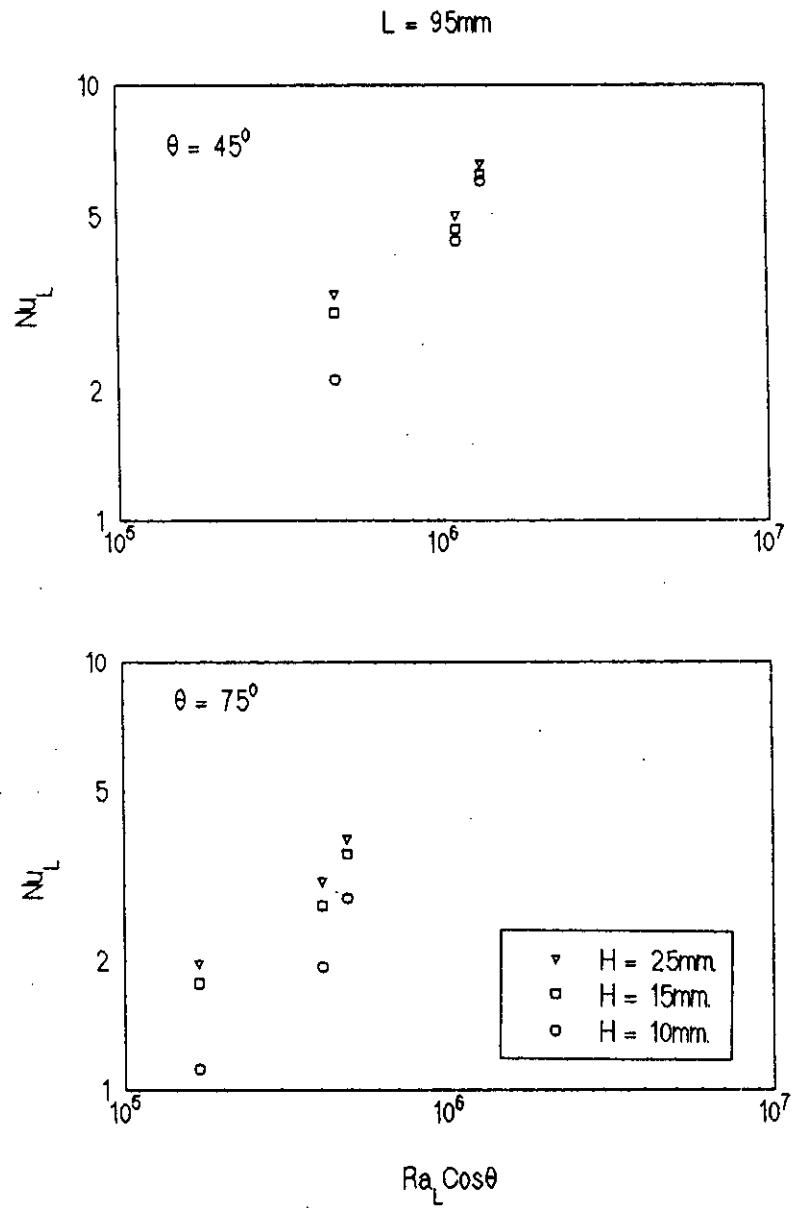
FIG. 6.38: PLOT OF AVERAGE NUSSELT NUMBER VS $RA_L COS\theta$ FOR L = 95MM

113
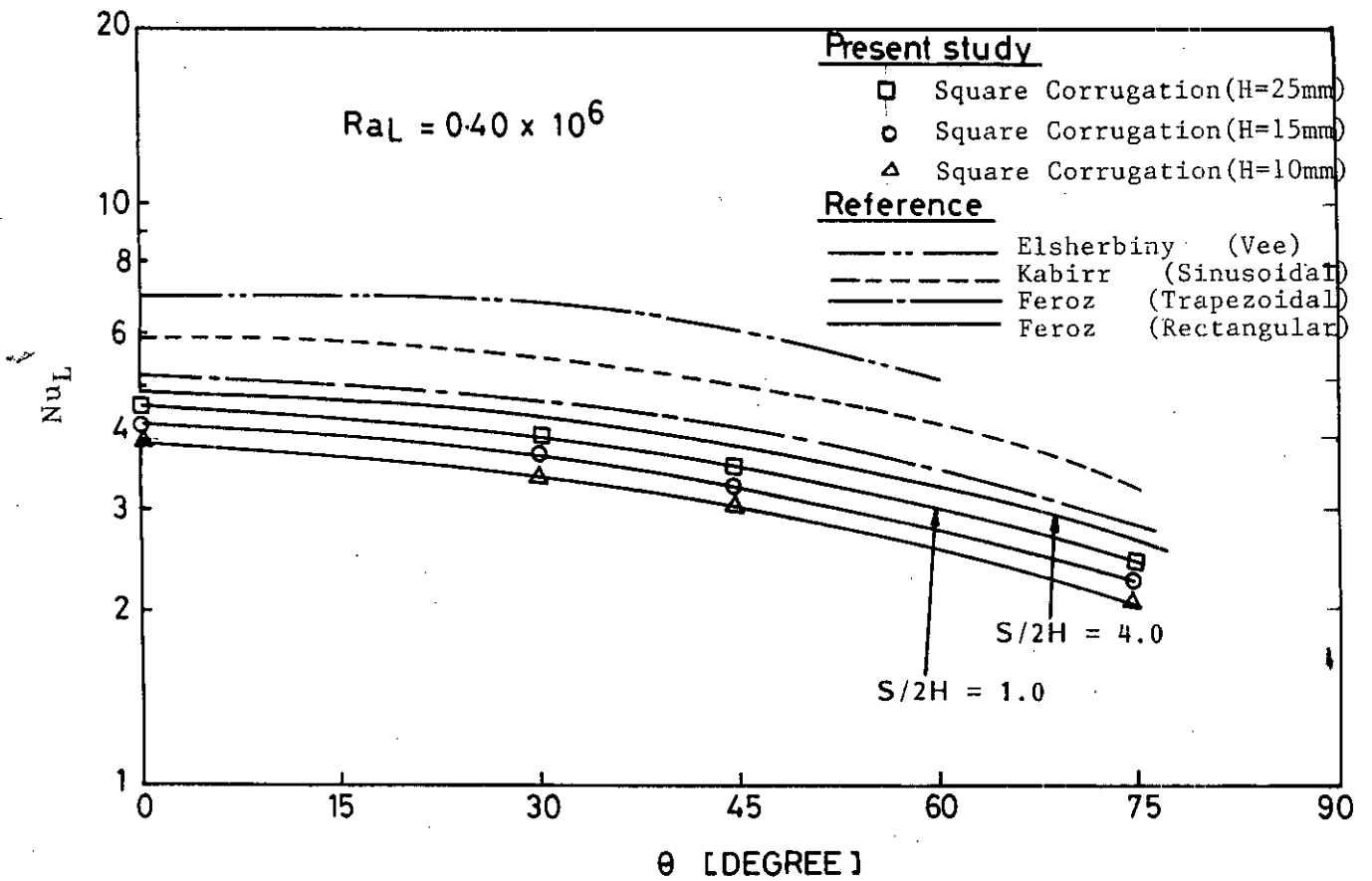
FIG. 6.39   COMPARISON OF THE EFFECT OF ANGLE OF INCLINATION
ON NUSSELT NUMBER OF THE PRESENT STUDY WITH
NUSSELT NUMBER OF OTHER RELATED WORKS.

114
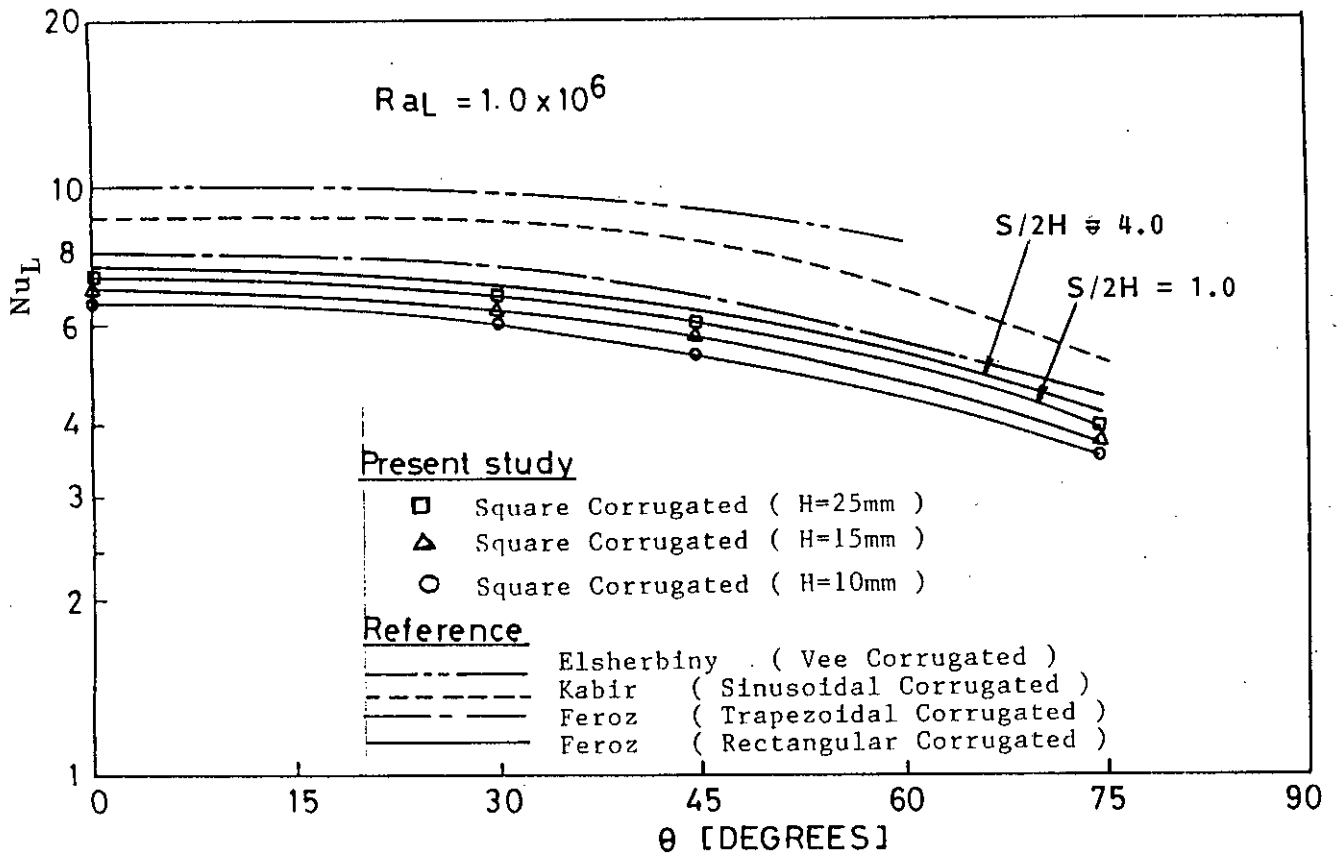
FIG. 6.40.  COMPARISON OF THE EFFECT OF ANGLE OF INCLINATION
ON NUSSELT NUMBER OF THE PRESENT STUDY WITH
NUSSELT NUMBER OF OTHER RELATED WORKS.

115
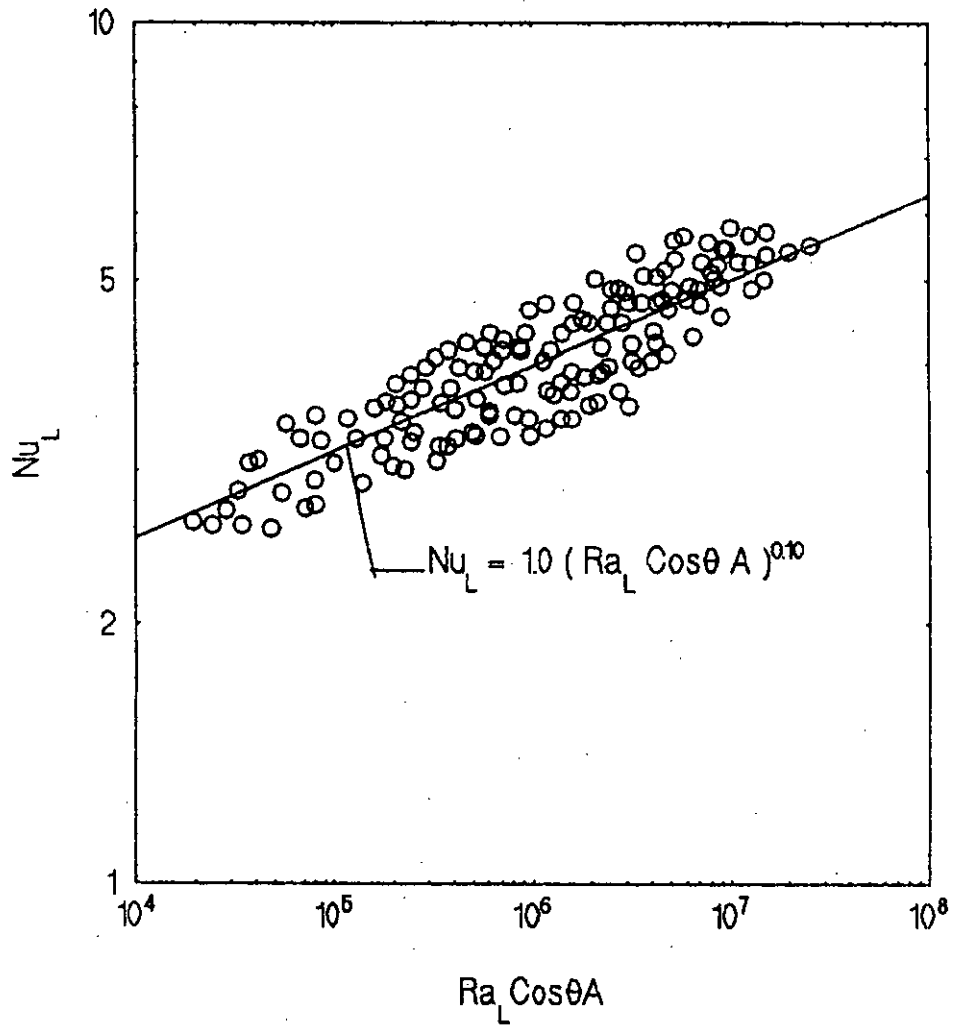
FIG. 6.41: GRAPHICAL REPRESENTATION OF THE CORRELATION FOR SQUARE CORRUGATION
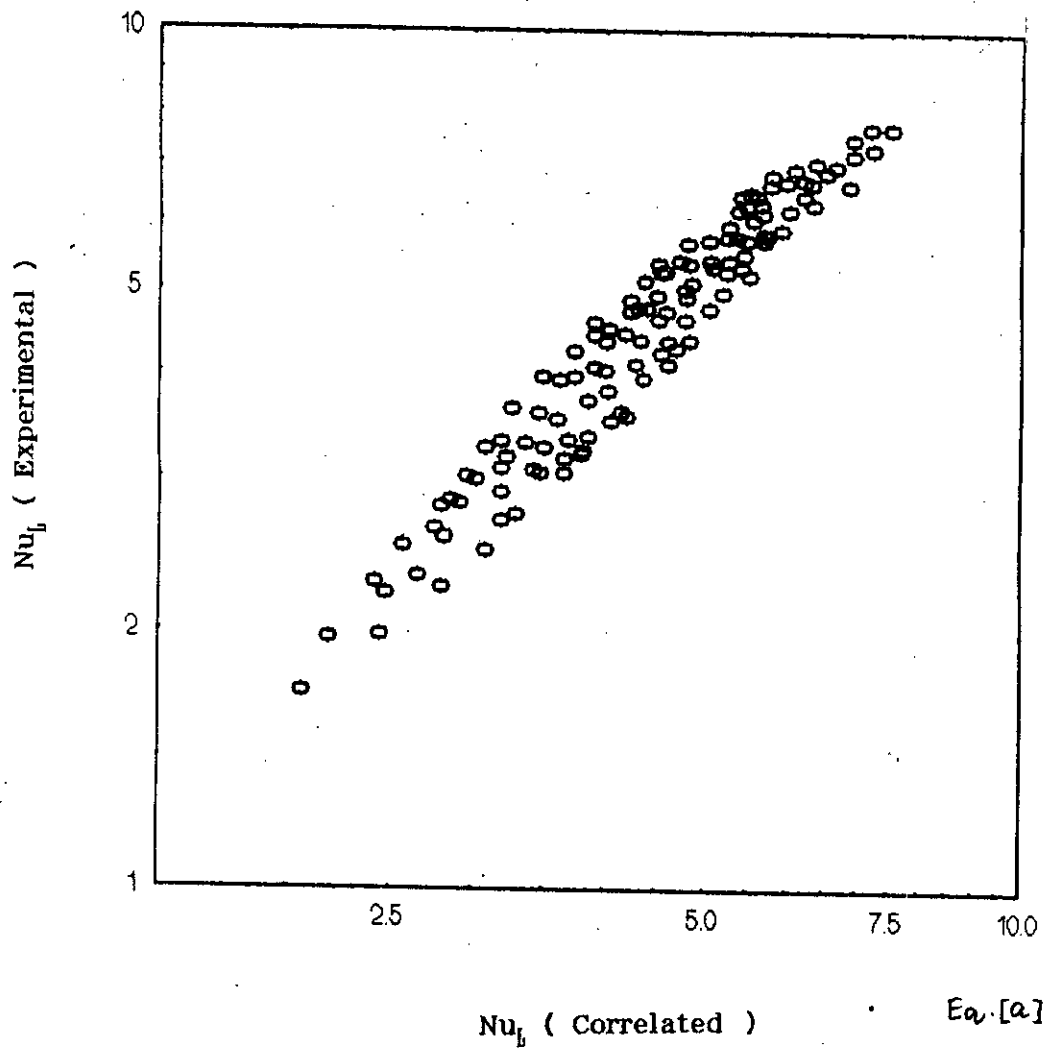
FIG. 6.42: GRAPHICAL REPRESENTATION OF THE CORRELATION FOR SQUARE CORRUGATION
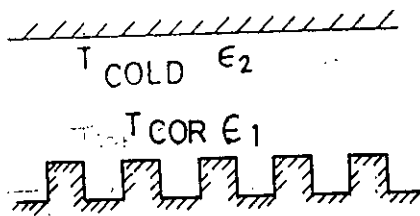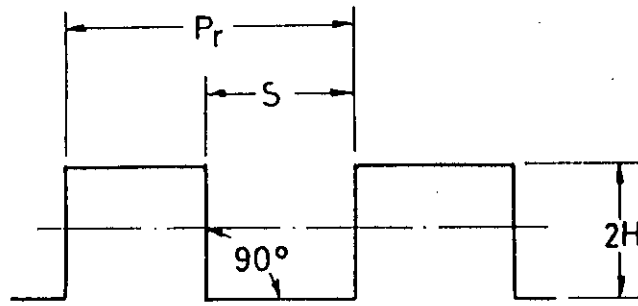
FIG. A.1.
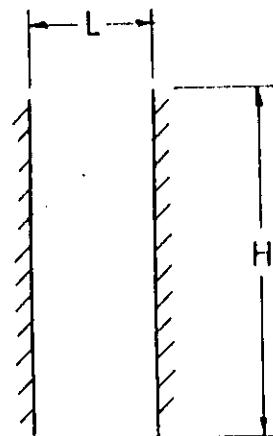


FIG. A.2.
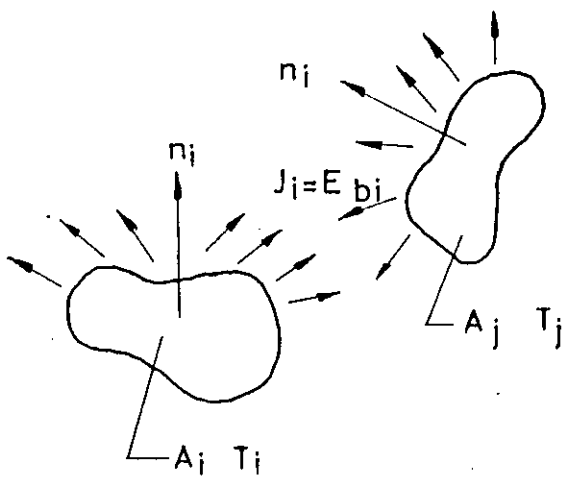


FIG. A.3.
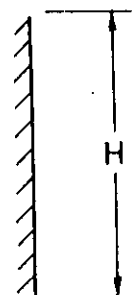


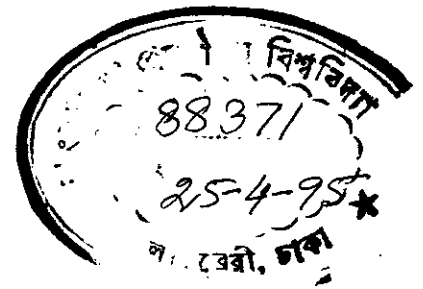FIG. A.4.
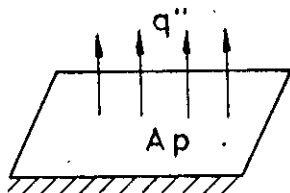


FIG. A.5.
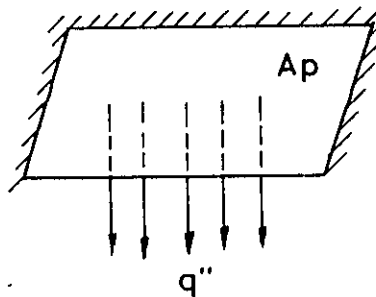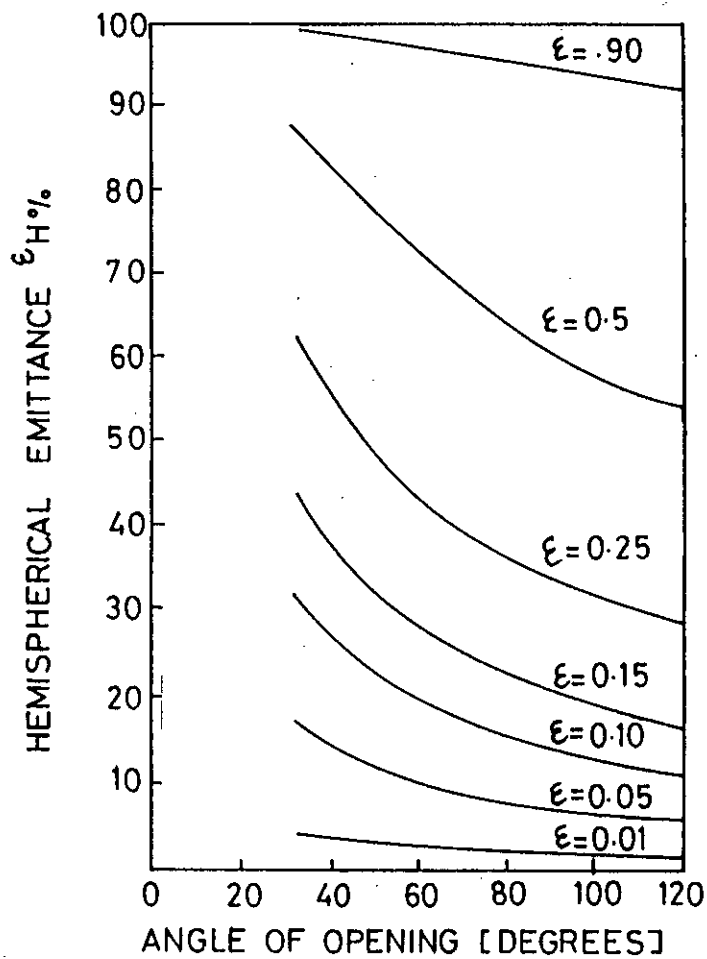


FIG. A.6.

FIG. C.1. CORRUGATION GEOMETRY



FIG. C.2. HEMISPHERICAL EMITTENCE Vs ANGLE
OF OPENING FOR SEVERAL PLANE
LONG WAVE EMISSIVITIES.

119